

University of Montana

ScholarWorks at University of Montana

Graduate Student Theses, Dissertations, &
Professional Papers

Graduate School

1997

Cordilleran partitioning and foreland basin evolution as recorded by the sedimentation and stratigraphy of the Upper Cretaceous Carten Creek and Golden Spike Formations central-western Montana

Amy M. Waddell
The University of Montana

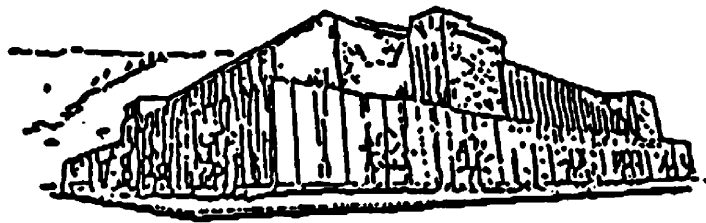
Follow this and additional works at: <https://scholarworks.umt.edu/etd>

Let us know how access to this document benefits you.

Recommended Citation

Waddell, Amy M., "Cordilleran partitioning and foreland basin evolution as recorded by the sedimentation and stratigraphy of the Upper Cretaceous Carten Creek and Golden Spike Formations central-western Montana" (1997). *Graduate Student Theses, Dissertations, & Professional Papers*. 7114.
<https://scholarworks.umt.edu/etd/7114>

This Thesis is brought to you for free and open access by the Graduate School at ScholarWorks at University of Montana. It has been accepted for inclusion in Graduate Student Theses, Dissertations, & Professional Papers by an authorized administrator of ScholarWorks at University of Montana. For more information, please contact scholarworks@mso.umt.edu.



Maureen and Mike
MANSFIELD LIBRARY

The University of **MONTANA**

Permission is granted by the author to reproduce this material in its entirety,
provided that this material is used for scholarly purposes and is properly cited in
published works and reports.

**** Please check "Yes" or "No" and provide signature ****

Yes, I grant permission

No, I do not grant permission

Author's Signature

Amy M. Wassell

Date

5/4/98

Any copying for commercial purposes or financial gain may be undertaken only with
the author's explicit consent.

**Cordilleran Partitioning and Foreland Basin Evolution
as recorded by the Sedimentation and Stratigraphy of the
Upper Cretaceous Carten Creek and Golden Spike Formations,
Central-Western Montana**

by

Amy M. Waddell

B.S., James Madison University, 1992

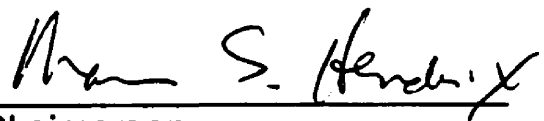
presented in partial fulfillment of the requirements for the degree of

Master of Science

The University of Montana

1997

Approved by:



Chairperson



Dean, Graduate School

5-13-98

Date

UMI Number: EP37915

All rights reserved

INFORMATION TO ALL USERS

The quality of this reproduction is dependent upon the quality of the copy submitted.

In the unlikely event that the author did not send a complete manuscript and there are missing pages, these will be noted. Also, if material had to be removed, a note will indicate the deletion.



UMI EP37915

Published by ProQuest LLC (2013). Copyright in the Dissertation held by the Author.

Microform Edition © ProQuest LLC.

All rights reserved. This work is protected against unauthorized copying under Title 17, United States Code



ProQuest LLC.
789 East Eisenhower Parkway
P.O. Box 1346
Ann Arbor, MI 48106 - 1346

Abstract

Waddell, Amy M., M.S. Geology

Cordilleran Partitioning and Foreland Basin Evolution as recorded by the Sedimentation and Stratigraphy of the Upper Cretaceous Carten Creek and Golden Spike Formations, Central-Western Montana

Committee Chair: Marc S. Hendrix, Ph.D. MSH

Recent stratigraphic and sedimentologic study of Upper Cretaceous nonvolcanic units in the Garrison, MT area provides more detailed interpretation of the upper-middle Carten Creek and lower Golden Spike formations. The facies and deposystems associated with these synorogenic formations record both foreland basin evolution, south of the Lewis and Clark Line (LCL), and the structural deformation of western Montana's fold-thrust belt. Sublithic-feldspathic sediment contained in the Coniacian-Santonian Carten Creek Formation eroded from the western orogenic wedge and allied Idaho Batholith. Upper-middle Carten Creek deposits represent a marginal-marine meandering-fluvial system that records a more terrestrial character upsection. The Campanian Golden Spike Formation is an amalgamation of interbedded volcanic and sublithic-nonvolcanic deposits. Opposing paleoflow of volcanic and nonvolcanic units (Gwinn and Mutch, 1965; Mackie, 1986) and abundant clasts of Mississippian Madison limestone suggest that Golden Spike sediment derived from the Elkhorn Mountain Volcanics, Sapphire Tectonic Block and uplift along the LCL. Depositional environments of the lower Golden Spike include eastward-facing alluvial fans, a southward-flowing fluvial system and a westward-spreading volcanic-alluvial apron. Lava flows and lahars (volcanic-debris flows) comprise the volcanic-alluvial deposits within the Golden Spike: reinterpretation of the unique megaconglomerate facies suggests deposition by multiple lahars that incorporated nonvolcanic detritus through superficial erosion. Overall, the Carten Creek Formation is part of a time-transgressive progradational shoreline that was presumably located in the foredeep depozone and extended north to south across western Montana, whereas the Golden Spike Formation represents wedge-top deposition within the eastward-propagating Cordillera. Golden Spike lava beds and lahar megaconglomerate suggest that concurrent volcanism related to the Elkhorn Mountain Volcanics occurred about 80-83Ma within the wedge-top depozone. The late Cretaceous stratigraphic sequence constrains the inception of uplift along the Lewis and Clark Line and subsequent partitioning of the foreland basin to early Campanian time.

Table of Contents

	PAGE
ABSTRACT _____	ii
TABLE OF FIGURES _____	v
INTRODUCTION _____	1
Acknowledgments	1
Purpose	2
Location	2
REGIONAL GEOLOGY _____	5
Introduction	5
Lewis and Clark Line	8
Partitioned Cordillera	10
Foreland Sedimentation	14
PREVIOUS INVESTIGATIONS _____	16
Age and Correlation	16
Carten Creek Formation	18
Golden Spike Formation	19
METHODS _____	26
SEDIMENTOLOGY AND STRATIGRAPHY _____	30
Introduction	30
Lithofacies of the upper-middle Carten Creek Formation	30
Lithofacies of the lower Golden Spike Formation	38
Environmental Interpretation of Lithofacies	57
Fluvial Deposition	57
Noncohesive Debris Flow Deposition	60

Table of Contents, Continued

	PAGE
SEDIMENTOLOGY AND STRATIGRAPHY, Continued	
Environmental Interpretation of Lithofacies, Continued	
Lahar and Volcanic-related Deposition	65
Provenance Analysis	68
Introduction	68
Carten Creek Formation	69
Golden Spike Formation	74
SUMMARY OF DEPOSITION _____	85
IMPLICATIONS OF LOCAL STRATIGRAPHY ON REGIONAL GEOLOGY ____	99
CONCLUSIONS _____	107
SUGGESTIONS FOR FUTURE STUDY _____	109
BIBLIOGRAPHY _____	110
APPENDIX _____	116

List of Figures

FIGURE	PAGE
1. Geologic map of and research localities in Garrison, MT and vicinity	4
2. Paleogeographic map of late Cretaceous North America	6
3. Regional sedimentation pattern in Campanian Northern Rocky Mtns	7
4. Opposing interpretations for Lewis and Clark Line development	9
5. Regional location of LCL, Sapphire Thrust Block and research area	11
6. Tectonic setting and location of research area in Clark Fork Sag	13
7. Palinspastically restored W-E cross-section of lithofacies in central MT	15
8. Upper Cretaceous and Paleocene synorogenic conglomerates	17
9. Sign commemorating 1883 union of Northern Pacific Rail Line	20
10. NNW-SSE cross-section of the Golden Spike Formation	22
11. Generalized stratigraphy of the Golden Spike type section	23
12. Measured section from the upper-middle Carten Creek Formation	31-33
13. Trough crossbedding in the upper-middle Carten Creek Formation	35
14. Mudchip-rich sandstone scour in the upper-middle Carten Creek Frm	35
15. Largest clast in the lower Golden Spike megaconglomerate facies	40
16. Remnant paleosol in lower Golden Spike megaconglomerate facies	41
17. Variation of matrix support in sandy cobble conglomerate of the GS Frm	43
18. Sandstone interbeds in sandy cobble conglomerate of the GS Frm	43
19. Grain-supported bed in the sandy cobble conglomerate of the GS Frm	44

List of Figures, Continued

FIGURE	PAGE
20. (a&b) Clast imbrication in matrix-supported sandy cobble congl.	45
21. Measured section from sandy cobble conglomerate in the GS Frm	46
22. Cobbles protruding from sandy cobble congl. into sandstone lens	47
23. Measured section from fluvial-related facies in the Golden Spike Frm	49
24. Schematic diagram of sed. structures in Golden Spike float slab 1F	51
25. Schematic diagram of sed. structures in Golden Spike float slab 1E	52
26. Measured section including megaconglomerate facies of the GS Frm	55
27. Styles of grading in sub-aerial, debris-flow conglomerate	61
28. Comparison of sediment movement by various flow mechanisms	63
29. (a&b) Imbricate clasts in modern debris-flow conglomerate	64
30. Clast in GS megaconglomerate offset along structural joint	66
31. Clast in GS megaconglomerate deformed during deposition	66
32. Illustrated explanation of lithologic percentages from clast counts	70
33. Provenance analysis of the upper-middle Carten Creek Frm	73
34. Provenance analysis of the lower Golden Spike Formation	75
35. Implied tectonic setting during deposition of the GS Formation	77
36. Compositional comparison of GS fluvial sandstone & "Moby Dick" clast	80
37. (a) Table of lithologic percentages from Golden Spike clast counts	82
(b) Graph of lithologic percentages related to GS clast dimensions	83

List of Figures, Continued

FIGURE		PAGE
38.	Environmental setting of upper-middle Carten Creek deposition	86
39.	Paleocurrent directions of the upper-middle Carten Creek Formation	87
40.	Environmental setting of initial GS deposition - "basal congl. unit"	91
41.	Paleocurrent directions of the lower Golden Spike Formation	92
42.	Fluvial deposits overlain by megaconglomerate in the GS Formation	94
43.	Environmental setting of GS megaconglomerate deposition	95
44.	Environmental setting of deposition succeeding GS Megaconglomerate	97
45.	Compositional comparison of Carten Creek and Virgelle Sandstones	101
46.	Schematic relationship between Carten Creek and Virgelle deposition	103
47.	Generalized cross-section of a foreland basin system	105

Introduction

Acknowledgments

Funding for this research primarily came from a Geological Society of America grant and McDonough scholarship. Drs. Marc Hendrix and Jim Sears provided additional financial support through their MONTS grant entitled "Constraints on the role of the Lewis and Clark Line during the Upper Cretaceous partitioning of the Northern Rocky Mountain foreland, western Montana: a combined structural and sedimentary basin analysis approach." UM Faculty, UM Travel, and AAPG Student Research (1997) awards also defrayed expenses.

Personal thanks go, of course, first to my family and close friends. This starving graduate student greatly appreciated your collective love, encouragement, and care packages. Immense gratitude goes to the following for field and lab assistance: Flint (my malamute), Ben Webb, Josh Goodman, Nancy Army, Lorin Amidon, Mary Alex Brooks, Shonna Rudolf, Derek Sjostrom, and Chris Greytak. Marc Hendrix's guidance and editing helped me bridge the gap between student and professional. Jim Sears' humor and enthusiasm for fieldwork constantly reminded me of why we are in this business, and Dave Alt served as a reality check to all the academia madness. Kelin Whipple offered great insight into debris flows by email. The Dutton, Rippingale, and

Hiesterman families thankfully granted access to their properties. Lastly to all those whom I neglected to mention, I am glad you were there.

Purpose

Sedimentologic and stratigraphic analyses of late Cretaceous sedimentation in western Montana are limited immediately south of the Lewis and Clark line. Previous research efforts apparently avoided the region due to structural overprinting and lack of biostratigraphic indicators. This thesis is an attempt to provide new detailed sedimentologic and stratigraphic data that better define the environmental and regional interpretations of the upper Carten Creek and lower Golden Spike formations. As part of a larger project, analysis of these synorogenic formations will better constrain the inception of late Cretaceous structural deformation within the Cordillera. Specifically, this research considers the role of the Lewis and Clark line in the evolution of western Montana's foreland basin system.

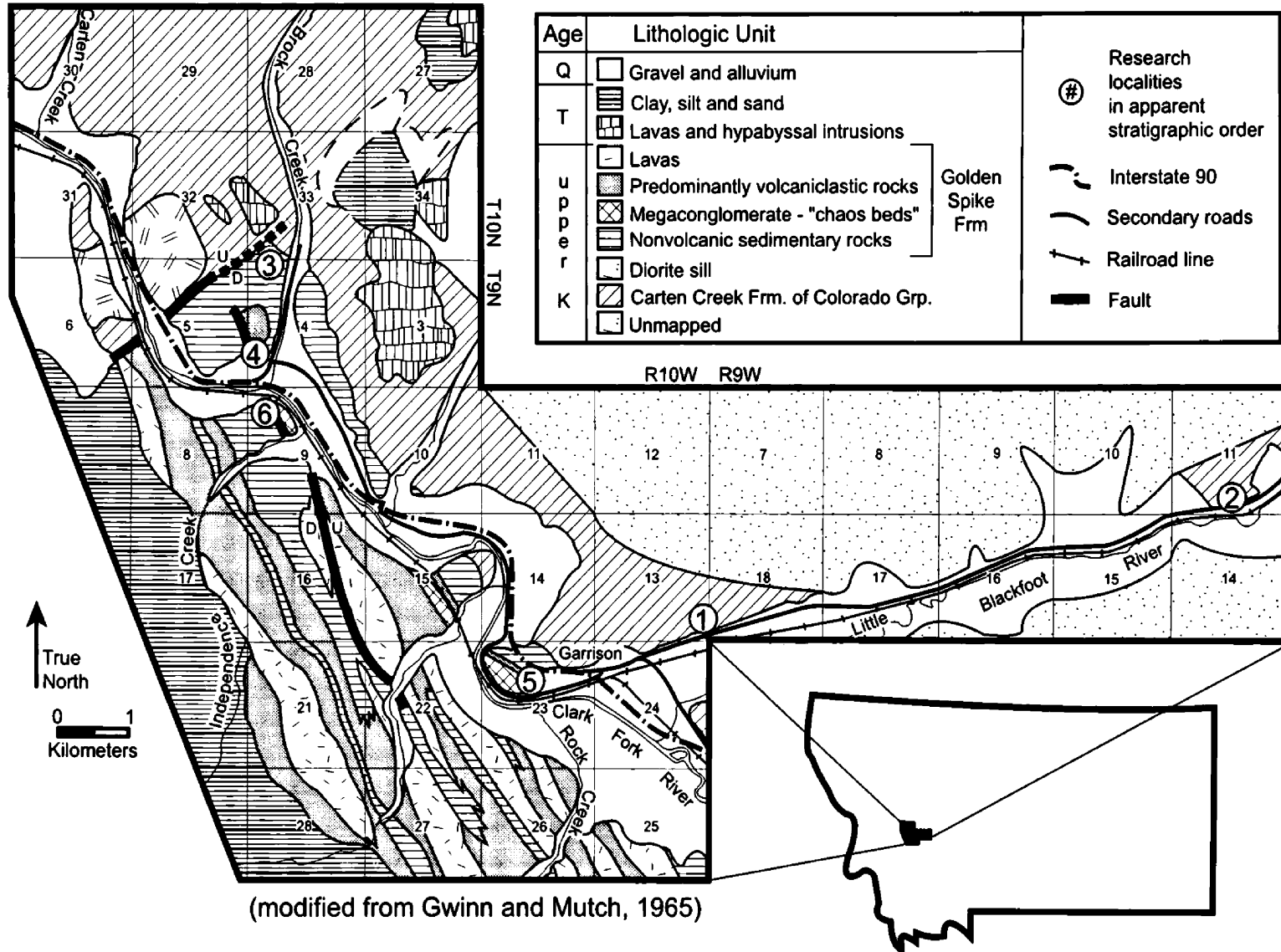
Location

The Coniacian to Campanian Carten Creek and Campanian-Maastrichtian Golden Spike formations outcrop around Garrison, MT (Powell County), approximately 70 miles southeast of Missoula. Analyzed exposures primarily occur in T9N-R10W, but two localities outcrop in section 33 of T10N-

R10W and section 11 of T9N-R9W (Figure 1). South-facing roadcuts of the upper-middle Carten Creek Formation, localities 1 and 2, respectively occur ~0.6 and 9.2km east of Garrison along State Highway 12 in the Little Blackfoot River valley.

The lower Golden Spike Formation generally outcrops along road and railroad-cuts that are easily accessible off Interstate 90 in the Clark Fork River valley. Southeast and east-facing outcrops of basal nonvolcanic strata occur along Brock Creek at ~0.3 (Locality 3) and 1.5km (Locality 4) north of the Phosphate Exit. An impressive southwest-facing outcrop of the megaconglomerate facies occurs ~1.2km west of town-center along Garrison's Frontage Road (Locality 5). The quarried, southeast hillside of locality 5, presently used as a junkyard, exposes interbedded volcanic and nonvolcanic strata. Locality 6, ~0.5km southeast of the Phosphate Exit and 0.3km northwest of Independence Creek, comprises a northeast-facing railroad-cut of sandy cobble conglomerate overlying the megaconglomerate facies. Additional exposures of sandy cobble conglomerate occur along the southeast hillside of locality 6.

Figure 1: Geologic Map of and Research Localities in Garrison, Montana and vicinity



Regional Geology

Introduction

The late Mesozoic collision between the North American and Farallon plates formed a north-south trending Cordilleran fold and thrust belt. Thrusting in western North America shortened the craton in excess of 100 kilometers (DeCelles and Mitra, 1995; Pang and Nummedal, 1995). Crustal deformation resulting from compression included Cretaceous Sevier-style ("thin-skinned") thrusting and late Cretaceous to early Tertiary Laramide-style ("thick-skinned") basement uplift (Dickinson et al., 1988). Eastward propagation of thrust plates resulted in an 800 to 1,650km wide foreland basin that extended from the Arctic to the Gulf of Mexico (Figure 2) (Jordan, 1981; Weimer, 1984; Schwartz and DeCelles, 1988; Pang and Nummedal, 1995). Uplift along the western margin acted as the dominant sediment source of the late Cretaceous foreland basin (Weimer, 1984).

According to stratigraphic and radiometric data, thrust movement related to the Sevier Orogeny in western Montana began about 100 Ma during the late Albian Age (Ruppel et al., 1981). Beginning in Campanian time, eruptions from the Elkhorn Mountain Volcanics, located east of the orogenic front in central-western Montana, supplied andesitic lava flows and volcanoclastic debris to the basin (Figure 3) (Gwinn, 1965; and Mutch, 1965; Wilson, 1970; Ruppel et al., 1981; Mackie, 1986). Repetitive shifts in deposition, from east to west, reflect

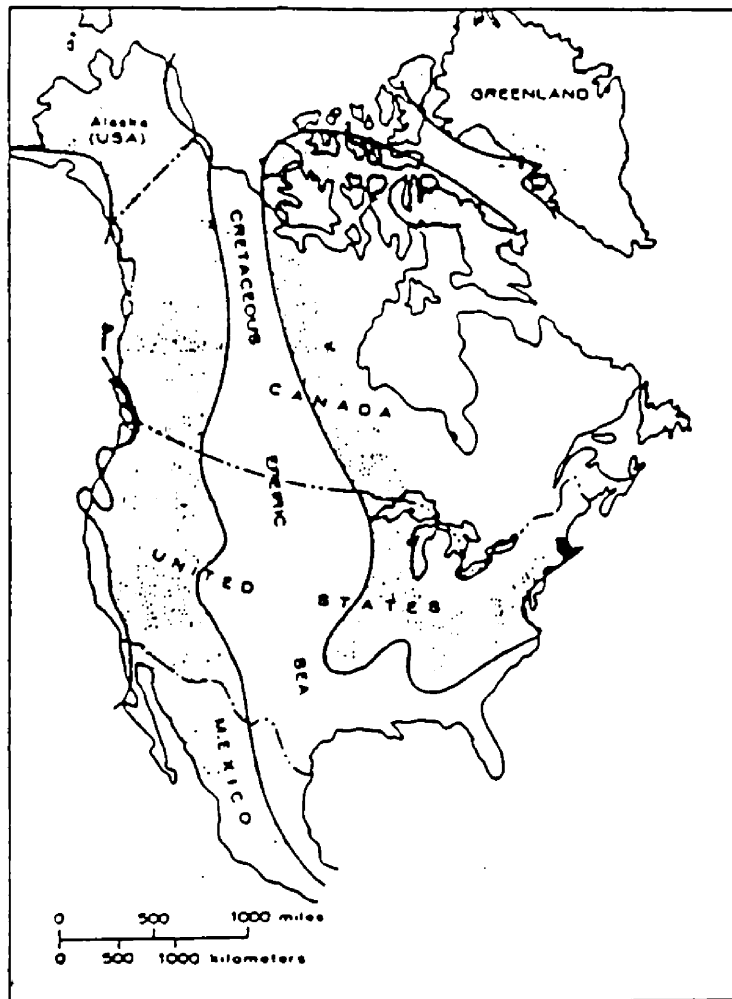


Figure 2: Paleogeographic map of late Cretaceous North America

(from Gill and Cobban, 1966 in Rice, 1980)

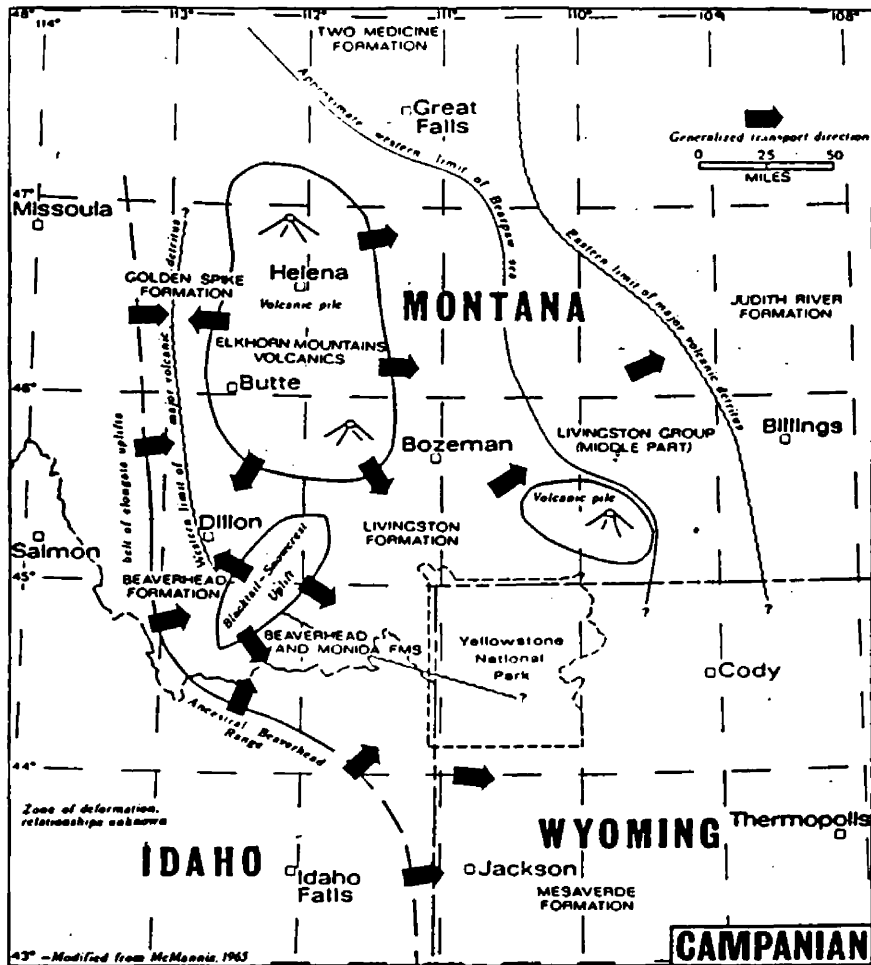


Figure 3: Regional pattern of Campanian deformation, volcanism and sedimentation in the Northern Rocky Mountains. (from Wilson, 1970)

late Cretaceous interplay between sources of sediment and subsidence rates (Gwinn, 1965).

Lewis and Clark Line

Slanting across the Idaho-Montana Cordillera, the Lewis and Clark Line (LCL) forms a shear boundary between two major thrust slabs that underwent differential movement (Wallace, 1990; Sears, 1988; 1994; Sears et al., in review). The LCL extends ~400km from near Wallace, ID to east of Helena, MT with a varying width of 30 to 50km, respectively (Ross et al., 1955; Sears, 1988; Sears et al., in review; Wallace, 1990). An *en echelon* set of southeast-plunging anticlines and synclines occur along the northeastern edge of the LCL and reflect shallow flexural slip levels (Gwinn, 1965; Mackie, 1986; Sears et al., in review). This folding, extending from Drummond to Helena (Ross et al., 1955), suggests that northeast-southwest compression accompanied crustal shear during the fragmentation of the Cordillera.

Two fundamentally different interpretive models have been suggested for the LCL (Figure 4), historically known as the Montana Lineament. Wallace et al. (1990) suggested that the LCL is a broad dextral shear zone created by differential shortening between the northern and southern regions. Sears (1988, 1994; Sears et al., in review) suggested that the LCL is a major Cretaceous transpressional shear zone related to clockwise thrust plate

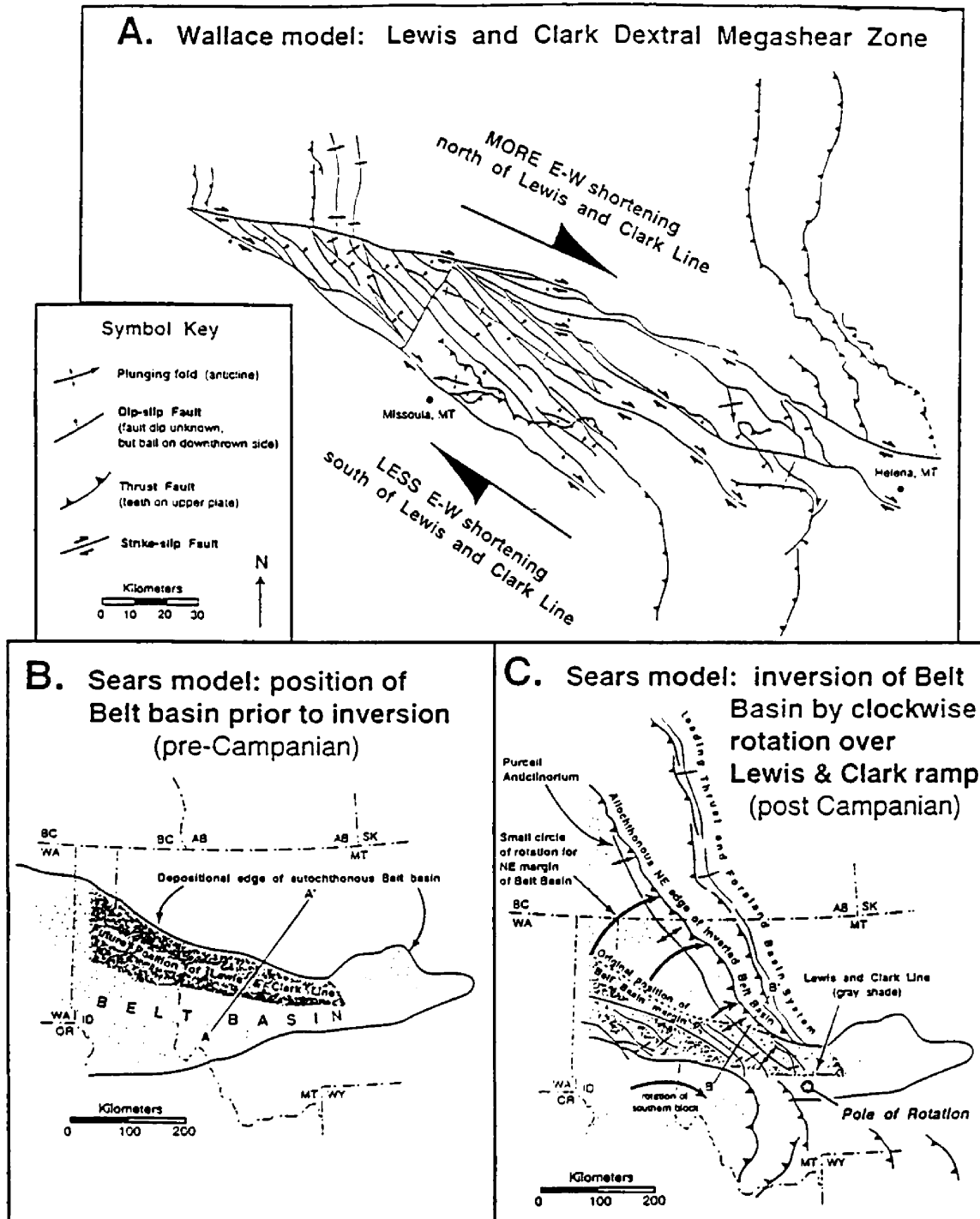


Figure 4: Schematic illustration of the opposing structural models for Lewis and Clark Line development. **4a:** Model by Wallace et al. (1990) suggesting that the LCL accommodates dextral shear between north and south sections of the fold-thrust belt. **4b&c:** Sears' (1988; 1994) model relating the LCL to 25-30° clockwise rotation of the inverted Belt Basin during late Cretaceous thrusting.

rotation. His model proposed that, from Campanian to Paleocene time, the southern thrust slab experienced sinistral shear against the northern plate. Sears et al. (in review) interpret dextral movement along faults of the LCL as post-Paleocene tectonic overprinting.

The rotational model (Sears et al., in review) suggests that compression along the LCL caused shallower strata to fold and deeper material to plastically flow upward into a “flower structure” (after Sylvester, 1988). In addition, Sears (1988; 1994) contends that the Belt Basin was thrust northeast over a southwest facing structural ramp that underlies the LCL at depth. This implies that the LCL delineates the restored northeastern boundary of the Belt Basin.

Partitioned Cordillera

Late Cretaceous uplift along the LCL fragmented the Idaho-Montana Cordillera into northern and southern thrust zones (Wallace, 1990; Sears, 1988; 1994; Sears et al., in review). North of the LCL, the Lewis-Eldorado-Hoadley thrust plate formed the Disturbed Belt, an arcuate region of closely spaced thrust faults and folds (Sears, 1988; 1994; Sears et al., in review). South of the LCL, the Sapphire Tectonic Block and subsequent Lombard-Elkhorn thrust plate comprised the Overthrust Belt (Ruppel et al., 1981; Schwartz and DeCelles, 1988; Sears, 1988; 1994; Sears et al., in review). My research concentrates on Santonian to Campanian sedimentation south of the LCL and east of the Sapphire plate (Figure 5).

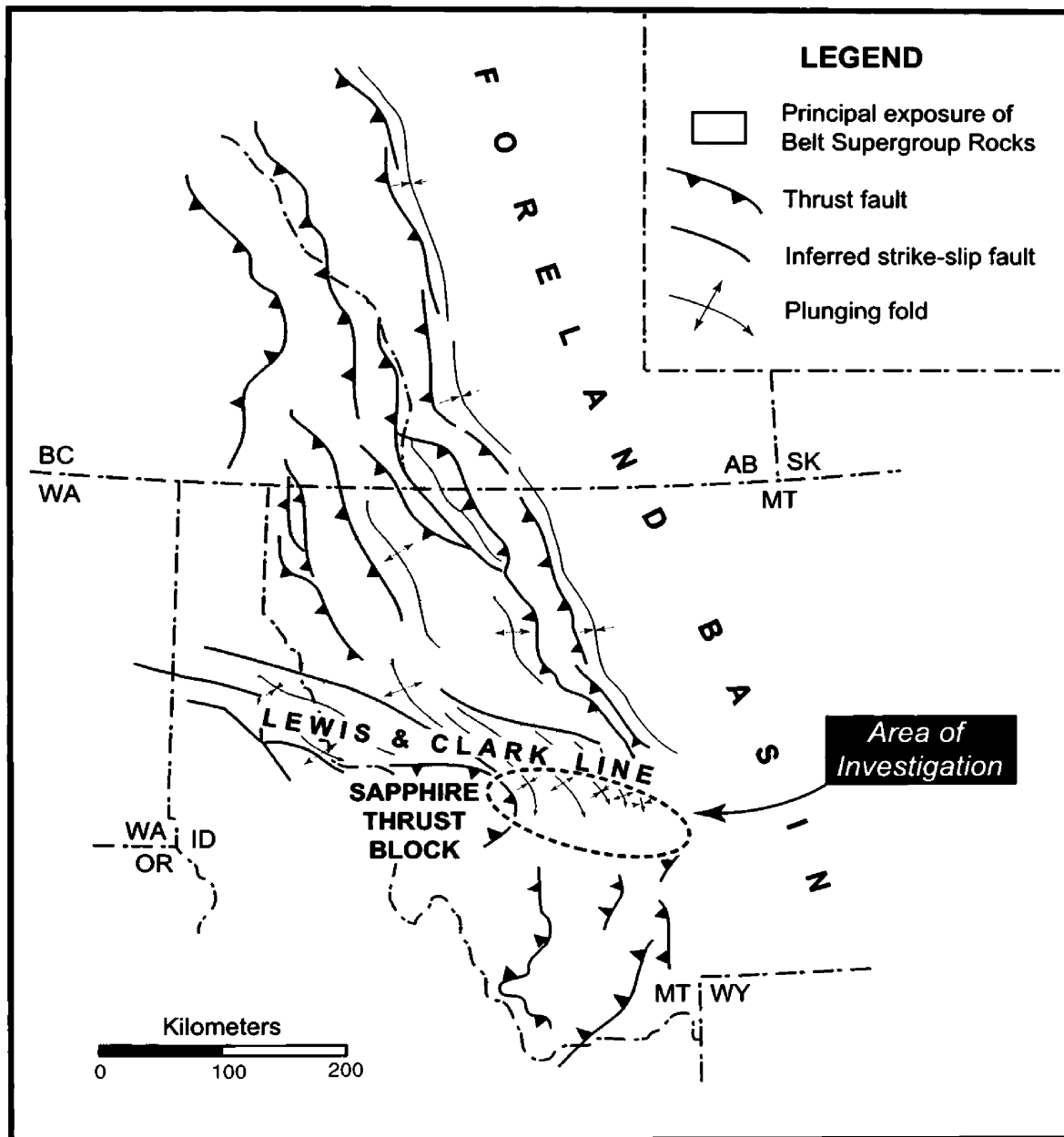


Figure 5: Regional location of the Lewis and Clark Line, Sapphire Thrust Block and research area in the Northern Rocky Mountain foreland basin.

The Garnet and Flint Creek Ranges define the northern and eastern crumpled boundaries of the Sapphire thrust plate, respectively (Figure 6). Both ranges contain tight folds and intrusions of granitic magma that presumably moved east along thrust faults (Ruppel et al., 1981; Alt and Hyndman, 1986). Garnet Range thrusting in the east began sometime after 88Ma, yet ceased in the west before ~82Ma (Ruppel et al., 1981). A granodiorite pluton in the western Garnet Range, known as the Garnet Stock (~82-79 Ma), cut thrust faults and intruded into a syncline along the LCL.

The 15 to 21km thick Sapphire Block apparently slid east off the rising Idaho batholith and emplaced during the late Cretaceous time (Hyndman, 1977; 1979; Ruppel et al., 1981). According to Ruppel et al. (1981), the lower member of the Elkhorn Mountain Volcanics (80-83Ma) and intrusion of the Boulder Batholith (74-80Ma) constrain the age of thrust faulting in the Lombard-Elkhorn thrust zone. However, Robinson et al. (1968) demonstrated that the main period of Lombard-Elkhorn thrusting involved the Elkhorn Mountain Volcanics and occurred between 76Ma and the late Eocene. Regardless, Ruppel et al. (1981) contended that emplacement of the Lombard-Elkhorn plate was coeval with movement on the eastern part of the Sapphire plate.

The LCL has a history of subsidence and sedimentation from the Proterozoic to recent times and is presumably a Precambrian zone of weakness (Peterson, 1981; Winston, 1986). The Sapphire Tectonic Block, Garnet Range, Flint Creek Range and Elkhorn Mountain Volcanics induced

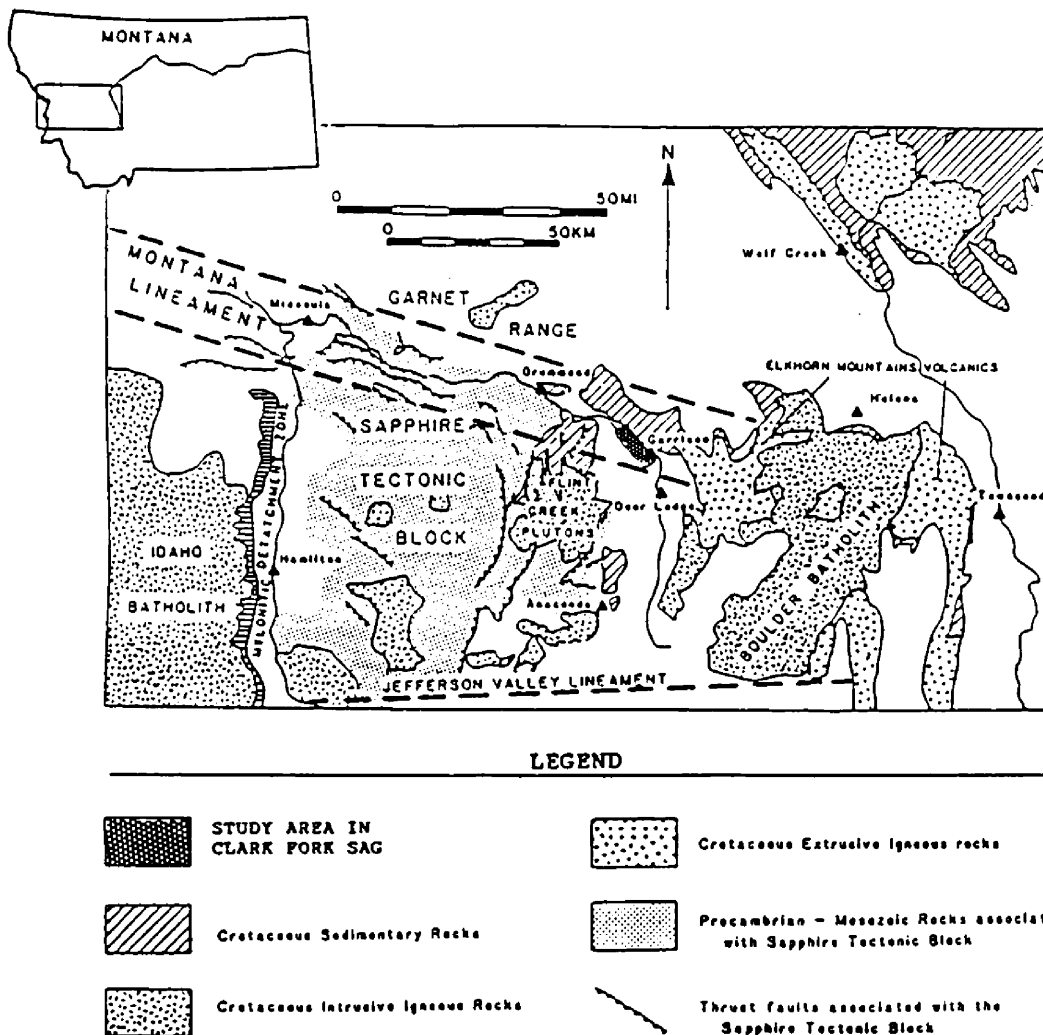
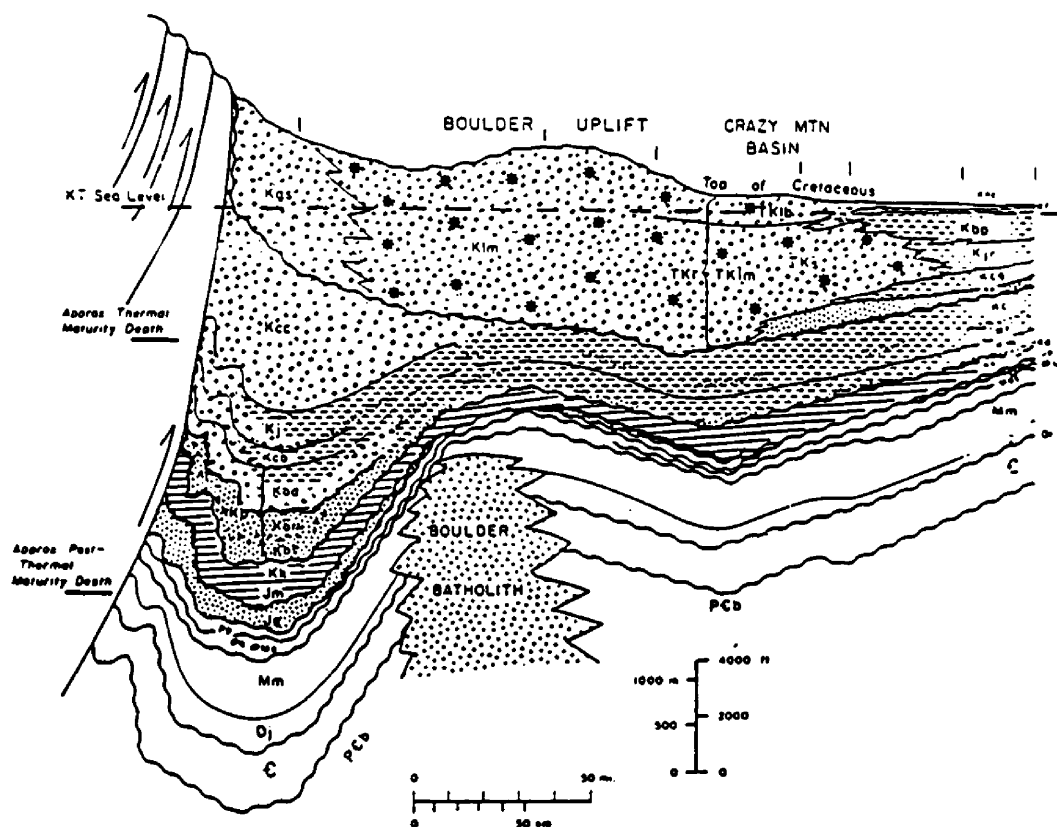


Figure 6: Tectonic map of central-western Montana that includes the location of Clark Fork Sag study area and its relationship to the surrounding Sapphire Tectonic Block, Garnet Range, Flint Creek Range and Elkhorn Mountain Volcanics. (modified from Hyndman, 1977 and Mackie, 1986)

localized subsidence along the LCL during late Cretaceous time (Gwinn, 1961 in 1965). The depression, known as the Clark Fork Sag, crosses folding trends of the Garnet and Flint Creek ranges (Figure 6) (Gwinn, 1965; Mackie, 1986).

Foreland Sedimentation

Cretaceous deposits preserved in Montana form a westward thickening clastic wedge as a result of foreland subsidence. Near Garrison, the Campanian Golden Spike Formation overlies 10,360 meters of Precambrian and Phanerozoic deposits (Figure 7) (Gwinn, 1960 in Mackie, 1986; Peterson, 1981). The southwestern flank of the N45°W trending Garrison anticline accommodates about 5,880 meters of Cretaceous strata (Gwinn, 1965). Montana's thickest Cretaceous sequence, approximately 6,240 meters, lies between Drummond and Garrison (Gwinn, 1960 in Mackie, 1986; Gwinn, 1965). However, it is uncertain if structural repetition south of the LCL affects the thickness of the Cretaceous sequence. In comparison, the thickness of the Cretaceous sequence preserved near Wolf Creek, east-northeast of the LCL in the Disturbed Belt, is 2,940 meters (Schmidt, 1963 in Gwinn, 1965).



Legend

Tklb--Billman Crk Frm	Kf--Frontier Frm	Pennsylvanian:
TKl -- Livingston Frm	Kbp--Bearpaw Shale	q--Quadrant Frm
TKIm--Maudlow Frm	Kjr--Judith River Frm	a--Amsden Frm
TKs--Sedan Frm	Kco--Cody Shale	Mo--Otter Frm
Kem--Elkhorn Mtn Volcanics	Ke--Eagle Sandstone	Mm--Madison Frm
Kgs--Golden Spike Frm	Kc--Colorado Shale	Dj--Jefferson Frm
Kcc--Carten Crk Frm	Kl--Lenep Sandstone	Cambrian (inclusive):
Kj--Jens Frm	Km--Montana Group	Pilgrim Limestone
Kcb--Coberly Frm	Kd--Dakota Frm	Park Shale
Kbd--Dunkelberg Frm	Jm--Morrison Frm	Meagher Limestone
Kb--Blackleaf Frm	Je--Ellis Group	Wolsey Shale
Kk--Kootenai Frm	Pp--Phosphoria Frm	Flathead Sandstone
Khc--Hell Crk Frm		PCb--Belt Supergroup

Figure 7: Palinspastically restored west to east cross-section of lithofacies in central Montana. (from Peterson, 1981)

Previous Investigations

Age and Correlation

The southwest limb of the Garrison anticline, related apparently to late Cretaceous - early Tertiary compression along the LCL, exposes both Carten Creek and Golden Spike strata (Mackie, 1986). W. A. Cobban (in Wallace, 1990) concluded an 88Ma basal age for the Carten Creek based on Coniacian mollusks. Upsection, the formation lacks sufficient biostratigraphic data for age determination (Gwinn, 1965; Wallace, 1990). However, the overlying Golden Spike restricts the Carten Creek's upper boundary age to, at youngest, early Campanian (Wallace, 1990). Andesitic volcanics within the Golden Spike correlate with the 80 to 83 Ma lower member of the Elkhorn Mountain Volcanics (Gwinn and Mutch, 1965; Ruppel et al., 1981; Mackie, 1986). Mackie's (1986) identification of the freshwater ostracod, Staringia, supports Golden Spike deposition extending into the Maastrichtian Age.

Numerous synorogenic conglomerates, of approximate age to the Golden Spike, outcrop along the entire length of the Rocky Mountain thrust belt (Figure 8) (Wilson, 1970; Ruppel et al., 1981; Mackie, 1986). In Montana, sedimentary units that are time-correlative with the Golden Spike include the southwestern Beaverhead Conglomerate, north-central Two Medicine Formation and central Livingston Group (Figure 3) (Gwinn, 1965; Gwinn and Mutch, 1965; Wilson, 1970; Ruppel et al., 1981; Mackie, 1986; Wallace, 1990;

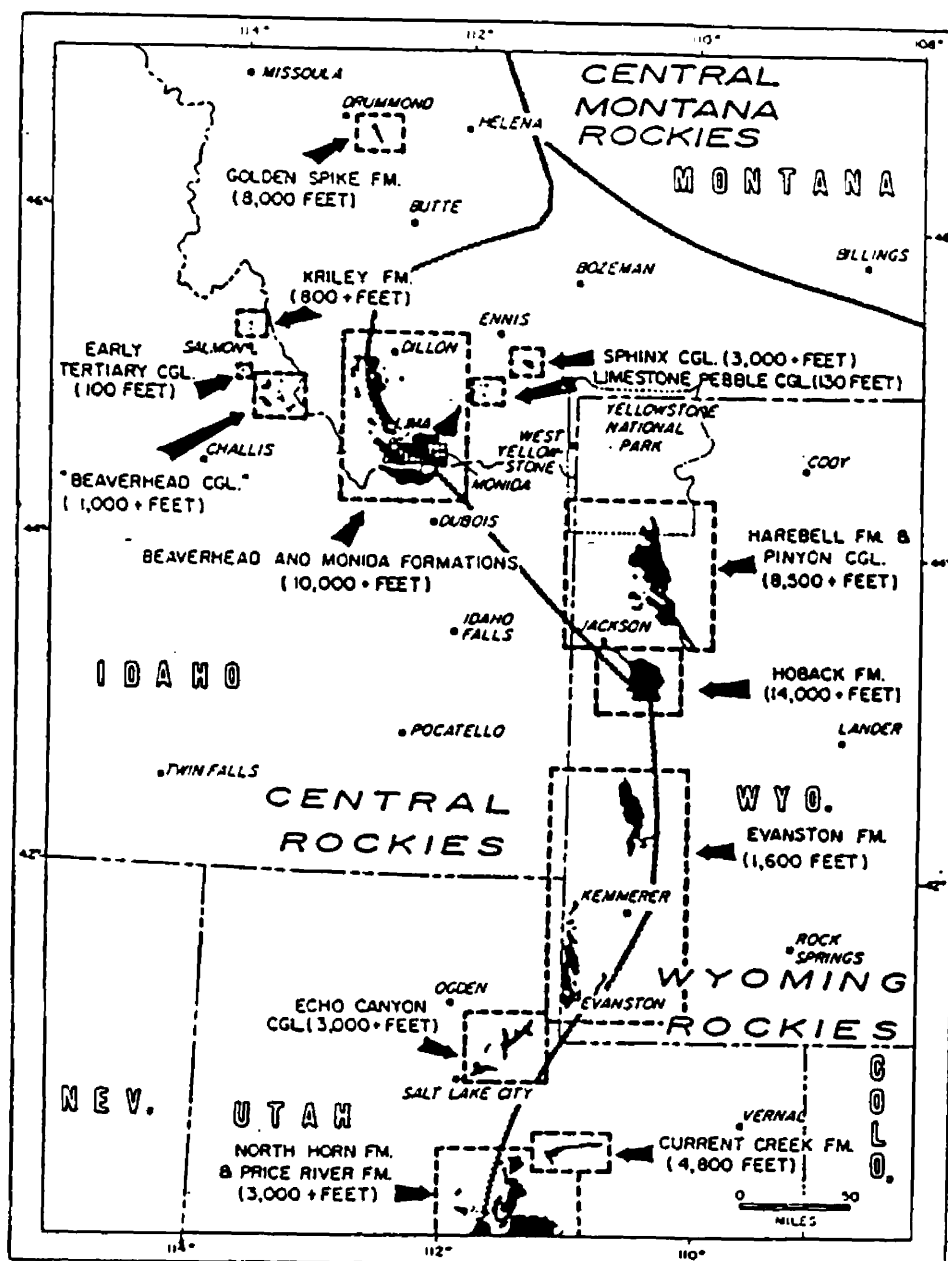


Figure 8: Upper Cretaceous and Paleocene synorogenic conglomerates distributed along the Rocky Mountain fold-thrust belt -- maximum unit thickness recorded in parentheses. (from Wilson, 1970)

Sears et al., in review). Local exposures of the Carten Creek and Golden Spike formations only exist east of the Sapphire Block and south of the LCL (Gwinn, 1965).

Carten Creek Formation

Gwinn (1965) referred to an 1,820m section of the Colorado Group, overlying the Turonian-Coniacian Jens Formation, as the Carter Creek Formation. However, the type locality lies ~1.6km east of Carten Creek (T10N-R10W) near Goldcreek, MT. Subsequent publications initiated a change in nomenclature to the more appropriate Carten Creek Formation (Ruppel et al., 1981; Wallace et al., 1990; Sears et al., in review).

Gwinn (1965) described the base of the Carten Creek as ~90m of planar laminated to low-angle cross-stratified sandstone thinly interbedded with shale. The basal sandstone contains brackish molluscan fauna that includes: Cardium cf. C. pauperculum, Volviceramus involutus, Pleuriocardia, Cymbophora arenaria, Tellina(?), Corbula, Scaphites and Placenticerus benningi (Gwinn, 1965; W. A. Cobban in Wallace, 1990). Brackish water fauna locally occur in the succeeding 1,200m section of green, gray, and tan sandstone, siltstone, shale and mudstone. Siliceous-rich sandstone, siltstone and mudstone interbed within this medial section above 273 meters. Dacite-andesite pebble conglomerate lenses occur in the upper medial section. Reddish gray, greenish gray and gray to buff sandy mudstone and siltstone

form the remaining 530m of the Carten Creek Formation. However in eastern outcrops of the upper Carten Creek, red beds are rare and brackish fauna sections are again common.

The Carten Creek Formation, composed of brackish and local freshwater deposits, signifies the final regression of the Cretaceous Sea from central-western Montana (Gwinn, 1965). Gwinn (1965) interpreted the basal mollusk-bearing deposits as nearshore marine and varicolored beds as terrestrial in origin. Repetitive brackish and fresh water deposits suggest the vacillation of depositional environments (Gwinn, 1965).

Golden Spike Formation

In 1883, the east and west ends of the Northern Pacific Railroad line joined near the mouth of Independence Creek, in section 9 of T9N-R10W, south of the Clark Fork River. The driving of a golden spike commemorated the transcontinental connection. The Golden Spike Formation is named after this historic event (Figure 9) (Gwinn and Mutch, 1965).

Northeast trending high-angle faults, presumably related to localized extension along the LCL, form the northwest and southeast boundaries of the 16km long Golden Spike Formation (Gwinn and Mutch, 1965; Mackie, 1986). Gwinn and Mutch (1965) first described the Campanian Golden Spike as interfingering nonvolcanic and volcanic deposits that thicken from west to east,

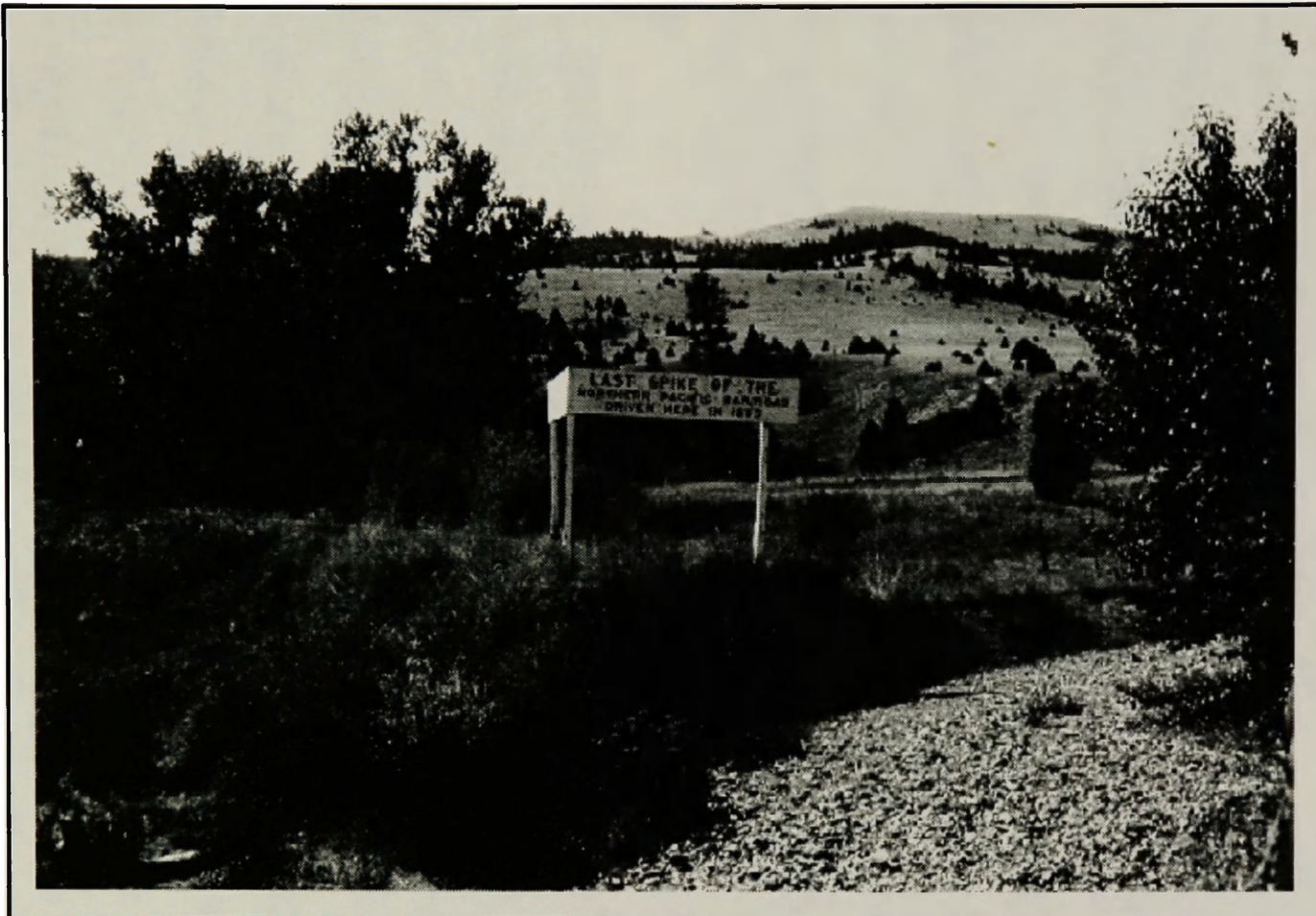


Figure 9: The Golden Spike Formation is named after the gold spike used to commemorate the 1883 joining of the eastern and western ends of the Northern Pacific rail-line. The type section (Gwinn and Mutch, 1965) is not far from Independence Creek where the historic event took place.

1,210 to 2,425m respectively (Figure 10). Paleocurrent indicators, variations in composition, and unit thickness indicate the Golden Spike Formation had multiple sediment sources (Gwinn and Mutch, 1965; Mackie, 1986). Primary source areas were the Sapphire Block and the Elkhorn Mountain Volcanics. The Sapphire thrust plate formed the western depositional margin of and provided nonvolcanic sediment to the Golden Spike (Gwinn, 1965; Gwinn and Mutch, 1965; Mackie, 1986; Waddell and Webb, 1997). The Elkhorn Mountain Volcanics supplied andesitic material from the east (Gwinn and Mutch, 1965; Mackie, 1986). The northwest-southeast trending nonvolcanic deposits collected in the Clark Fork Sag and interfingered with volcanic material flowing from southeast to northwest (Gwinn, 1965; Gwinn and Mutch, 1965; Mackie, 1986).

At its northwest end, the Golden Spike is composed of 97 percent nonvolcanic quartz, quartzite, chert and carbonate rock debris (Gwinn and Mutch, 1965). Nonvolcanic beds pinch out towards the southeast where volcanic-related deposits dominate (Gwinn and Mutch, 1965; Mackie, 1986). Extrusive and brecciated volcanic strata constitute 3% of the formation around Brock Creek, but comprise approximately 60-70%, 4.5km southwest, near Rock Creek (Gwinn, 1965; and Mutch, 1965).

Gwinn and Mutch (1965) identified six stratigraphic units in the Golden Spike Formation (Figure 11): (1) The "basal conglomerate unit" comprises a ~140m section of nonvolcanic pebble conglomerate and chert-rich sandstone

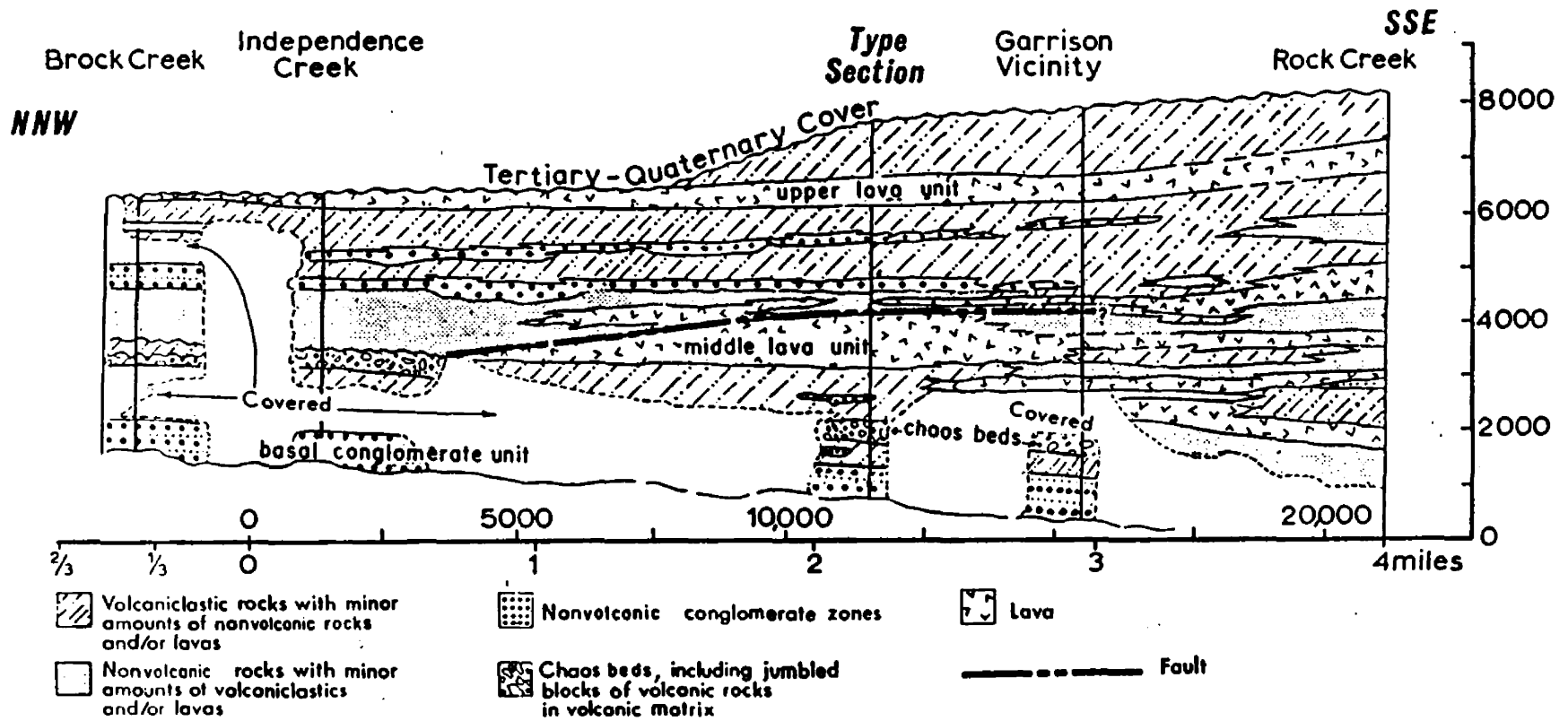


Figure 10: North-northwest to south-southeast cross-section of Golden Spike stratigraphy along strike. Measurement in feet. (from Gwinn and Mutch, 1965)

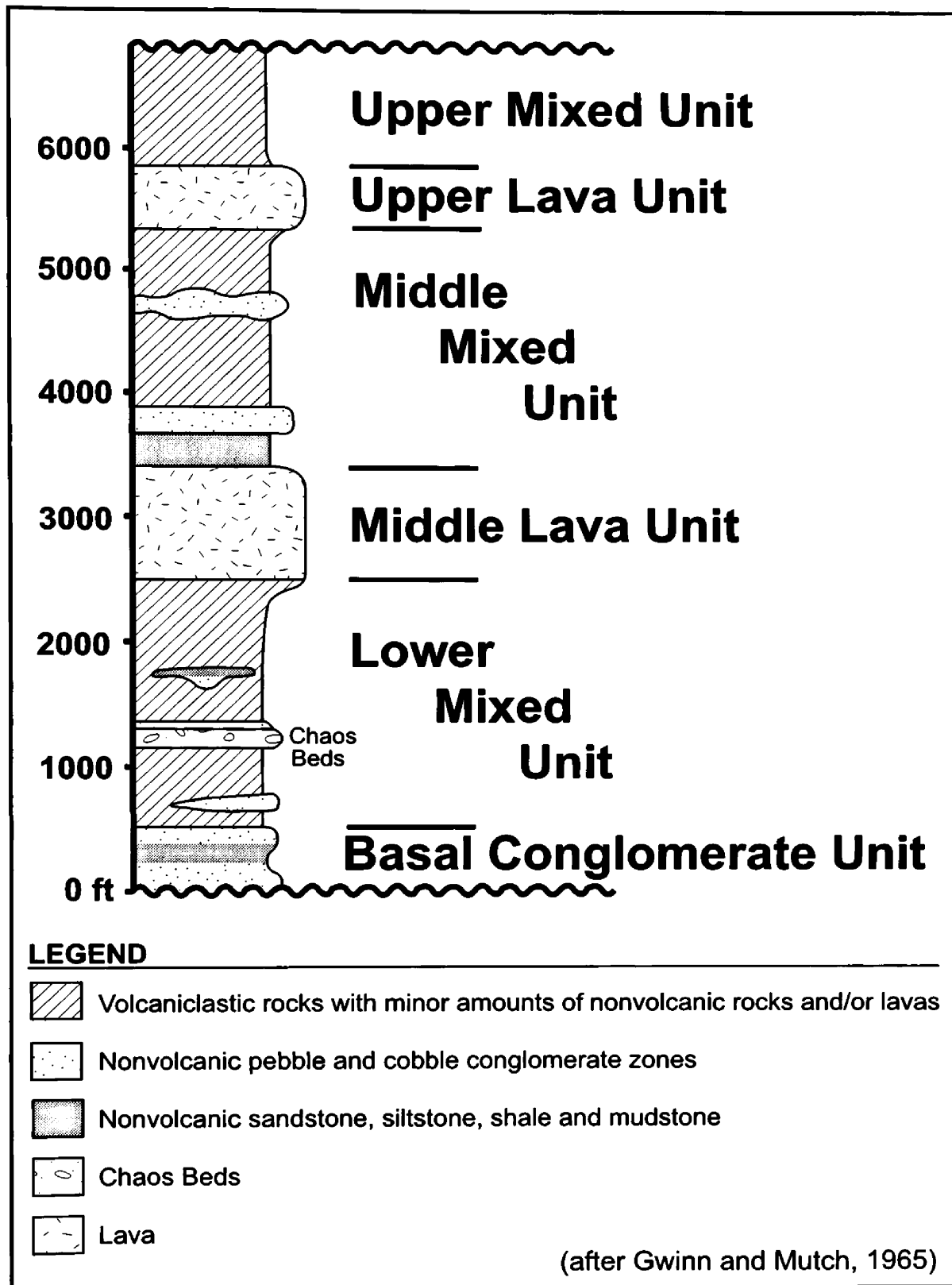


Figure 11: Generalized stratigraphy of the Golden Spike type section.

that vertically interbed with siltstone and mudstone. Two to four thick cobble conglomerate intervals also occur within this basal unit. (2) A thick amalgamation of volcanoclastic and nonvolcanic deposits characterize the ~635m "lower mixed unit". Poorly indurated megaconglomerate, known as the "chaos beds", occurs 150 to 210m above the unit's base. The "chaos beds" subunit is an unsorted mixture of nonvolcanic and volcanic, pebble to boulder sized detritus in a fine grained volcanoclastic matrix. A few thin lava flows and isolated stromatolitic algal limestone deposits also occur within the "lower mixed unit". (3) The ~275m thick "middle lava unit" contains aphanitic and porphyritic-aphanitic andesite flows that locally interbed with autoclastic flow breccias. Lava flows contain calcic plagioclase phenocrysts in the more porphyritic sections. Clinopyroxene phenocrysts also occur in Golden Spike volcanic specimens, but are less common. (4) Poorly exposed deposits of the ~580m thick "middle mixed unit" are similar to those of the "lower mixed unit" with few exceptions. Interbedded nonvolcanic, volcanoclastic, and lava flows typify this unit. Nonvolcanic cobble conglomerate, thicker volcanic breccias, and one crystalline tuff occur higher in the section. The "chaos beds" megaconglomerate does not recur in the "middle mixed unit". (5) The "upper lava unit" is an ~160m thick section of at least three aphanitic andesite flows that locally appear porphyritic. Volcanoclastic deposits also interbed with lava flows in this unit. (6) The final 285m, of the Golden Spike Formation, is a poorly exposed repetitive sequence of nonvolcanic and volcanic interbeds, known as the "upper mixed unit". Nonvolcanic lithologies include sandstone, siltstone,

and mudstone. However, volcanoclastic breccia, sandstone, siltstone, and mudstone apparently dominate the unit. Several porphyritic andesite flows and thin welded tuffs also occur high in the section.

Gwinn and Mutch (1965) noted that only a small percentage of the volcanic rocks in the Golden Spike appeared pyroclastic in origin. Most volcanoclastic material is matrix-rich and presumably deposited through mudslides, landslides, and water (Gwinn, 1965; and Mutch, 1965). Gwinn and Mutch (1965) interpreted the megaconglomerate "chaos beds" as a single large-scale landslide, possibly induced by a seismic shock, that resulted from Elkhorn Mountain volcanism. Mackie (1986) proposed that a hot lahar, or volcanic-debris flow, deposited the megaconglomerate in a single layer.

Nonvolcanic deposits tend to be better sorted and more distinctly bedded than the volcanic rocks, yet display extreme textural and compositional immaturity (Gwinn and Mutch, 1965; Mackie, 1986). Previous interpretations of nonvolcanic facies include braided stream and meandering river deposits on an eastern-sloping, piedmont-valley flat complex (Gwinn, 1965; Gwinn and Mutch, 1965; Mackie, 1986). The intermittent silt and shale layers of this formation are presumed to be overbank deposits as they also grade laterally into river channel deposits (Gwinn and Mutch, 1965).

Methods of Study

Facies Analysis

Both the Carten Creek and Golden Spike formations tend to outcrop poorly. The few, well-exposed sections that exhibited the least amount of structural overprint were utilized for sedimentologic and stratigraphic analysis. Favorable sections were measured at submeter resolution, while field observations of outcrops not well suited for section measurement were recorded on photomosaics. Locally, trough crossbedding and imbricated clasts supplied paleocurrent data. Designation of lithofacies was based on key assemblages of sedimentary structures and textures in both formations. Facies identification subsequently enabled the interpretation of depositional environments.

Compositional Research

Representative samples of the Carten Creek and Golden Spike formations were selected for thin section analysis either randomly or incrementally at several meter scale within measured-section and photo-mosaic outcrops. Thin sections of the sampled sandstone, pebble conglomerate, and conglomerate-matrix were analyzed for provenance information. Point counting of thin sections followed a modified Gazzi-

Dickinson method (Dickinson, 1970) in which the lithologies of 500 grains were systematically identified. Provenance information for the Golden Spike Formation also comes from the lithologic identification of ≥ 1 cm clasts in two conglomeratic facies. Totally, ten clast counts (CB CC1-6 and SCC CC1-4) were conducted on Golden Spike megaconglomerate and sandy cobble conglomerate.

Due to the nature of conglomerate exposure, sampling for clast counts included two types of procedures: random starting-point and systematic census. Clast counts sampled from random starting-points were conducted on all sandy cobble conglomerate (SCC CC1-3) and one exposure of megaconglomerate (CB CC6). Generally, the megaconglomerate facies (CB CC1-5) underwent systematic sampling that involved taking a census of clasts within a 1x1 meter station. Although stations were marked along base of the megaconglomerate outcrops due to the inherent danger of loose rock, the samples obtained include a variety of lithologies and appear representative of lateral deposits exposed uphill. Depending on station selection, immense clasts could potentially comprise an entire square meter block. Some counts are clast compilations from individual stations in direct contact with one another. For instance, CB CC1 inclusively tabulates a 1x2m block, and CB CC2&3 are censuses of 1x3m blocks.

Due to extreme clast-size variability in Golden Spike conglomerates, both lithology and diameter measurement were recorded in clast counts. Compositional percentages were first calculated based on the total presence

of lithology in count and then recalculated for lithologic population proportional to clast size. However, initial counts (CB CC1-3 and SCC CC4) reported data in only three clast-diameter categories: 1-6cm (small), >6cm-<50cm (medium), and ≥ 50 cm (large). Data from succeeding clast counts included, along with lithology, all long and intermediate clast axes to better represent any volumetric differences. To enable comparison of all clast count results, numeric weights were applied to lithologic totals in the medium and large categories of preliminary counts (CB CC1,2&3 and SCC CC4) relative to the smaller category value. Data from the later, more size-descriptive clast counts was used to set these numeric weights by determining a ratio of area covered by clasts within the three size-factions.

Specifically, clasts from the subsequent counts were arranged by long-axis length into the same small, medium and large size categories initially identified. Since the megaconglomerate facies incorporates pebble to boulder sized clasts, the median-clast length was obtained and computed as median-area in centimeters for each size-faction in CB CC4,5&6. Mean-area in centimeters was calculated for SCC CC1,2&3 from the total clast-coverage of the small and medium categories because extremely large clast sizes do not occur in the sandy cobble conglomerate. Within a count, the areas compiled for each size-faction were converted into a dimensionless ratio with respect to the smallest category -- i.e., the areas of categories 1, 2 and 3 were divided by category 1's area. Ratios that derived from clast counts performed on the same conglomerate facies were then averaged to establish one set of numeric

weights. Ultimately, lithologic totals from the medium and large categories of CB CC1,2&3 were multiplied by 11 and 384, respectively, while the medium size-faction value in SCC CC4 was weighted by 4.

Sedimentology and Stratigraphy

Introduction

Profiles of the Carten Creek and Golden Spike formations include lithofacies descriptions, environmental interpretations, provenance analyses, and a regional synopsis. Lithofacies and environmental discussions reflect data obtained from measured sections (Carten Creek - Figure 12; Golden Spike - Figures 21, 23 and 26) and photomosaics (Carten Creek - Appendix plates 1a-f; Golden Spike - Appendix plates 2, 3, 4a-c, 5 and 6a & b). This study focuses on the upper-middle interval of the Carten Creek Formation and the lower third of the Golden Spike Formation ("basal conglomerate" and "lower mixed" units by Gwinn and Mutch, 1965) as recorders of late Cretaceous foreland basin evolution.

Lithofacies of the Upper-Middle Carten Creek Formation

Coarse - Very Coarse Sandstone with Volcanic-Pebbles






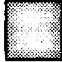




Tan lithic-feldspathic sandstone containing dacite-andesite pebbles characterizes this facies (Locality 1 in Figure 1). Sandstone is coarse to very-coarse grained; grains are moderately sorted and commonly angular to subround. Tabular sandstone beds commonly exhibit large-scale planar

Figure 12 :

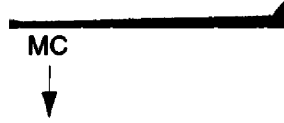
Carten Creek Formation Measured Section - Legend

Scale of stratigraphic column is in meters.

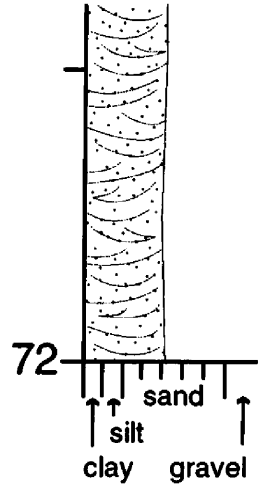
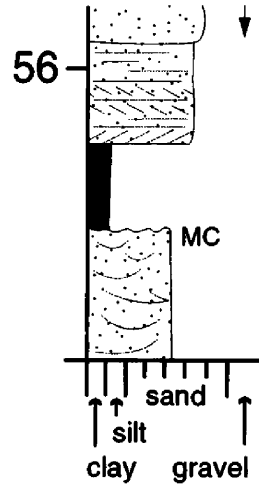
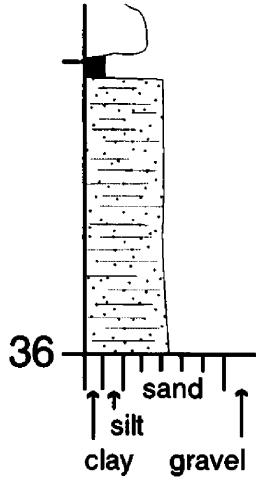
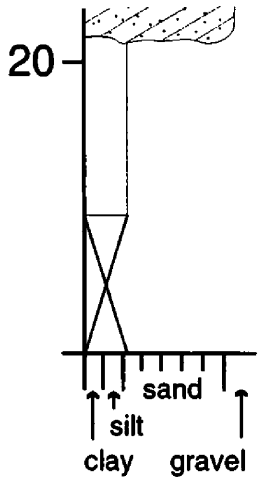
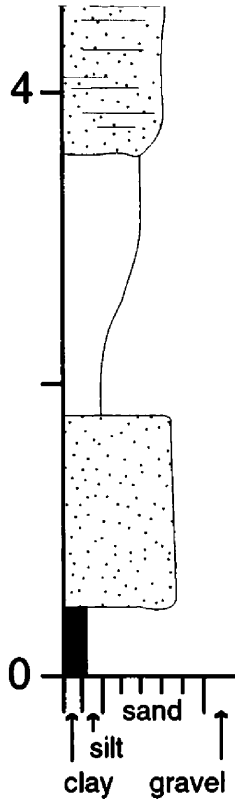
"X" indicates covered zone.

	Tan Sandstone		
	Varied-Color Siltstone to Fine Sandstone		Planar Laminations
	Black/Gray Silty Shale		Trough Crossbeds
	Brown/Red Silty Mudstone		Planar Foresets
VP - Volcanic Pebbles			Trough Crosslaminations
MC - Scattered Silty Mudchips			Planar Crosslaminations
MCC - Silty Mudchip Conglomerate			Convolute Planar Laminations
WF - Scattered, Carbonized Woody Fragments			
CN - Scattered Caliche Nodules			

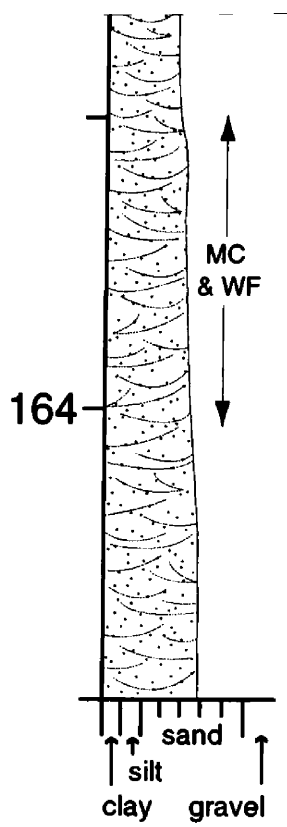
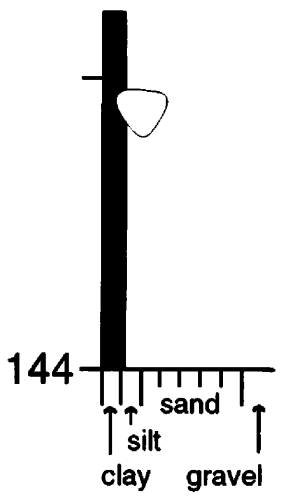
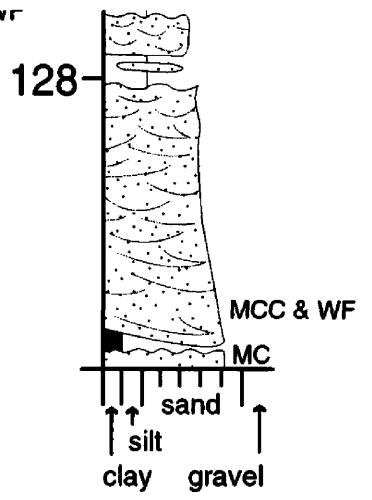
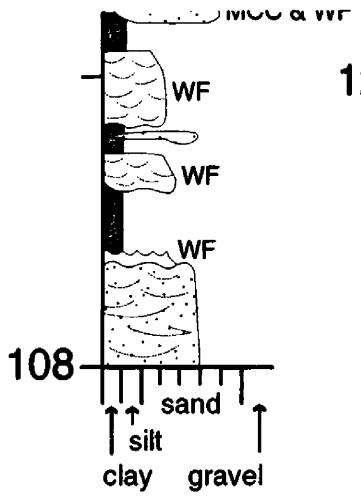
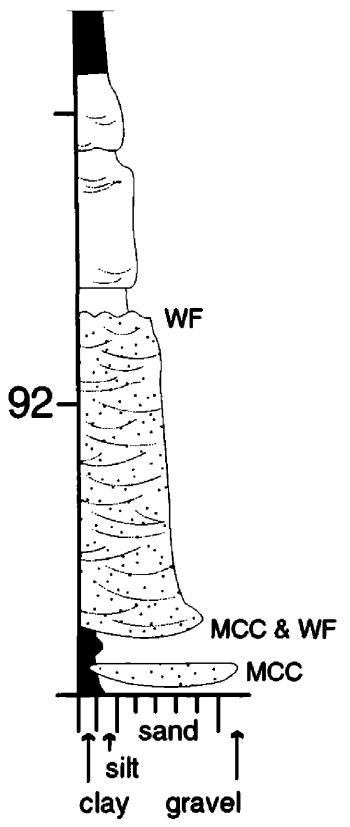
THIS SPACE
FOR
OVERSIZED
IMAGES



Car



THIS SPACE
FOR
OVERSIZED
MAGNET



foresets and local planar laminations. Subround volcanic pebbles and subangular silty mudchips mantle planar foresets and accumulate above denudation surfaces.

Volcanic pebbles are abundant and typically ≤ 2 cm in diameter, but 5-6 cm pebbles are not uncommon. Silty mudchips occur locally and are highly variable in size, ranging between ~0.5 to 15 centimeters. Carbonized wood fragments are rare and similarly vary in size.

Coarse-grained bases generally erode slightly into underlying black shale deposits. The pebbly sandstone of this facies generally grades vertically into a medium to coarse grained sandstone with large-planar foresets, planar laminations, and local trough crossbedding. Black shale also sharply overlies the upper contact of deposits in this facies.

Fine to Very-Coarse Sandstone with Local Mudchip Conglomerate

Tan to white, feldspathic-rich sandstone in this facies contains subround to angular grains and is moderately sorted. Deposits commonly fine upward from coarse to fine grained sandstone, but greenish gray to tan mudchip conglomerate and very-coarse sandstone is present at the base of some beds. Mudchip conglomerate comprises abundant light to dark gray silty-mudchips in a lithic-feldspathic matrix.

Deposits containing abundant large-scale trough crossbedding (Figure 13) comprise the majority of this facies. Locally, medium to very-coarse grained beds contain large-scale planar foresets, planar laminations, and



Figure 13: Large-scale trough crossbedding abundantly occurs in the fine-coarse sandstone facies of the upper-middle Carten Creek Formation (Locality 1). Rock hammer used for scale.



Figure 14: Mudchip-rich sandstone scouring into underlying shale in the Carten Creek Formation (Locality 1). Two large wood particles are outlined to ease observation. Camera lens cap in upper-right of photo provides scale.

sparse dacite-andesite pebbles. In rare exposures, the planar laminations are convoluted and trough topsets are preserved.

Mudchips, particles of carbonized wood, clay drapes, and very-coarse sand grains commonly mantle trough crossbeds, planar foresets, planar laminations, and denudation surfaces. Basal deposits also contain abundant mudchips, wood debris, and local tool marks. Likewise, wood particles and fine mudchips commonly appear in the scour pits of linguoid and sinuous ripples that locally occur on top of trough-crossbedded deposits. The subround to angular mudchips greatly vary in size; most are ≤ 3 cm in diameter, but diameters ≥ 10 cm are not uncommon in conglomerate sections.

Sandstone deposits are tabular to wedge shaped and several to tens of meters wide. Thickness of trough-crossbedded sandstone sections varies notably but apparently does not exceed 9 meters. Beds mainly composed of planar and convoluted laminations range up to ~ 2.5 m thick. Deposits with large-scale planar foresets are ≤ 0.4 m thick and commonly occur near the volcanic-pebble sandstone facies. Locally, mudchip-rich sandstone vertically interbeds with thin (≤ 0.25 cm) layers of dark gray clayey siltstone.

Basal contacts are irregular and commonly erode into the underlying finer grained rock types (Figure 14). This facies either grades upward into siltstone and mudstone or is sharply overlain by black shale (Localities 1 and 2 in Figure 1). Stacked fine to coarse sandstone deposits also occur laterally and vertically.

Massive Siltstone - Fine Sandstone

Greenish tan, greenish gray, and purple siltstone to fine grained sandstone generally characterizes this facies, but tan medium grained deposits also occur locally. Fine sandstone contains subround to angular grains that display moderate sorting. Beds commonly maintain constant grain size or fine upward, but rarely coarsen upward. Intermittent with the shale and mudstone facies, deposits commonly occur as tabular beds and lenses, $\leq 1.2\text{m}$ and $\leq 0.5\text{m}$ thick respectively, although beds occurring in the Carten Creek measured section are locally several meters thick. Other thin ($\leq 0.25\text{m}$) beds of fissile clayey-siltstone locally interfinger with coarser grained rock types.

Typical deposits have an irregular or well-defined scoured base and appear massive. Locally beds contain clay drapes, small and large scale trough crossbeds, basal mudchips, carbonized wood fragments, and/or planar laminations. Rare topsets of trough crossbedding are exposed in outcrop. Rippled bed tops, climbing ripples, convoluted laminations, basal black chert pebbles, and siltstone concretions also appear rarely in this facies.

Massive Silty Shale

Massive silty shale is dark greenish-gray to black, fissile and organic-rich. Beds are generally $\leq 2.5\text{m}$ thick, but shale also occurs as thin drapes on foresets and denudation surfaces. The erosion of shale by overlying coarser-grained deposits resulted in great variation of bed thickness within this facies.

Accordingly, thin beds and lenses of massive siltstone and very fine-fine sandstone occur within thick deposits of shale. Locally, shale beds contain carbonized wood fragments and scattered nodules of dark gray micrite. A rare layer of nodular micrite occurs at ~88m within the Carten Creek's measured section (Figure 12).

Mottled Silty Mudstone

Greenish tan, brownish gray, and reddish brown silty mudstone to clayey siltstone predominate much of the upper Carten Creek Formation (after Gwinn, 1965). Deposits appear locally mottled with red discoloration. Mudstone thickness ranges from several meters to only a decimeter due to the same erosive processes affecting the massive shale facies. Micritic nodules, typically ≤ 2 cm and locally ~5cm in diameter, are common in the mudstone facies.

Lithofacies of the Lower Golden Spike Formation

Matrix-Supported Megaconglomerate Facies

The Golden Spike Formation contains spectacular megaconglomerate that outcrop along the Frontage Road in Garrison, Montana and Interstate 90 at the Phosphate Exit (Localities 5 and 6 in Figure 1). Gwinn and Mutch (1965) first described the poorly sorted, matrix-supported megaconglomerate as the "chaos beds." Stacked megaconglomerate deposits outcrop along a roadside

exposure in Garrison, MT and are approximately 155 meters thick. (Appendix plate 4a-c). Gwinn and Mutch (1965) measured unit thickness of the megaconglomerate along the type-section, ~0.9km northeast of Garrison, to be approximately 62 meters. Thickness of the Garrison exposure may be artificially high due to structural repetition, but is consistent with the overall westward thickening of the Golden Spike Formation.

This lithofacies contains pebble to boulder sized clasts in a fine grained matrix. Matrix texture varies between clay and poorly sorted very-fine sand. Matrix material comprises 75-80% of the megaconglomerate at the base (Garrison Frontage Road Locality) and increases to 85-90% both upsection and westward (South Phosphate Exit Locality - Appendix plate 5).

Clasts range in shape from round to angular, but are dominantly subround. The largest clast ("Moby Dick" - Figure 15) measures 17.2 x 4.4 meters and is likely cannibalized from underlying white sandstone deposits of the Golden Spike. Subangular, red-brown clasts composed of volcanoclastic breccia are approximately 5 to 7 meters in diameter. Large boulder sized and volcanic clasts are more prevalent to the east in deposits along the Garrison Frontage Road than in the south Phosphate Exit exposure.

Although individual beds are difficult to detect within this unit, contacts are observable over short distances. For example, the remnant of a mottled paleosol horizon beneath "Moby Dick" (Figure 16) suggests bedding. Bedding within the Chaos Beds is also evident from several interfingering lava and volcanoclastic flows.



Figure 15: Megaconglomerate of the lower Golden Spike Formation (Locality 5) containing clasts that greatly range in size. The 17m long, white sandstone boulder in center of photo is the largest clast observable in the facies. Dark volcanoclastic boulders are also visible in the photo. People - one man circled - congregating at base of outcrop provide scale.



Figure 16: Mottled mudstone layer beneath large white clast ("Moby Dick") is one of few bedding indicators in the megaconglomerate facies of the lower Golden Spike Formation (Locality 5). Black outline is added to distinguish the remnant paleosol from surrounding matrix-supported conglomerate deposits. Stratigraphic up from right to left side of photo and scale indicated by decimeter increments on staff.

Sandy Cobble Conglomerate Facies

Sandy cobble conglomerate characterizes portions of the lower Golden Spike Formation (Appendix plates 5 and 6a & b). Stacked conglomerate of this facies varies from clast-rich with matrix support to fully grain-supported (Figure 17); matrix support is typically moderate to poor. Tabular and lens shaped deposits of tan sandstone define bedding within the conglomerate deposits (Figure 18).

Clast sizes range from pebble to cobble. In exposures underlying the megaconglomerate deposits (Localities 3 and 4 in Figure 1), clast diameters do not typically exceed 25 centimeters. In deposits directly overlying the Chaos Beds clast diameters are larger but generally less than 40 centimeters (Locality 6 in Figure 1). Clast and sand grain shapes range from subangular to subrounded.

Within the sections of grain-supported conglomerate, imbricated and horizontally oriented clasts are common (Figure 19). Clast imbrication also occurs locally in the matrix-supported conglomerates (Figures 20a&b). Matrix is poorly sorted and composed of very-fine to coarse sand and pebbles.

Vertical grain-size transitions, from conglomerate to overlying sandstone, are both gradational and sharp (Figure 21). Gradational transitions begin with moderately matrix-supported conglomerate that becomes more grain-supported upsection. Grain-supported conglomerate may contain imbricated cobbles and is commonly overlain by pebbly coarse-grained



Figure 17: Sandy cobble conglomerate varying between clast-rich with moderate matrix-support to fully grain supported. Conglomerate near bottom of photo is matrix poor, but matrix-support increases higher in outcrop (Locality 4). Rock hammer for scale.



Figure 18: Bedding in sandy cobble conglomerate of the Golden Spike Formation designated by a lens-shaped interbed of tan sandstone (Locality 3). Part of another sandstone bed is visible in photo at the base of the outcrop. Rock hammer for scale.

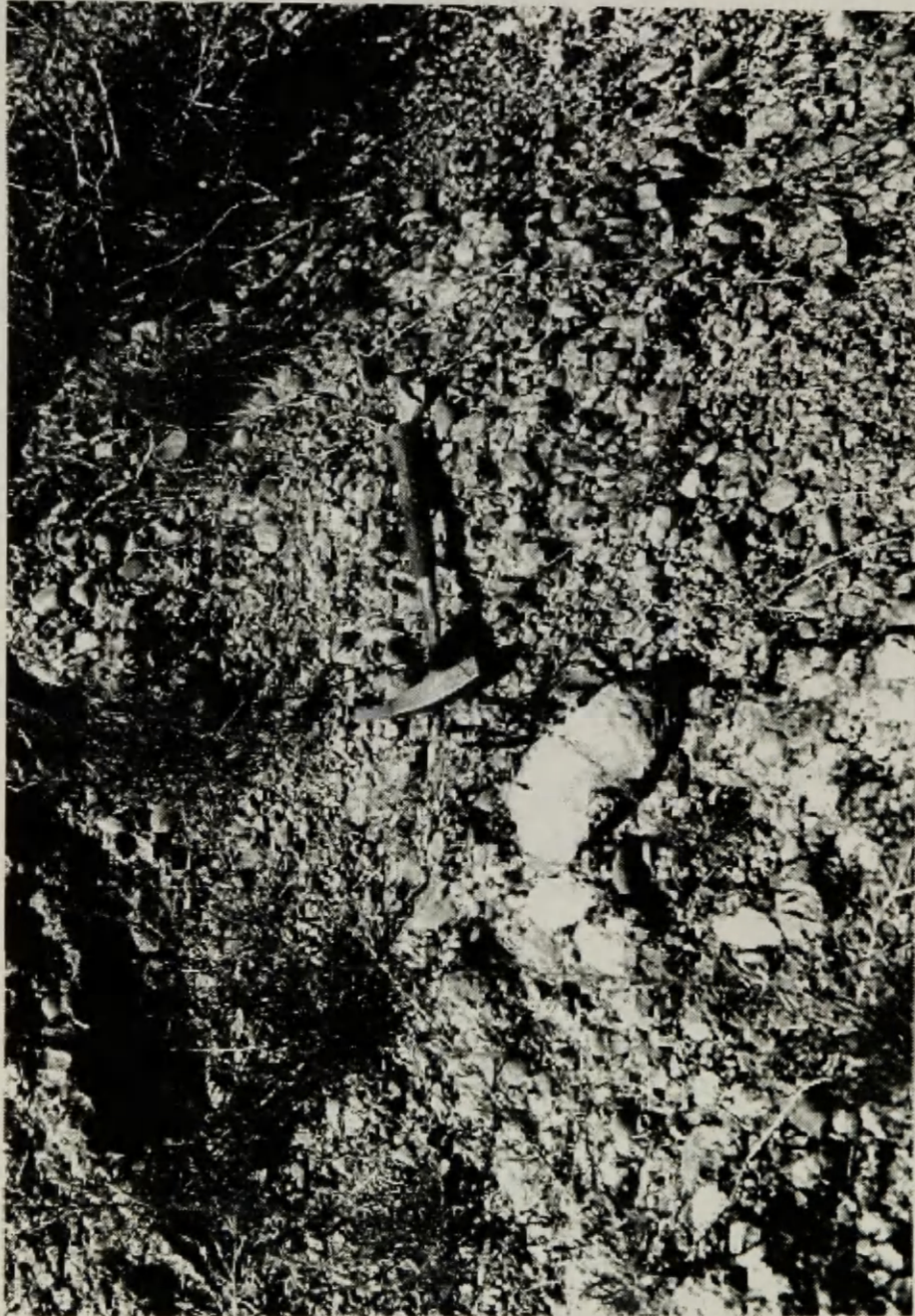


Figure 19: Grain-supported bed within the sandy cobble conglomerate facies of the lower Golden Spike Formation (Locality 4) is more homogeneous in texture than underlying matrix-supported bed (contact dashed). Clast imbrication in grain-supported conglomerate is most apparent in upper-right corner of photo. Rock hammer for scale.

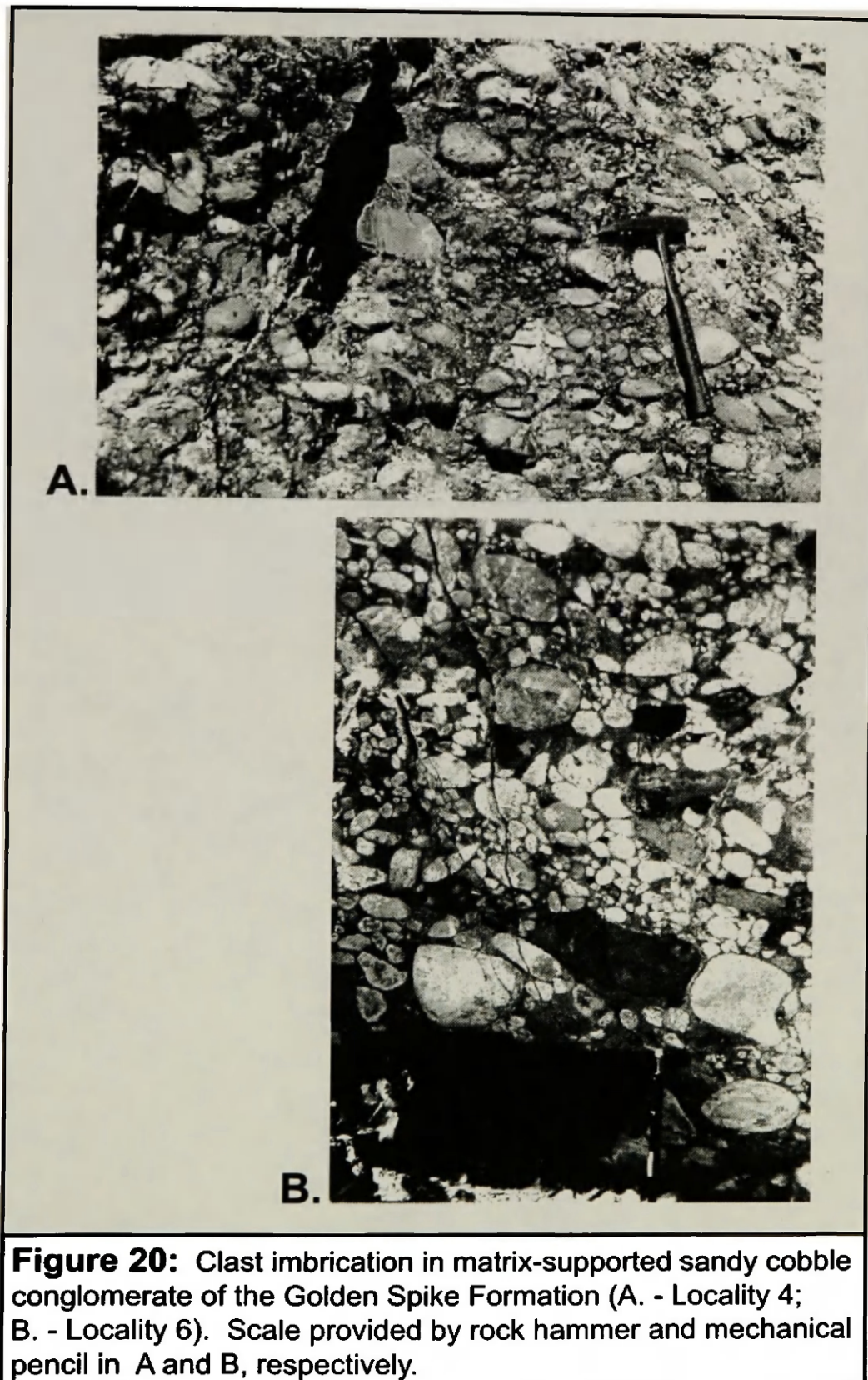


Figure 21:
Golden Spike Formation
Measured Section Involving
Sandy Cobble Conglomerate (SCC) Facies
 Scale of stratigraphic column is in meters.
 "X" indicates covered zone.

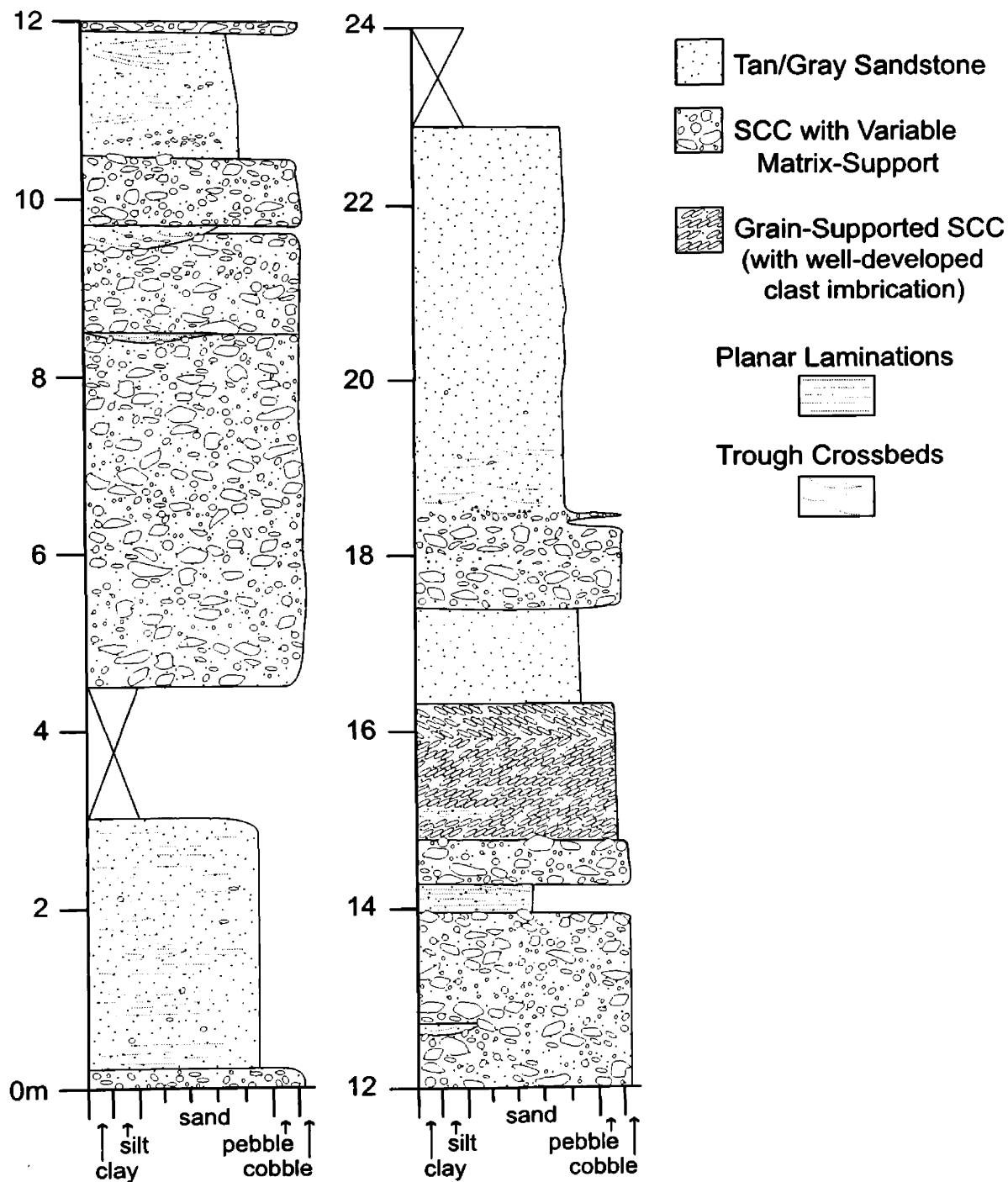




Figure 22: Sandstone lens in sandy cobble conglomerate of the Golden Spike Formation (Locality 6). Cobbles from conglomerate commonly protrude into overlying sandstone lenses and tabular beds. Camera lens cap at bottom-center of photo denotes scale.

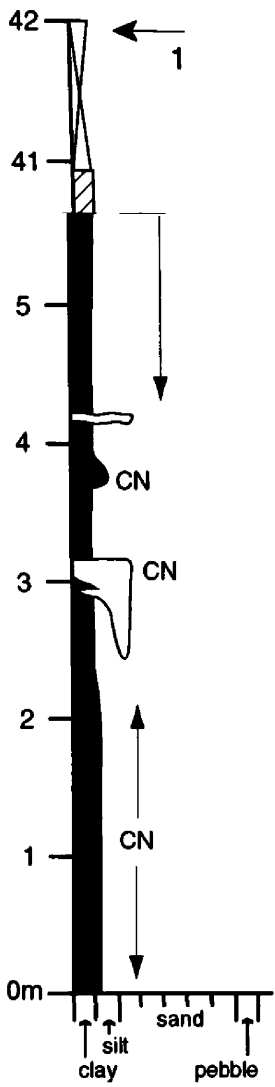
sandstone. Sharp contacts are characterized by moderately matrix-supported conglomerate overlain by decimeter scale beds of medium sandstone with planar laminations or trough crossbedding. Cobbles commonly protrude from underlying conglomerate beds into overlying sandstone deposits (Figure 22).

Clast-Supported Pebble Conglomerate Facies

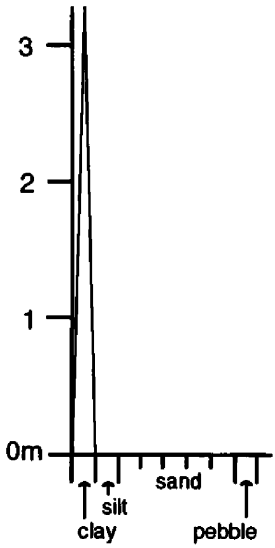
Bluish gray, sublithic conglomerate occurs in broad, shallow scours approximately 10-15m wide and less than 50cm thick (Appendix plates 2 and 3). Conglomerate vertically grades into sandstone, and laterally interfingers with siltstone and shale (Localities 4 and 5 in Figure 1; Figure 23). Grain-support is typical. Pebbles are subround to subangular and generally ≤ 3 cm in diameter. Indurated pebbles commonly deform rip-up mud clasts contained in conglomerate beds. Sorting ranges from moderate to poor. Trough crossbeds and clay drapes occur locally.

Very-Fine to Coarse Grained Sandstone Facies

Sublithic sandstone of this facies comprises subround to angular grains that are moderately sorted. Grain size fines upward from coarse to very-fine within deposits. Medium to very-coarse grained sandstone beds commonly contain trough crossbeds with subround pebbles locally mantling foresets. Finer sandstone beds are generally planar laminated, but may show low-angle trough crossbedding. In general, beds are tabular, broad wedge, and small



THIS SPACE
FOR
OVERSIZED
MASSES



3:

(<1m wide) lens shaped. However, lenticular sandstone deposits are commonly finer grained than the other bed types.

Tan to greenish tan sandstone beds interfinger with the sandy cobble conglomerate facies and exhibit planar laminations and trough crossbeds. Tabular tan sandstone occurring downsection of the megaconglomerate facies is ≤ 1.4 m thick. Similar beds exposed upsection of the megaconglomerate are commonly thin (<40cm). Lens shaped deposits of tan sandstone are typically less than 35cm thick and pinch out in or mantle the top of an underlying sandy cobble conglomerate bed.

Sandstone occurring in gradational contact with the clast-supported pebble conglomerate facies is commonly bluish gray, but locally outcrops white or light gray. Analysis of cut and polished float block slabs indicates planar laminations, trough crossbeds, pebble lags, clay drapes, rip-up mud clasts, and/or fluid escape structures are present in bluish gray sandstone deposits (Figures 24 and 25). Bluish gray sandstone beds are generally laterally continuous at the scale of the outcrop (~10m) and do not exceed 1.5m in thickness.

Massive Siltstone - Very Fine Sandstone Facies

Sublithic shaley-siltstone to silty-sandstone comprises this facies which is commonly associated with bluish-gray sublithic sandstone. Shaley-siltstone locally contains scattered very-fine sand grains. Very-fine sandstone and siltstone grains are subround and moderately sorted. Beds are greenish gray

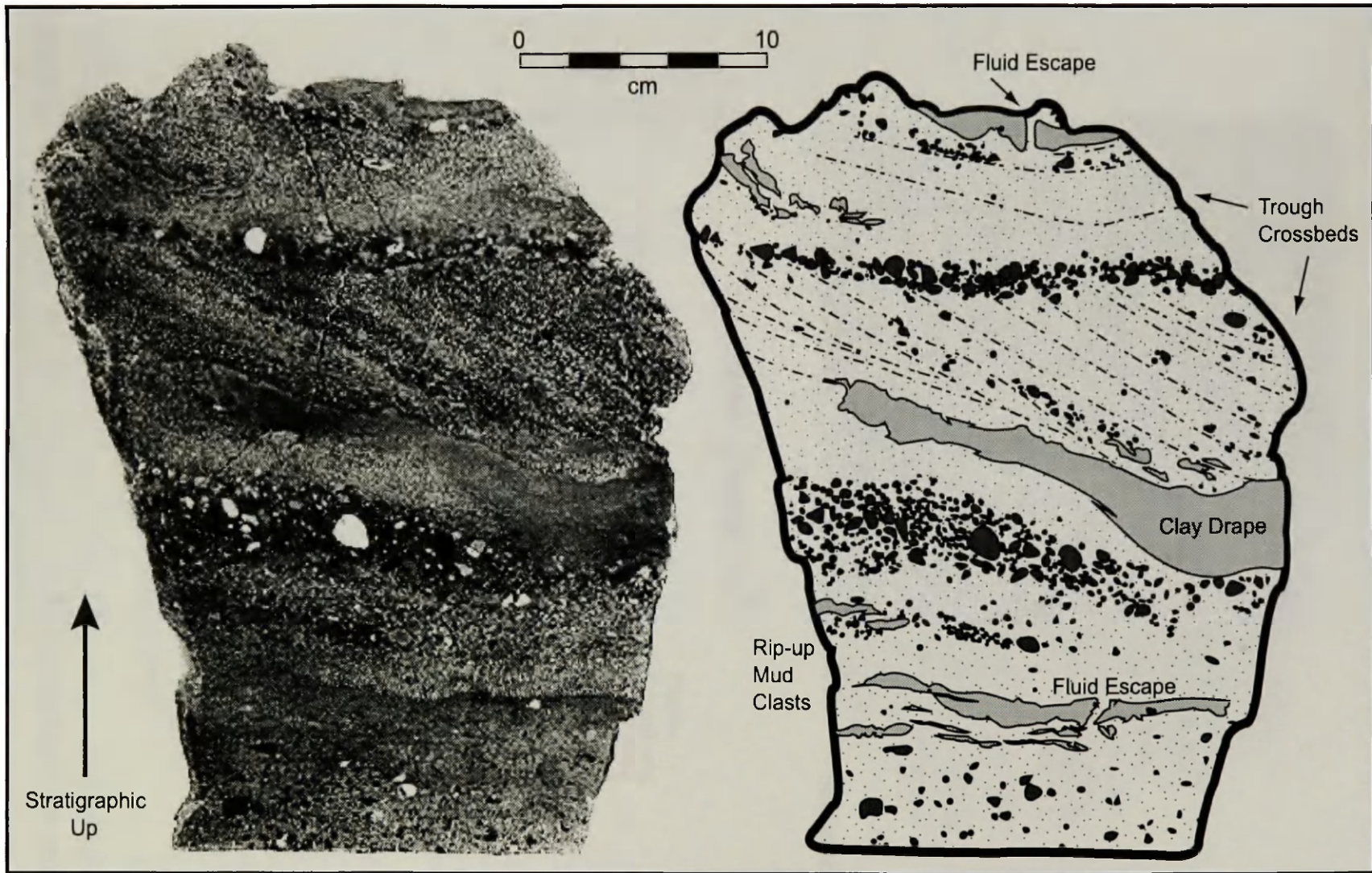


Figure 24: Schematic Diagram of Sedimentary Structures in Float Slab 1F of the Lower Golden Spike Formation

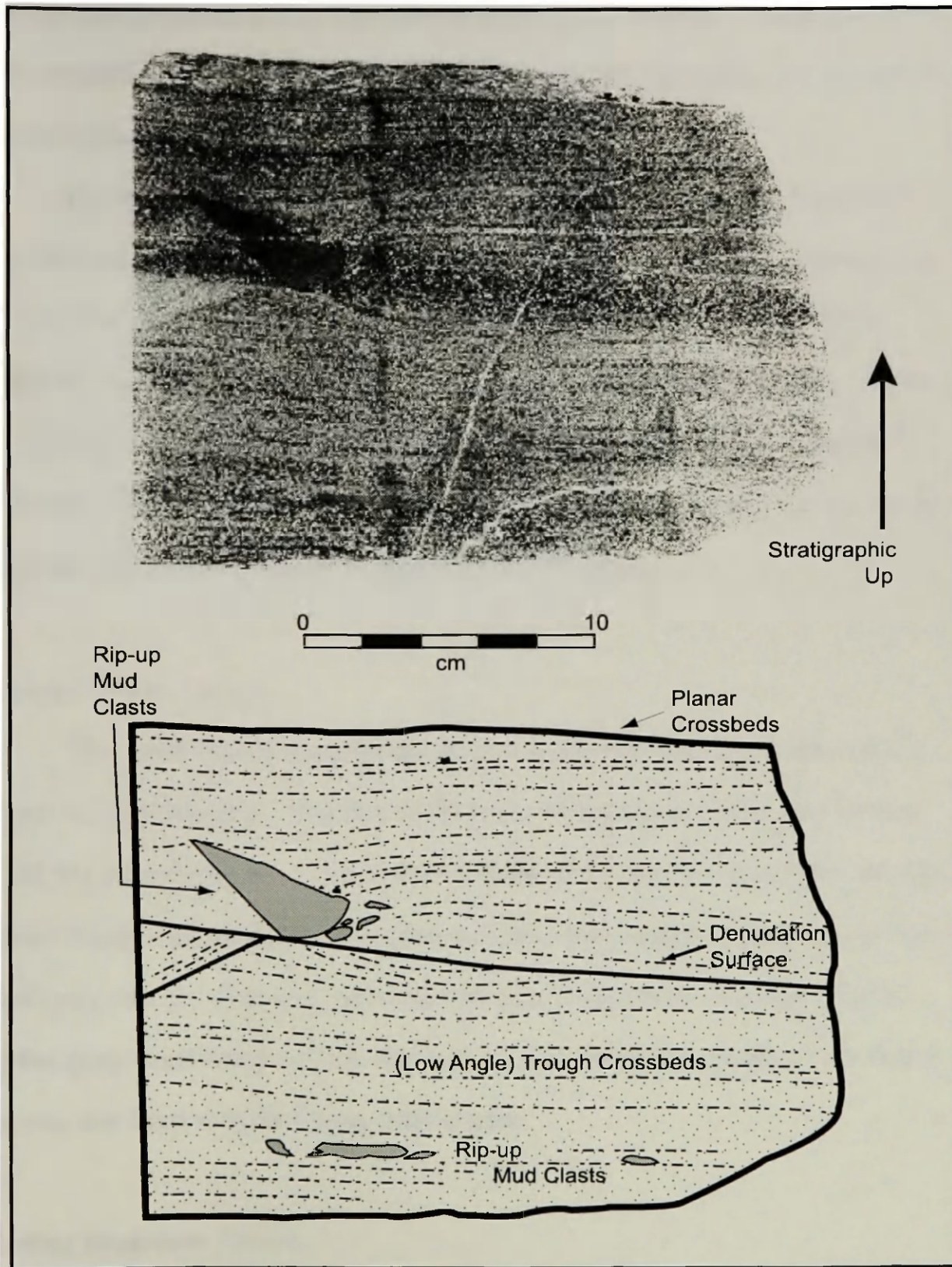


Figure 25: Schematic Diagram of Sedimentary Structures in Float Slab 1E of the Lower Golden Spike Formation

and appear massive due to an opaque weathered coating. Deposits occur in lens shaped or tabular forms with variable thickness that does not exceed 85 centimeters.

Basal contacts can be either erosive or gradational. Some siltstone to very-fine sandstone deposits have irregular bases and scour into underlying shales and mudstones. Erosive sandstone beds locally contain micritic nodules similar to those encased in the surrounding shale deposits. Other deposits in this facies fine upward from the underlying coarser sandstone deposits. Upper contacts of siltstone beds typically grade into mudstone facies and may contain fragments of carbonized plant debris.

Massive Shale Facies

The shale facies is generally gray in color, but may locally be reddish-brown or reddish-gray. Massive shale beds are typically one to two meters thick, but alternating 5 - 10cm beds of shale and greenish-gray siltstone also occur locally. Shale beds commonly contain calcareous nodules composed of dark gray micrite. Nodules, typically 1 to 3cm in diameter, have a white or lighter gray weathering rind on the surface and septarian cracks in the center. Cracks are filled with dark gray calcite spar.

Mottled Mudstone Facies

Mottled green-purple to red silty mudstone deposits are typically associated with the shale and siltstone facies. An erosional remnant of

mottled mudstone occurs beneath the largest clast, nicknamed "Moby Dick", in the megaconglomerate facies (Locality 5 in Figure 1). Beds are typically ≤ 10 cm thick, but may reach 90cm locally. Basal contacts are gradational with underlying siltstone and silty shale. Upper contacts are commonly irregular and appear erosive. Deposits contain numerous calcareous nodules and sparse carbonized wood.

Algal Limestone Facies

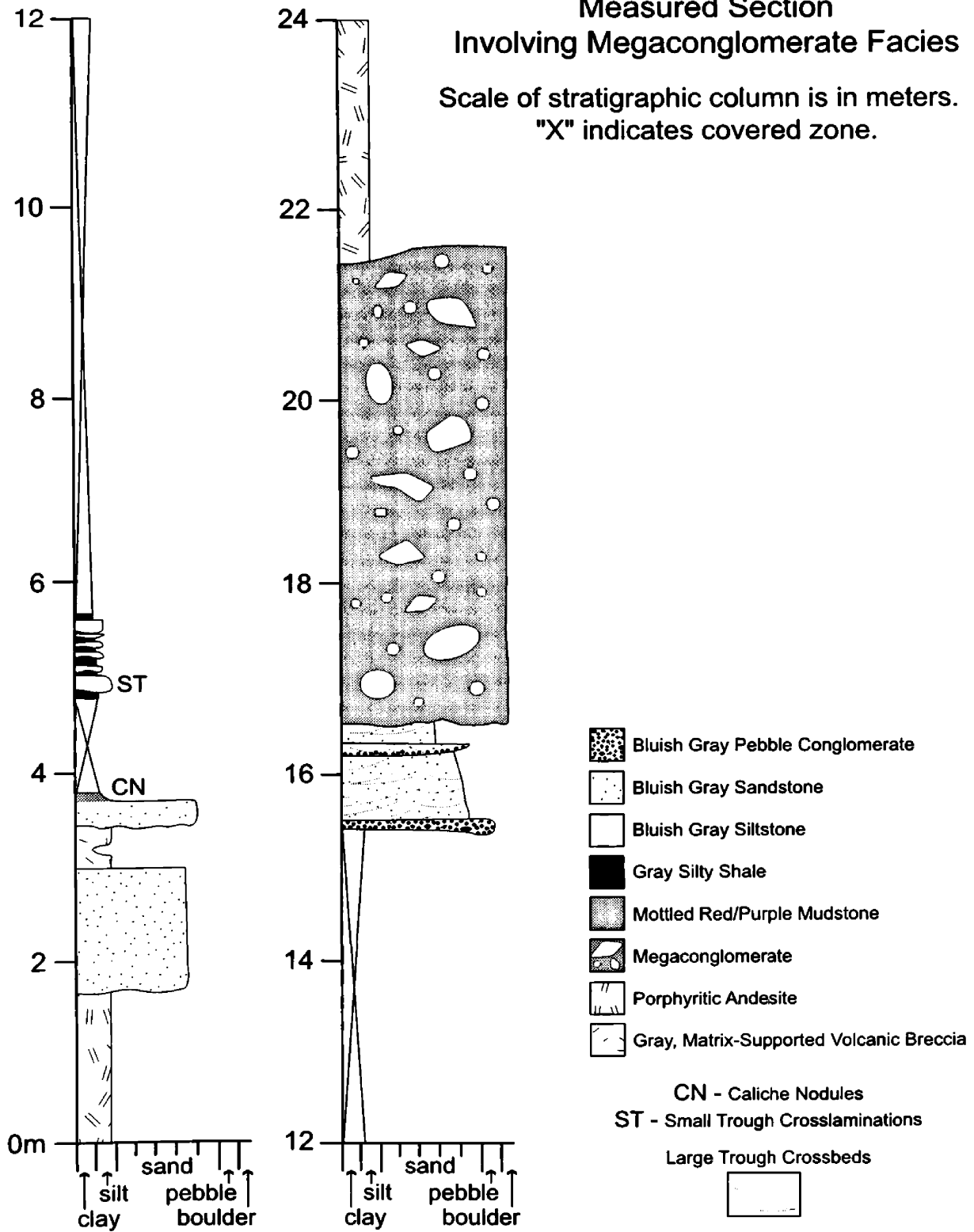
Gwinn and Mutch (1965) described two exposures of algal limestone with ostracod debris in the Golden Spike's "lower mixed unit". One outcrop of light gray, sparry biomicrite is illustrated in Figure 23. Stromatolites within this exposure vary between 2 to 10cm wide and are oval shaped.

Volcanic/Volcaniclastic Facies

Thick (>10 m) volcanic deposits intertongue with the matrix-supported megaconglomerate in Garrison, MT and at the Phosphate Exit localities (Appendix plates 4a-c and 5). Interfingering of volcanic and volcaniclastic material also occurs with other nonvolcanic units underlying the megaconglomerate facies (Figures 23 and 26), but apparently at a lesser (≤ 5 m) scale. Common rock types include porphyritic andesite, autoclastic breccia, and matrix-supported volcaniclastic breccia. Volcanic deposits (typically andesite and welded breccia) contain blocky plagioclase and

Figure 26 : Golden Spike Formation Measured Section Involving Megaconglomerate Facies

Scale of stratigraphic column is in meters.
"X" indicates covered zone.



platy biotite crystals. Plagioclase observed in porphyritic andesite is commonly zoned.

The matrix-supported, volcanoclastic breccia commonly contains euhedral biotite, hornfels chips, zoned plagioclase crystals, and irregularly rounded microcrystalline felsic clasts. Plagioclase crystals appear either resorbed or broken. The subangular-subrounded felsic clasts are inversely graded in one deposit (Figure 23) from 2mm to 20cm. Matrix material of these deposits is clay sized. Beds are generally grayish-green, but may also appear dark gray or reddish brown.

Environmental Interpretation of Lithofacies

Fluvial Deposition

Mudchip-rich sandstone (Carten Creek Formation) and clast-supported pebble conglomerate (Golden Spike Formation) vertically grade into coarse-medium sandstone and represent high-energy thalweg deposits within a channel sequence. Mudchips dispersed in trough-crossbedded channel deposits presumably eroded off banks and levees, although the reworking of clay drapes could also account for many clasts. Lenses of mudchip-rich sandstone may locally represent catastrophic levee breaches in the Carten Creek Formation. Repetitive, upward-fining basal lag and trough-crossbedded deposits in the Carten Creek and Golden Spike formations (Figures 12 and 23) are consistent with the point bar model of meandering rivers (Walker, 1984).

Vertical changes in grain size and sedimentary structures represent velocity gradation within the channel deposits of both formations. Scoured and coarse-grained bases with local tool marks (Carten Creek Formation) suggest current velocity along the channel floor was in the upper flow regime during peak flood time (Walker, 1984; Boggs, 1995). Planar laminations and dune foresets indicate the average discharge velocity was within the upper-lower flow regime (Boggs, 1995). Clay drapes between beds, on foresets, and along denudation surfaces indicate periodic and significant reductions in current flow.

Wood particles and mudchips constitute a significant part of the Carten Creek's bedload. The rare preservation of trough topsets, in channel deposits,

indicates the Carten Creek river system routinely was highly concentrated in sediment (Collinson and Thompson, 1982). Accordingly, local convoluted laminations, related to liquefaction, suggest high rates of sand deposition (Collinson and Thompson, 1982).

Coarser-grained channel units grade upward into siltstone and laterally interfinger with shale and mudstone (Appendix plates 1a-f, 2, and 3). Lateral accretion surfaces, dipping approximately 10 to 15 degrees, imply high-sinuosity in the fluvial system of the Carten Creek Formation. Extensive consumption of the cut-bank, suggested by abundant mudchips, also supports meandering. The Golden Spike fluvial deposits lack lateral accretion surfaces. However, the waning flow velocity, represented by upward fining sequences, suggests low-sinuosity channel migration and bar aggradation occurred in the lower Golden Spike.

Tabular beds of siltstone to fine sandstone, present in both formations, erode underlying shale deposits and represent intermittent high energy events such as crevasse splays. Deposits commonly appear massive, but local beds in the Carten Creek Formation exhibit mudchips, small-scale troughs, planar laminations, and ripples. Overbank sequences also reflect rapid deposition by the rare preservation of trough topsets and climbing ripples.

Local finer-grained beds are attributable to, but not required of, chute development. One possible deposit that erodes lateral accretion surfaces occurs from 119.6 to 120.5m in the Carten Creek measured section. Black chert pebbles are locally present at gradational contacts in Golden Spike

siltstone and imply sporadic velocity increases that may relate to poorly developed chutes.

Four sequences comprising large-scale planar foresets, horizontal laminations, rare convoluted laminations, and local trough crossbeds occur low in the Carten Creek measured section. These units, comprising the volcanic-pebble sandstone and portions of the fine to coarse sandstone facies, suggest longitudinal and/or chute-convergence bars. Greenish gray to black shale generally underlies and sharply caps bar sequences.

In both formations, massive shale represents flood plain development within a fluvial system. Upper shale bed contacts tend to be irregular due to erosion by overlying coarser units. Chert, jasper, and quartzite pebbles locally occur near the top of Golden Spike shale deposits and imply deposition related to an ensuing high energy event. Lenses of very-fine grained sandstone and siltstone within shale beds suggest distal or small crevasse splays. Mottled mudstone beds represent paleosol horizons that developed on floodplain and bar surfaces in both formations. The micritic nodules, or caliche, are the result of calcium enrichment (Mack and James, 1992). Caliche development occurs when precipitation rates are too low to adequately flush carbonate through the soil horizon (Reeves, 1976 in Gavin, 1986) or when the water table fluctuates (Mack and James, 1992).

Tan tabular sandstone interfingering with the Golden Spike's sandy cobble conglomerate facies indicates consistent water currents and may

represent either braided stream development on or under-laden flood waters that flowed over an alluvial fan surface. According to Johnson (1965), flood waters relatively free of solid material often follow major debris flow waves and may remobilize and deposit sediment. Smaller tan sandstone lenses may also represent rills and gullies created by rain erosion (Blair and McPherson, 1994).

Noncohesive Debris Flow Deposition

The sandy cobble conglomerate facies of the Golden Spike Formation was deposited in a high energy environment by highly sediment-concentrated events. Some deposits, albeit suggestive of fluvial deposition, may also represent sandy noncohesive debris flows (Figure 27). According to Kelin Whipple (personal communication, 1997), sandy debris flows are highly susceptible to material separation during flow. The separation of sediment within a flow creates a debris snout, intermittent waves of concentrated material and a wet tail (Johnson, 1965). Stacked conglomerate beds suggest repetitive debris snout and/or wave deposits within an alluvial fan system (Johnson, 1965). Lens shaped sandstone beds imply the winnowing and remobilization of finer grained material by succeeding waves of the same debris flow episode (Johnson, 1965). Accordingly, debris flow dewatering could produce enough clear water flow to rework finer grained sediment. However, underlying sand and gravel deposits may absorb water released

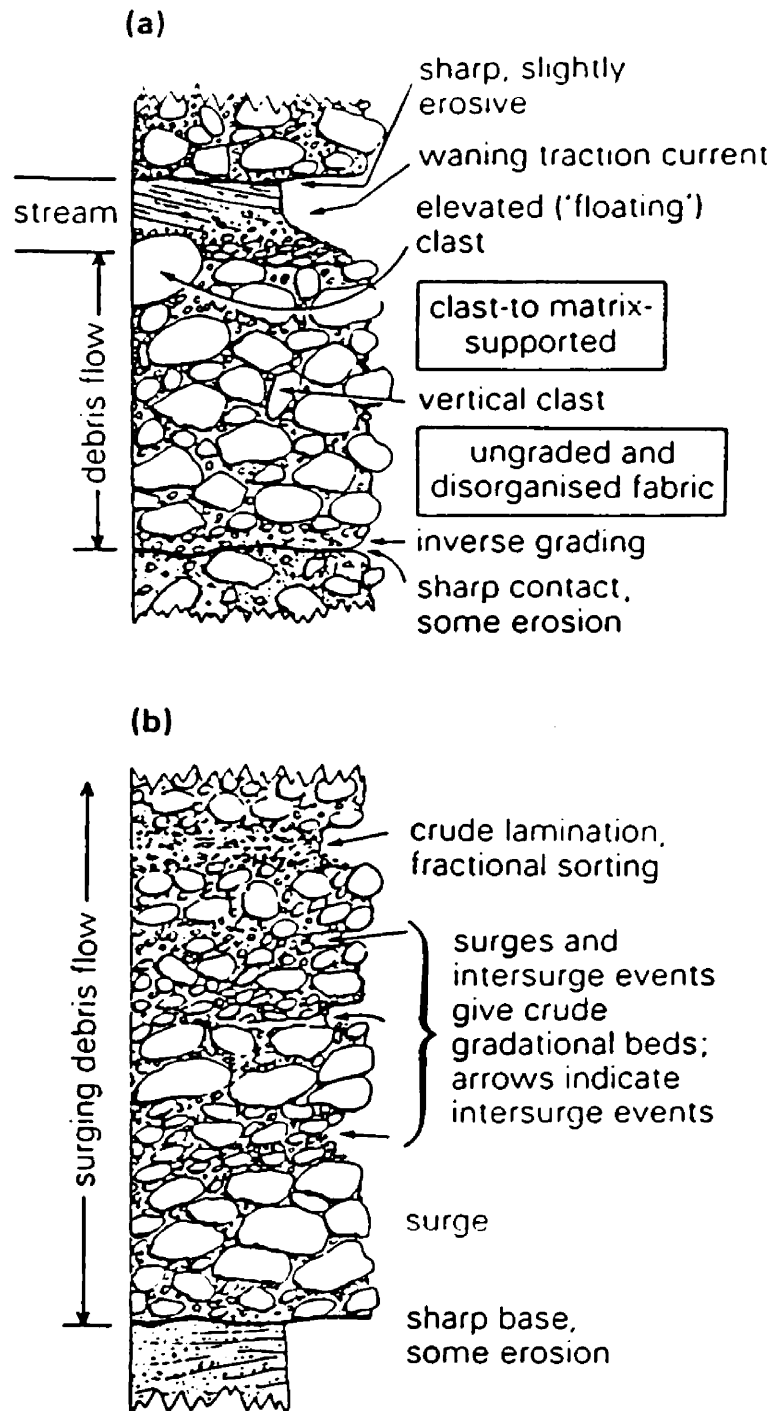


Figure 27: Styles of grading possible in debris-flow conglomerate due to different sub-aerial processes of deposition. Beds can vary from a few decimeters to meters thick. (from Nemec and Steel, 1984)

during debris flow 'freezing' (Jahns, 1949 in Johnson, 1965).

Video footage of Japan's Sakura Island in the 1980's shows that flow partitioning leaves the debris flow's tail a sediment concentrated slurry deprived of coarser debris. According to Johnson (1965), water content within a flow progressively increases with distance behind the debris flow snout. An increase in water content could change the tail of a sandy debris flow into a hyperconcentrated flow (Figure 28). Hyperconcentrated flows are defined by Smith and Lowe (1991) as "non-Newtonian fluid-solid mixtures possessing little or no strength and generating deposits intermediate in nature between those of debris flows and dilute streamflows."

A hyperconcentrated tail could potentially produce sedimentary features traditionally associated with fluvial systems. While this remains to be demonstrated by lab experimentation, witnessed debris flow events are known to have left deposits that appear fluvial in origin (Kelin Whipple, personal communication, 1997). For example, the 1995 floods that mobilized debris in the Blue Ridge Mountains of Virginia deposited imbricate clasts both in matrix and grain support (Figures 29a&b). Similarly, Johnson (1965) described a conglomerate unit with touching pebbles in silty matrix and a pebble-cobble conglomerate unit with platy clast imbrication on the Surprise Canyon alluvial fan in Panamint Valley, California.

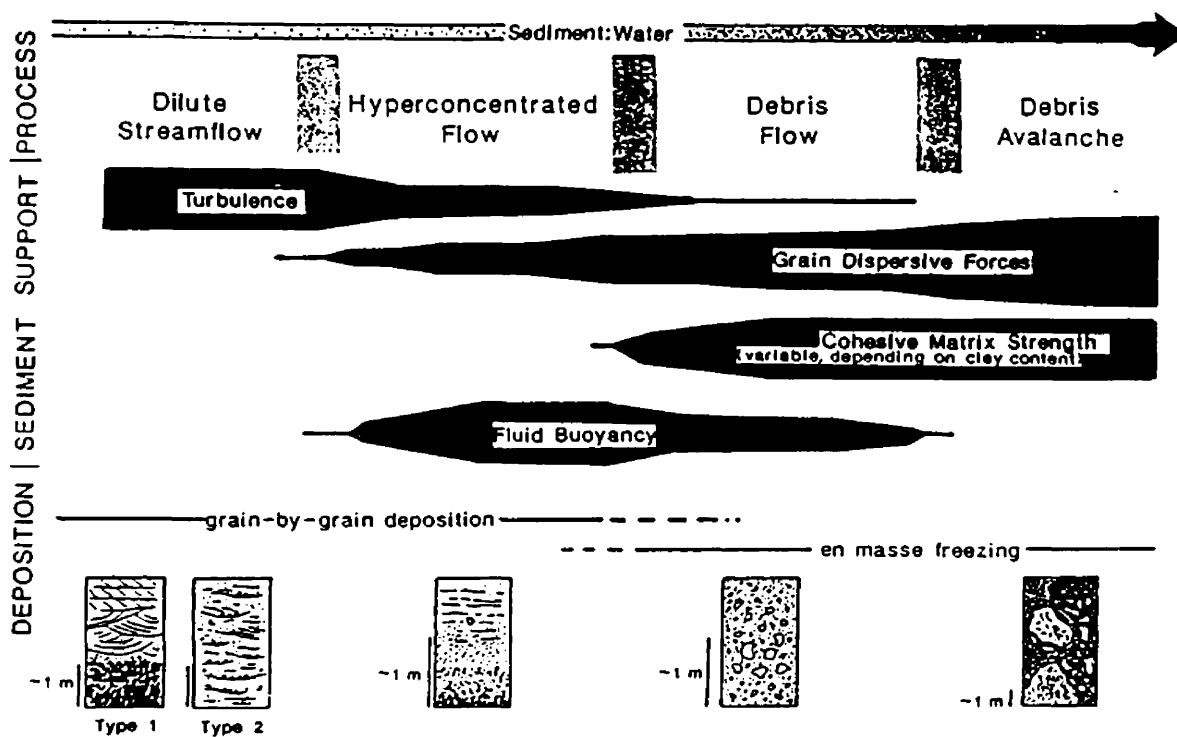


Figure 28: Schematic comparison of sediment movement by various flow mechanisms with idealized models of deposits. Transition between depositional processes relates to gradual changes in the sediment to water ratio and, consequently, flows may involve multiple forms of sediment support. (from Smith and Lowe, 1991)



Lahar and Volcanic-related Deposition

Crude bedding within the thick matrix-supported megaconglomerate of the Golden Spike Formation indicates that a single depositional event, as previously interpreted (Gwinn and Mutch, 1965; Mackie, 1986), is improbable. Rather, I interpret the megaconglomerate facies to be multiple subaerial debris-flow deposits. Although the megaconglomerate contains nonvolcanic clasts, matrix material representative of a magmatic arc provenance and abundant individual volcanic clasts suggest lahars were the dominant depositional mechanism. Multiple lahar deposits suggest a volcanic alluvial fan environment created the megaconglomerate facies.

Mackie's (1986) interpretation that the megaconglomerate resulted from hot lahar deposition is suspect. He cites only individual clast deformation as evidence of high temperature. While I concur that some clasts are distorted and jointed, my field analysis cannot confirm any influence of heat. Movement along conjugate joints clearly offset and deformed duraclasts (Figure 30). Collisions with indurate pebbles during debris flow deformed dark gray shale and siltstone clasts (Figure 31). Furthermore, no clear distinction between baking and weathering rinds is evident, and most clasts are free of external coatings.

Although lahars are typically clay-poor (Smith and Lowe, 1991), superficial erosion may explain both the clay-rich content and the nonvolcanic detritus within the megaconglomerate facies. Clay within a lahar originates from diagenetic alteration of metastable volcanic grains, hydrothermally altered



Figure 30: Faults occurring in Golden Spike megaconglomerate deform and offset large clasts (Locality 5). The sheared clast depicted in photo is outlined for better illustration, and arrows depict direction of movement along fault. Camera lens cap in center of photo provides scale.

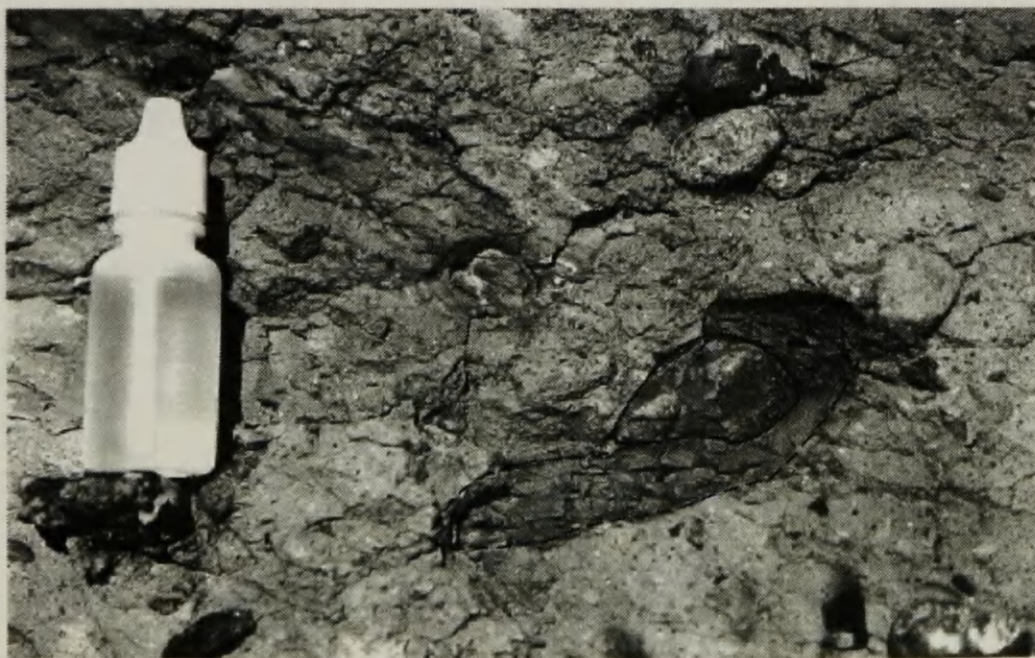


Figure 31: Dark gray, muddy siltstone clast (dashed outline) in Golden Spike megaconglomerate (Locality 5) was deformed by a more resilient clast (solid outline) during debris-flow movement. Acid bottle, used for scale, is 8cm tall.

source material, and the consolidation of soil during flow (Palmer and others, 1991; Smith and Lowe, 1991). Since debris flows characteristically engulf and incorporate loose material encountered along their paths (Johnson, 1965), volcanic-debris flows may contain nonvolcanic clasts from the surrounding landscape (Smith, 1991). Intermixing of lahars with nonvolcanic-debris flows from the western thrust front is also feasible as lahars can travel many tens of kilometers (Palmer and others, 1991; Smith and Lowe, 1991).

Modes of transport for the volcanic/volcaniclastic facies in the Golden Spike Formation include lava and volcaniclastic flows. Matrix-supported, volcaniclastic breccia likely represents lahar deposits as suggested by Gwinn and Mutch (1965). Clasts of hornfels embodied in breccia are presumably baked mud chips and suggest the volcanic-debris flows were hot. The characteristic green color is diagnostic of chloritization affecting the metastable volcanic debris (Tucker, 1991). X-ray diffraction of clay particles conducted as adjunct analysis to this research corroborates the presence of chlorite.

Provenance Analysis of Lithofacies

Introduction

Framework-grains in the Carten Creek and Golden Spike formations are compositionally comparable with relatively few exceptions. Mackie (1986) thoroughly characterized the specific composition of framework-grains in his description of the Golden Spike's sedimentary petrology. In general, the mineral grains recognized in thin section include: monocrystalline quartz, polycrystalline quartz, chert, potassium feldspar, plagioclase, biotite, muscovite, chlorite, pyroxene, and accessory "heavy" minerals. Volcanics, plutonics, sandstone, siltstone, limestone, dolomite, quartzite, and micaceous schist comprise the detrital lithic fraction identified during point counting. Porphyritic andesite is the primary igneous component, but granite grains also occur in Carten Creek specimens. Compositional data from point counts are plotted on ternary diagrams as percent ratios of quartz, feldspar, and various lithic fragments (Figures 33-36). The proximity of compositional data to fields outlined in the ternary diagrams (after Dickinson and Suczek, 1979) provides a basis for the interpretation of tectonic setting and provenance for both formations.

Clast counts conducted in this study provide a detailed provenance history of the megaconglomerate and sandy cobble conglomerate facies in the Golden Spike Formation. Lithologic data from clast counts are reported in two ways (Figure 37a): 1) compositional percentage based on population, where

each occurrence of a clast registers as one count, and 2) composition proportionally related to the sample area covered by clasts. The difference between population-based and area-related percentages indicates the effect that highly variable clast sizes have on compositional calculations. In general, a small ($\leq 5\%$) positive or negative difference exists between the two percentages calculated for specific lithologies represented in a count, although about 10% of the lithologic groups yield differences of $\sim 10\%$. Positive differences mean the lithologic percentage based on simple clast recurrence within a count is less than the proportion related to clast area and negative differences indicate the opposite (Figure 32). When substantial, negative differences imply that Golden Spike clasts of a specific lithology average 3.5cm in diameter as determined from the median long-axis of category 1 clasts within counts. Strong positive differences ($>10\%$) illustrate that the average clast diameter within a lithologic population is $>3.5\text{cm}$, and may exceed 50cm. Vertical change in the mean clast size of a given lithology likely reflects tectonic activity, the unroofing trends of sediment sources and residence time of clasts within the environment. Therefore, only the lithologic percentages related to area are graphed (Figure 37b) for compositional comparison of the major conglomerate facies in the Golden Spike Formation.

Carten Creek Formation

Sandstone composition of the upper-middle Carten Creek Formation varies between lithic-feldspathic, subfeldspathic, and sublithic. Well-rounded

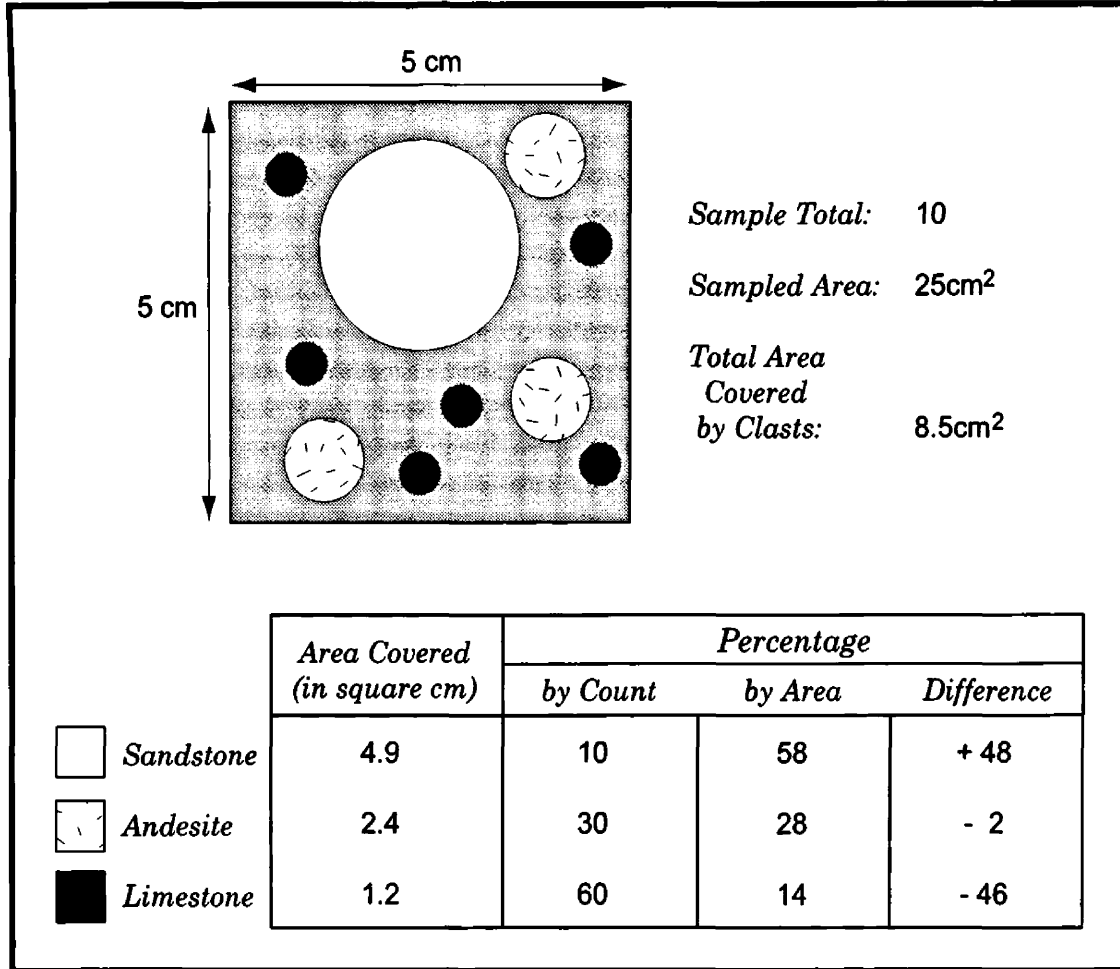


Figure 32: Schematic clast count illustrating the effect of variable clast size on lithologic percentage computation. (Clast areas are determined from the mathematical equation for the area of an ellipse.) Positive and negative differences in compositional proportions directly relate to clast size. Substantial positive changes in percentage indicate the prevalence of large clasts within certain lithologies; an abundance of small-sized clasts is represented by a significant negative difference.

quartz grains with broken silica-overgrowths occur locally and represent recycled sediment. Monocrystalline quartz with straight and sweeping extinction is pervasive in thin section but polycrystalline quartz, chert and local chalcedony is also present. Twinned plagioclase forms large blocky crystals that are consistently (sub)angular. Lithic fragments include dacite, porphyritic andesite, granite, quartzite, limestone, sandstone, siltstone and rare micaceous schist. Limestone grains, commonly deformed due to compaction, comprise solid micrite with local sparite-filled cracks. Two sandstone grains noted in thin section contain round quartz particles in a fine grained matrix and likely derived from a mature arenite. Less common minerals observed include biotite, muscovite and rare (sub)round clinopyroxene.

Point count data indicate that sandstone commonly contains 9% matrix and 23% cement on average. Bent and fragmented micas locally constitute pseudo-matrix. Sparite and poorly formed silica overgrowths occur along grain boundaries, but calcite is the primary cement.

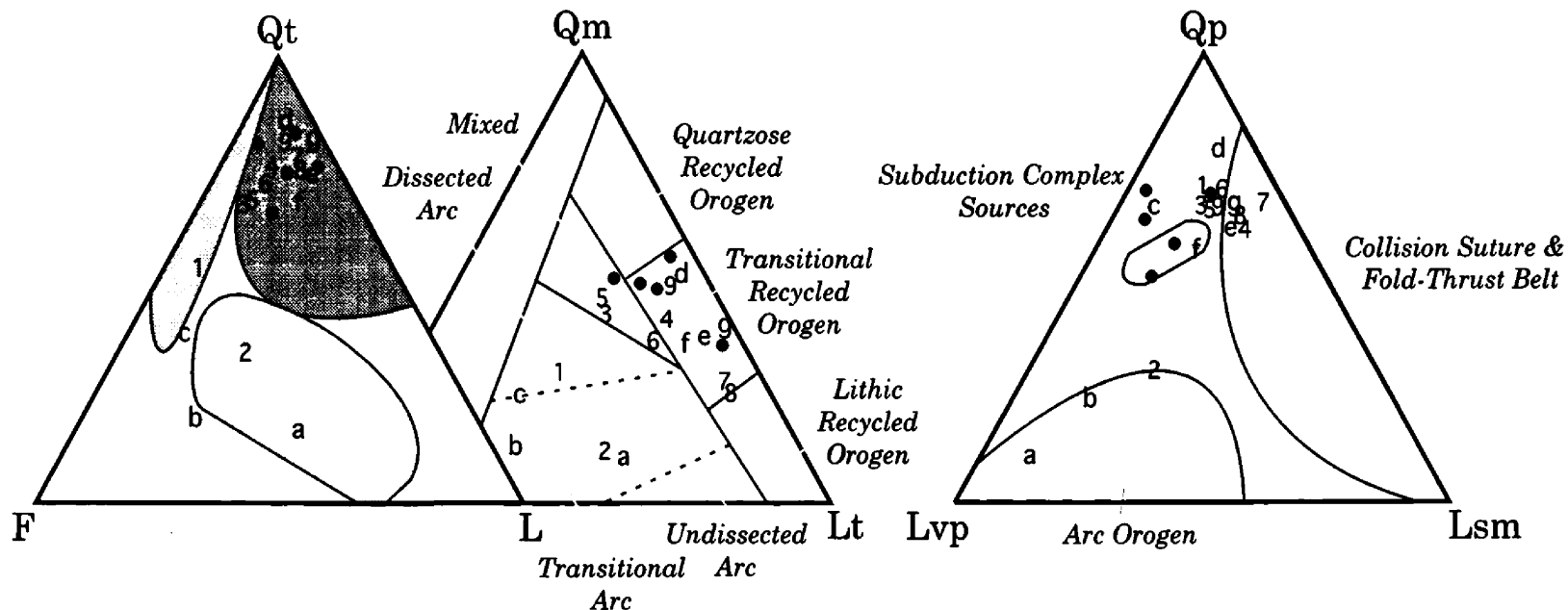
Since partial replacement by calcite commonly obscures plagioclase identification, cement estimations may include an unknown proportion of framework-grains. However in counting, close attention was given to the identification of plagioclase grains that were either partially or completely replaced by calcite. Furthermore, thin sections displaying heavy alteration of framework grains were eliminated from statistical analysis.

Framework-grain compositions suggest that a continental volcanic system eroded in association with exposed older lithofacies to form the upper-

middle Carten Creek Formation. Compositions of sandstone plotted on a QtFL diagram illustrate that the majority of sediment in the Carten Creek derived from a recycled orogen (Figure 33a). However, the feldspar-rich bar and thalweg deposits are representative of a magmatic arc provenance that is slightly outside the field defined by Dickinson and Suczek (1979). Analysis of compositional data on a QmFLt diagram depicts both a mixed source and repetitive changes in provenance from transitional arc to transitional recycled-orogen (Figure 33b). Mixed and transitional provenance types suggest a close association between the arc and recycled orogen sources.

The composition of Carten Creek sandstones is slightly discordant with QpLvplsm tectonic fields (Figure 33c). Nonetheless, over half of the specimens congregate in or near the designated collision suture and fold-thrust belt setting, and three represent an arc orogen. The implication that erosion of a subduction complex relates to Carten Creek sedimentation is inconsistent with the known, Cretaceous tectonics of western Montana. Divergence of Carten Creek compositions from designated tectonic fields is presumably related to atypical volcanism within the foreland system. Similarly, Graham et al. (1993) described modern sands in the basins of western China eroding from a collision suture and fold-thrust belt source that compositionally reflect a relict volcanic-tectonic setting.

Figure 33:
Tectonic Provenance and implied Setting of the Carten Creek Formation



LEGEND

Recycled Orogen
 Continental Block
 Magmatic Arc

1 - 9 Carten Creek Sandstone from Measured Section (Locality 1)

a - g Carten Creek Sandstone from Photomosaic Section (Locality 2)

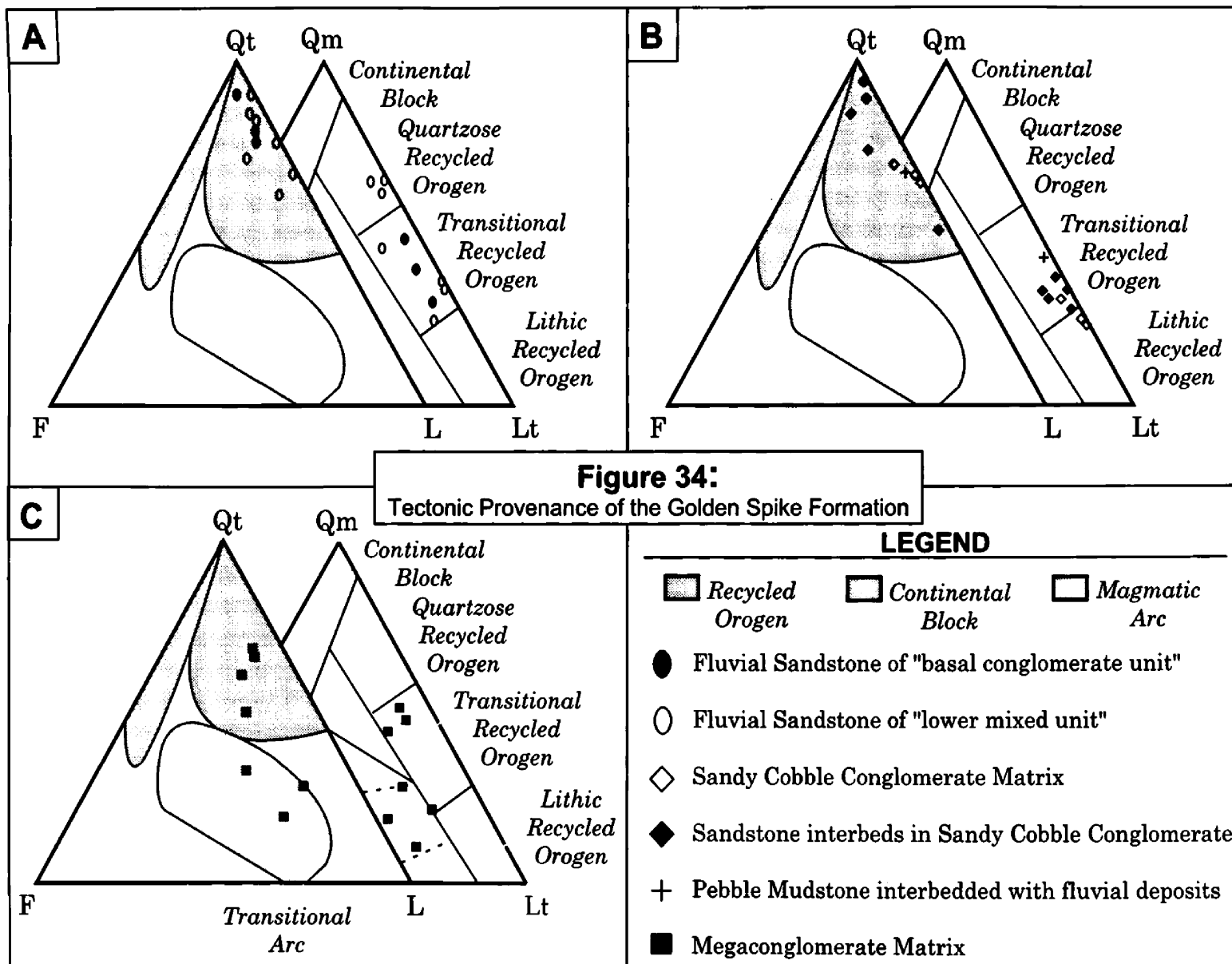
● Carten Creek Sandstone from Reconnaissance Random Sampling

Golden Spike Formation

Point Count Analysis

In the lower Golden Spike Formation, sandstone and sandy cobble conglomerate compositions plot in the recycled orogen provenance on QtFL and QmFLt diagrams (Figure 34a&b). In general, the framework-grain compositions of these facies denote a transitional recycled-orogen source, like that represented in the Carten Creek. Composition of matrix and sandstone interbeds in sandy cobble conglomerate locally represent a lithic recycled-orogen provenance due to an increased proportion of carbonate grains (Figure 34b). The more quartzose composition of some fluvial sandstones likely reflects superior weathering of sediments within the meandering river system (Figure 34a).

Megaconglomerate matrix moderately differs in composition from the other lower Golden Spike deposits as illustrated in QtFL and QmFLt diagrams. Specifically, the composition of matrix in megaconglomerate represents both recycled orogen and magmatic arc sources (Figure 34c). On the QmFLt diagram, some megaconglomerate matrix compositions suggest a transitional recycled-orogen provenance. Comparing all samples of Golden Spike facies that plot within this provenance field, megaconglomerate matrix is similar in composition to the meandering-fluvial deposits, but is more quartzose than the matrix and sandstone interbeds in the sandy cobble conglomerate. The compatible composition of megaconglomerate matrix and underlying fluvial



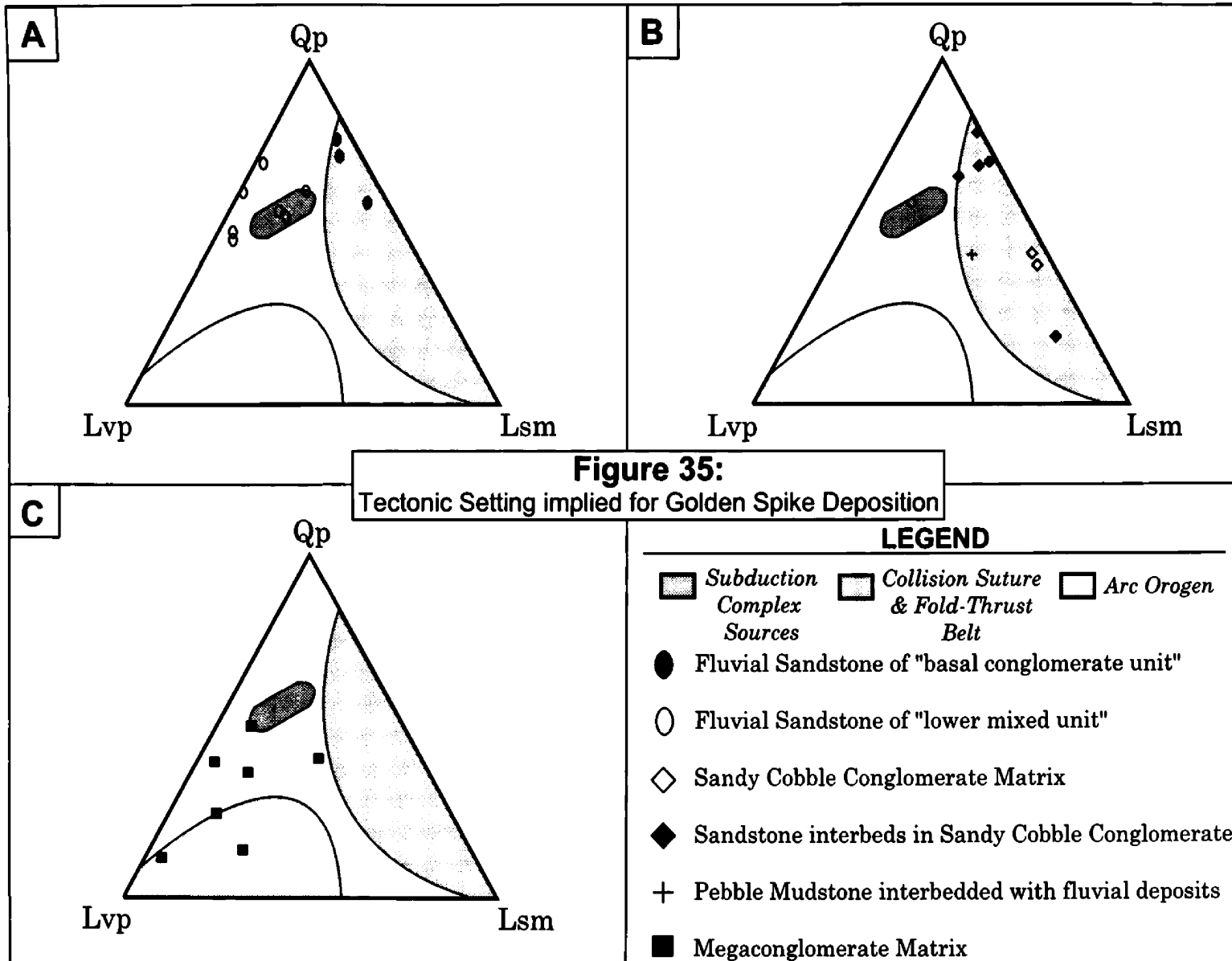
sandstones supports the idea, proposed in this work, of deriving the megaconglomerate's nonvolcanic component from superficial intraformational erosion.

On the QpLvpLsm diagram, the composition of megaconglomerate matrix represents an arc-orogen (Figure 35c) that corresponds to extensive Elkhorn Mountain volcanic activity in the region (Gwinn and Mutch, 1965). A collision suture and fold-thrust belt tectonic setting is also depicted in the lower Golden Spike Formation by the compositions of basal fluvial sandstone, sandy cobble conglomerate matrix and sandstone interbeds (Figure 35a). However, fluvial sandstone compositions in the "lower mixed unit" (after Gwinn and Mutch, 1965) plot outside the designated QpLvpLsm tectonic fields like the Carten Creek Formation. Although unlike the Carten Creek, these Lvp-rich deposits presumably reflect the early influence of Elkhorn Mountain Volcanics (Figure 35b).

Clast Count Analysis

Clast counts conducted on the Golden Spike provide detailed information on the rock-types and formations exposed in the fold-thrust belt. With local exception, limestone and quartzite clasts dominate both the sandy cobble conglomerate and megaconglomerate facies. The various nonvolcanic rock formations span the Precambrian, Paleozoic and Mesozoic Eras.

Clast of dark gray crinoidal sparmicrite and fossiliferous sparite (grainstone) are abundant in Golden Spike conglomerates and probably



eroded from the Mississippian Madison Formation. Massive, dark gray sparite/micrite clasts could have also derived from the Cambrian Silver Hill and Red Lion formations. Regardless, trilobite-bearing micrite noted in sandy cobble conglomerate indicates the presence of the Red Lion Formation. Clasts of gastropod-ostracod rich sparite probably derived from limestone units in the Cretaceous Kootenai Formation. Lastly, hematitic intrasparite with blocky biomicrite clasts and local glauconite grains is an unidentified enigma that occurs in three clast counts in very small percentages and likely is of Paleozoic age.

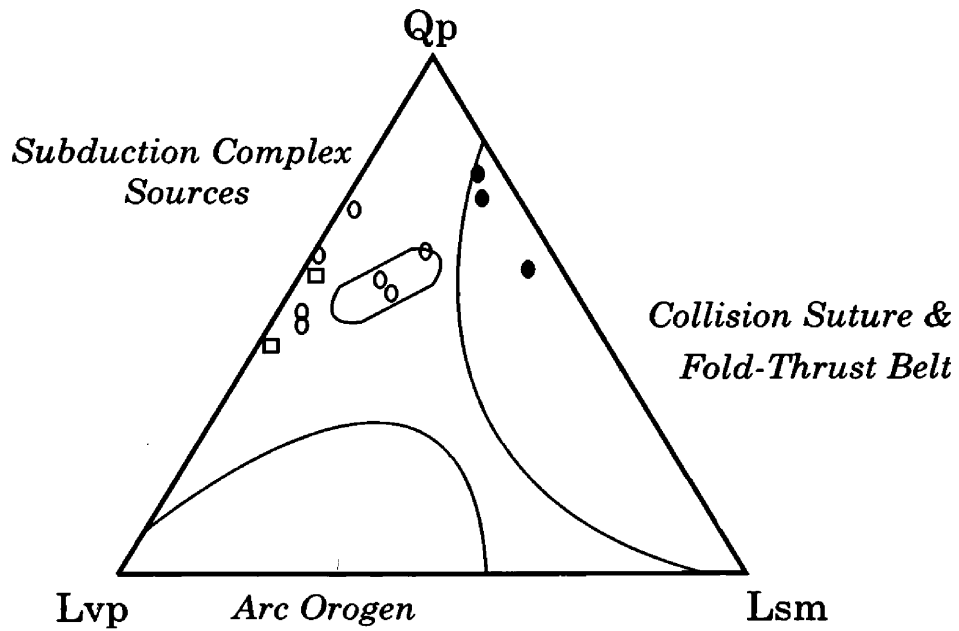
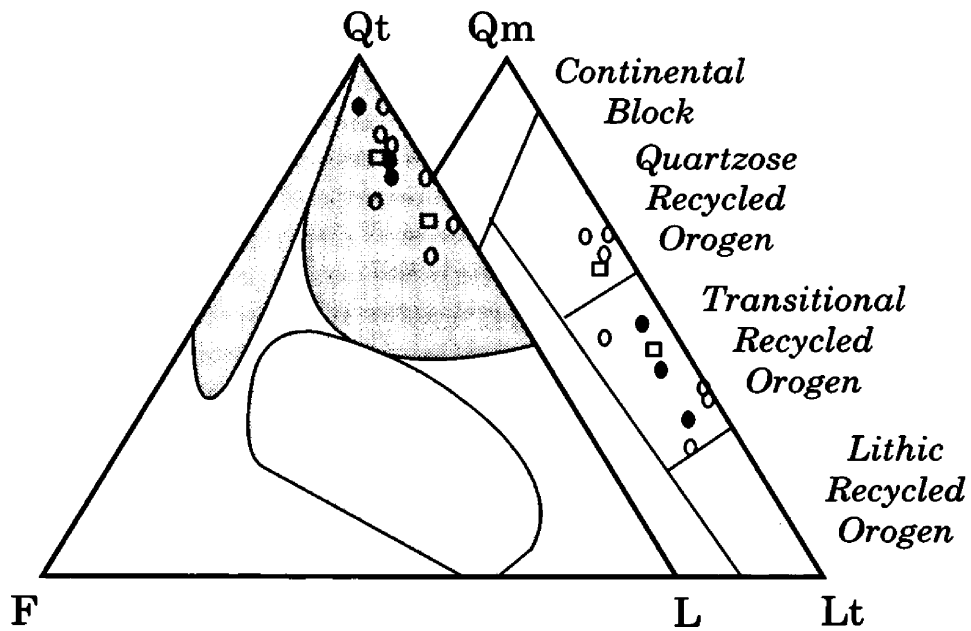
Quartzite clasts in the Golden Spike are fine to coarse grained and typically red, pink or orangish brown in color although white, tan, dark gray and green quartzite also occurs. Erosion of the middle Proterozoic Bonner Formation is evident in the Golden Spike by the red-pink, subfeldspathic quartzite clasts with local ripple crossbeds and red argillite rip-up chips. Other sources of quartzite represented in Golden Spike conglomerates potentially include the Proterozoic Mt. Shields, Pilcher and Garnet Range formations. Brown and white subfeldspathic meta-arenite with local glauconite grains, derived from the Cambrian Flathead Formation, also comprises part of the quartzite population. (However, some white clasts of identical composition retain a sandstone texture, i.e. no sutured quartz grains, and therefore were not included as quartzite during lithology percentage calculations.)

Chert and tan dolomite constitute moderate proportions in Golden Spike conglomerates (Figure 37a). Chert is predominantly black and commonly

spiculitic. Other chert clasts are red, green, gray and white. Black chert potentially eroded from the Mississippi Madison, Permian Phosphoria and Cretaceous Kootenai formations. A possible source of the red and green chert is the middle Proterozoic McNamara Formation. The Dunkleberg Member of the early Cretaceous Blackleaf Formation also may have provided varicolored cherty porcellanite debris. Tan, white and pink sucrosic sparite and dolomite likely eroded from the Pennsylvanian Amsden Formation. Dark gray crystalline dolomite is representative of the Cambrian Hasmark Formation.

Sandstone and siltstone clasts in the Golden Spike conglomerate facies include various lithologies. The Pennsylvanian Quadrant Formation presumably supplied white fine grained arenite to the Golden Spike, although some clasts could also come from white sandstone deposits in the Cambrian Flathead Formation. Red to pink, subfeldspathic-lithic arenite likely eroded from red sandstone units in the Cretaceous Kootenai Formation. Green sublithic-feldspathic arenite with pink orthoclase is present in two sandy cobble conglomerate counts, but remains unidentified by formation. Large bluish-gray sublithic arenite and pebble conglomerate clasts, exclusively occurring in the megaconglomerate facies, eroded from meandering-fluvial deposits in the Golden Spike and denote cannibalization of the formation. Compositional comparison of "Moby Dick" to meandering-fluvial sandstone strongly implies that the megaconglomerate's largest clast also eroded from the Golden Spike Formation (Figure 36) -- specifically, the lower "lower mixed unit" (after Gwinn

Figure 36:
 Composition and Tectonic Provenance Comparison between
 Lower Golden Spike Fluvial Sandstone and "Moby Dick" Clast



LEGEND

- | | |
|---------------------|--|
| □ Recycled Orogen | ● Fluvial Sandstone of "basal conglomerate unit" |
| □ Continental Block | ○ Fluvial Sandstone of "lower mixed unit" |
| □ Magmatic Arc | □ "Moby Dick" clast in Megaconglomerate |

and Mutch, 1965). Erosion of the relatively soft Cretaceous Colorado Group provided the black shale and siltstone to the Golden Spike megaconglomerate.

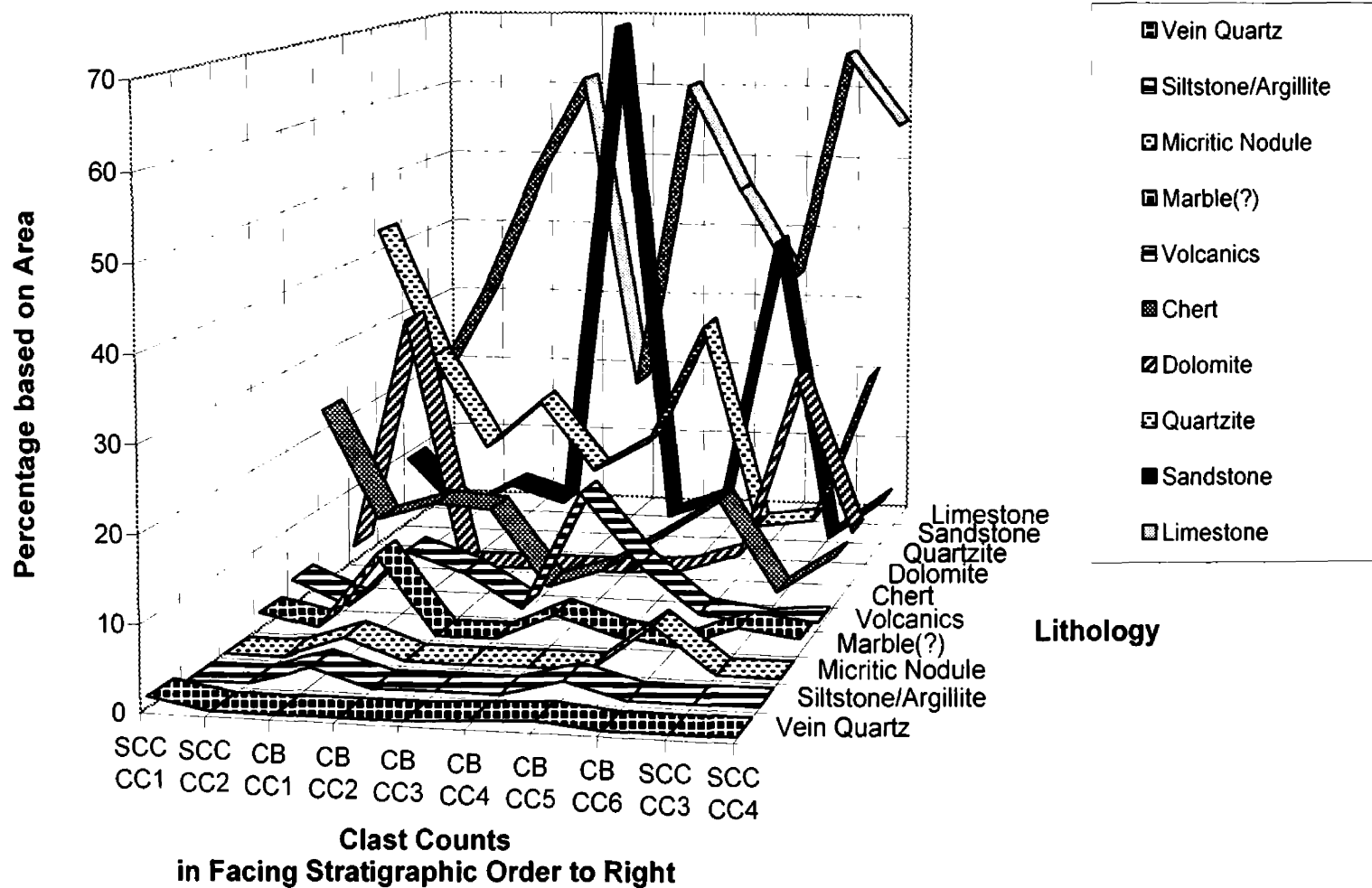
Comparison between the lithologic percentages of conglomerate facies distinguishes overall erosional trends (Figure 37b). After initial decreases of ~10%, fluctuating quartzite proportions remain relatively consistent but chert percentages gradually decrease throughout the lower Golden Spike. Proportion of limestone increases in the megaconglomerate facies and ranges among 45 - 65% upsection, except where large boulders of cannibalized sandstone affect the area-based percentages. Increased proportions of sandstone contained in the megaconglomerate facies reflect immense clast dimensions more often than physical abundance. Dolomite, however, generally disappears in megaconglomerate, while volcanic proportions show a distinctive increase. Conversely in the sandy cobble conglomerate, dolomite is common and volcanics dwindle.

Changing percentages of lithology relate to the tectonic setting affecting the conglomerate deposits. The relative abundance of limestone suggests uplift and constant erosion of a carbonate-bearing source. Potential sources include uplift along the Sapphire thrust margin and/or the Lewis and Clark Line (LCL). Vein quartz and marble may represent hydrothermal and contact metamorphic zones within the Garnet Range. Volcanic pebbles in sandy cobble conglomerate eroded from an arc located within the fold-thrust belt, as discussed for the ternary compositional plots. The Elkhorn Mountains are the

Cobble Count Sample #	Quartzite Percentage			Chert Percentage			Limestone Percentage			Dolomite Percentage		
	(by Count)	(by Area)	(difference)	(by Count)	(by Area)	(difference)	(by Count)	(by Area)	(difference)	(by Count)	(by Area)	(difference)
SCC CC1	31.2	42.6	11.4	25.8	22.5	-3.3	20.7	17.6	-3.1	2.5	2.0	-0.5
SCC CC2	31.2	25.7	-5.5	22.0	8.5	-13.5	34.8	31.0	-3.8	9.2	32.4	23.2
CB CC1	19.4	13.5	-5.9	11.8	10.9	-0.9	49.7	48.1	-1.6	0	0	0
CB CC2	17.5	19.9	2.4	9.0	10.3	1.3	66.7	61.4	-5.3	0	0	0
CB CC3	29.8	10.8	-19	3.0	0.6	-2.4	61.7	18.4	-43.3	0	0	0
CB CC4	20.7	14.9	-5.8	10.6	3.1	-7.5	53.4	60.6	7.2	0	0	0
CB CC5	28.9	30.6	1.7	8.6	7.7	-0.9	48.2	46.1	-2.1	0.4	0.6	0.2
CB CC6	8.8	4.0	-4.8	13.2	12.4	-0.8	42.7	33.8	-8.9	4.4	2.8	-1.6
SCC CC3	5.6	5.0	-0.6	2.8	1.1	-1.7	63.4	65.2	1.8	26.8	26.1	-0.7
SCC CC4	22.9	24.4	1.5	10.9	6.0	-4.9	51.2	55.5	4.3	4.6	6.4	1.8
Cobble Count Sample #	Volcanics Percentage			Sandstone Percentage			Siltst./Argill Percentage					
	(by Count)	(by Area)	(difference)	(by Count)	(by Area)	(difference)	(by Count)	(by Area)	(difference)			
SCC CC1	1.0	3.2	2.2	16.1	9.0	-7.1	0	0	0			
SCC CC2	0.9	0.2	-0.7	0.9	1.8	0.9	0	0	0			
CB CC1	6.5	7.4	0.9	1.6	5.8	4.2	1.1	2.1	1			
CB CC2	6.4	4.9	-1.5	0.4	3.5	3.1	0	0	0			
CB CC3	4.0	0.7	-3.3	1.0	69.4	68.4	0.5	0.1	-0.4			
CB CC4	8.4	15.4	7	1.4	2.3	0.9	0	0	0			
CB CC5	6.9	6.7	-0.2	3.0	4.9	1.9	2.6	1.9	-0.7			
CB CC6	1.5	1.0	-0.5	19.1	40.4	21.3	0	0	0			
SCC CC3	0	0	0	0	0	0	0	0	0			
SCC CC4	1.1	0.6	-0.5	6.3	5.4	-0.9	0	0	0			
Cobble Count Sample #	Vein Quartz Percentage			Marble(?) Percentage			Micritic Nodule Percentage					
	(by Count)	(by Area)	(difference)	(by Count)	(by Area)	(difference)	(by Count)	(by Area)	(difference)			
SCC CC1	1.5	1.3	-0.2	1.0	2.0	1	0	0	0			
SCC CC2	0	0	0	0.9	0.4	-0.5	0	0	0			
CB CC1	0	0	0	7.6	9.6	2	2.2	2.5	0.3			
CB CC2	0	0	0	0	0	0	0	0	0			
CB CC3	0	0	0	0	0	0	0	0	0			
CB CC4	0.5	0.4	-0.1	4.9	3.2	-1.7	0	0	0			
CB CC5	0.4	0.7	0.3	0.9	0.9	0	0	0	0			
CB CC6	0	0	0	0	0	0	10.3	5.5	-4.8			
SCC CC3	0	0	0	1.4	2.6	1.2	0	0	0			
SCC CC4	0	0	0	2.9	1.6	-1.3	0	0	0			

Figure 37a: Actual percentages of lithologies present in the sandy cobble conglomerate and megaconglomerate facies of the Golden Spike Formation; clast counts listed in facing stratigraphic order from top to bottom. Differences relate to the effect of clast size on percentage computation.

Figure 37b: Compositional Analysis of Conglomerates in the Golden Spike Formation



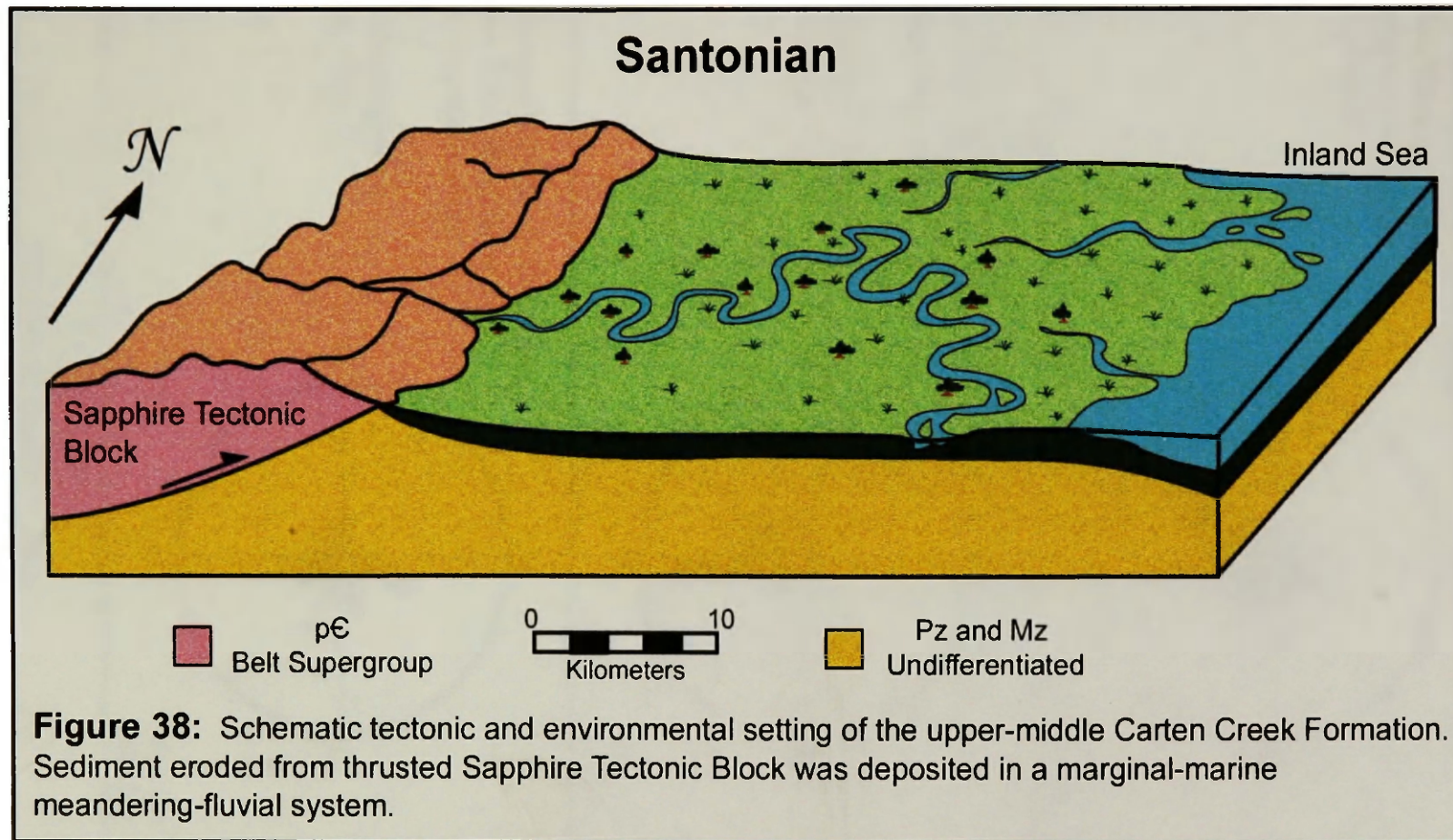
predominant volcanic influence on the megaconglomerate facies. (Of note, many large volcanic boulders were missed by stations during systematic sampling; therefore, volcanic clast content may be under represented in the megaconglomerate facies.) Increasing proportions of sandstone, siltstone/argillite and micritic nodules within the megaconglomerate further support superficial erosion of the landscape by lahars.

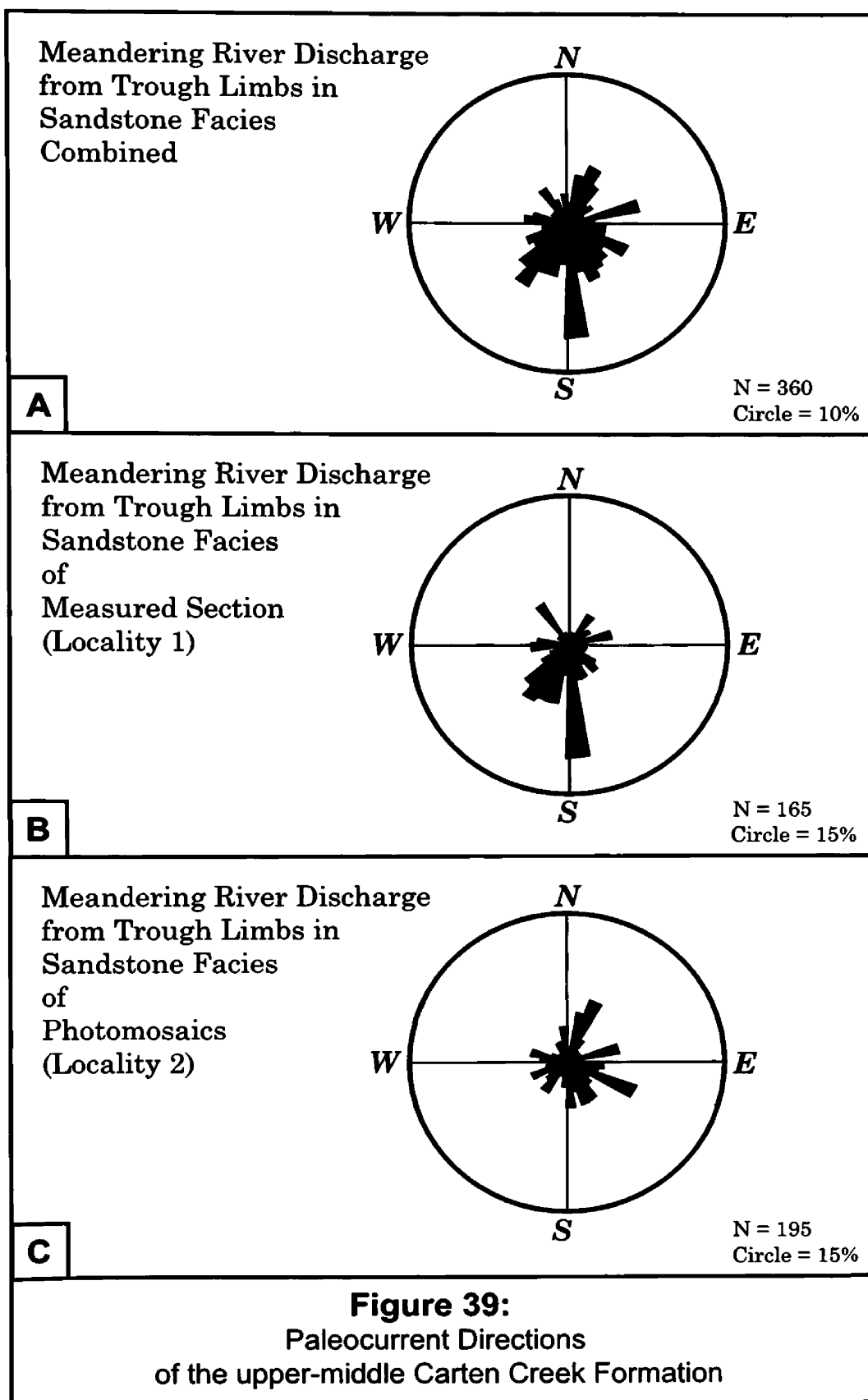
Summary of Deposition in Late Cretaceous Central-Western Montana

Increased sediment supply, related to middle-late Cretaceous uplift of the orogenic wedge, created the Carten Creek Formation and initiated the final regression of Cretaceous seas from the Clark Fork Valley area (Gwinn, 1965). Consequently, the thick Carten Creek sequence records both marine and terrestrial deposition. Biostratigraphic control on lower marine units implies a Santonian to earliest Campanian age for subsequent fluvial deposits in the upper-middle Carten Creek Formation.

Transition upsection from a brackish-marine environment and presence of longitudinal bar forms suggest that the meandering fluvial system represented in the upper-middle Carten Creek comprises part of a deltaic environment (Figure 38). Rivers drained dominantly to the south as represented by the primary direction of paleoflow in outcrop CC1 (Locality 1 in Figure 1; Figure 39a&b). However, bearings routinely vary up to 180° within deposits and paleoflow depicted in the Carten Creek photomosaics (CC2 - Locality 2 in Figure 1) suggest more eastward flow (Figure 39c). The abundant variation in discharge direction presumably relates to the highly-sinuuous geometry of the meandering river system.

Abundant volcanic detritus combined with recycled sediments in the upper-middle Carten Creek is atypical of foreland sedimentation as implied by





the designated provenance fields of Dickinson and Suczek (1979). Yet, early Cretaceous intrusion of the Idaho batholith and related-volcanism occurred within the Cordillera of western North America (Mallory, 1972). Composition of the Carten Creek Formation compares to that of the Idaho arc-terrain (Ziebell, 1943) except for scarce, well-rounded clinopyroxene that presumably eroded from another source.

Portions of the Idaho batholith's Atlanta lobe dated between 85 and 95 Ma (Bennett and Kiilsgaard, 1983) sufficiently predate deposition of the upper-middle Carten Creek Formation. Evidence for volcanic eruption of the Idaho arc-terrain also exists in the Atlanta lobe (Myers and Carlson, 1982). Rocks in the Bitterroot lobe of the Idaho batholith suggest no volcanic activity (D.W. Hyndman, personal communication, 1997) although ~12km of overburden eroded away to expose present structural levels (Hamilton, 1983; Jordan and Rodgers, 1994).

Tectonic loading from late Cretaceous uplift of the Sapphire, Garnet and Flint Creek ranges locally subsided the Clark Fork Sag (Gwinn, 1965; and Mutch, 1965; Mackie, 1986). This isolated basin provided sufficient accommodation space for the thick Golden Spike Formation (Mackie, 1986). Mackie (1986) suggested the Clark Fork Sag is a pull-apart basin because of the northeast-trending normal faults that form the northwestern and southeastern boundaries of the Golden Spike outcrop belt.

Whether those transtensional features along the Lewis and Clark Line (LCL) are syndepositional to or succeeded formation of the Golden Spike is not clear. However, normal faulting related to Eocene Basin and Range extension is common in western Montana. Furthermore, the facies assemblage of the Golden Spike Formation is inconsistent with that of a pull-apart basin (Miall, 1984).

The variety of lithologies present in the Golden Spike Formation is representative of a recycled orogen provenance associated with local syndepositional volcanic activity. Numerous nonvolcanic clasts, including debris of the Belt Supergroup, originated from the Sevier thrust front to the west (Gwinn, 1965; and Mutch, 1965; Mackie, 1986; Reynolds, 1986). I submit that uplift along the LCL to the north/northwest provided detritus from the Mississippian Madison Formation and accounts for much of the abundant limestone clasts. Volcanic material in the Golden Spike Formation derives from the early Campanian Elkhorn Mountains to the east and indicates that deposition of the Golden Spike began around 80-83Ma (Gwinn, 1965; and Mutch, 1965; Ruppel et al., 1981; Mackie, 1986).

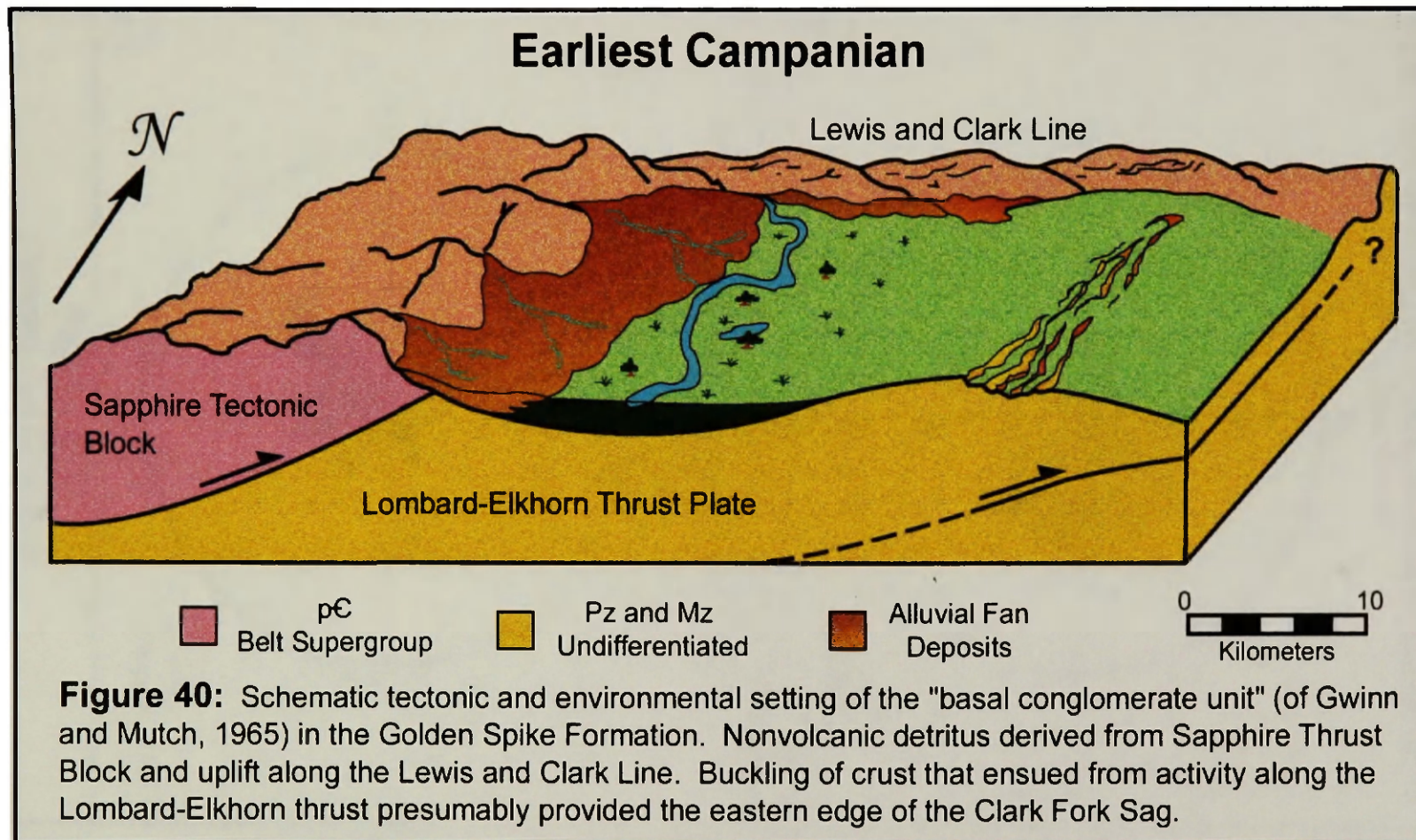
Detritus that shed east into the Clark Fork Sag originally mantled the Cordilleran hinterland and presumably traveled to the Sapphire thrust front by way of a fluvial system. Fluvial channel conglomerates containing pebble to boulder sized clasts locally outcrop in the Cramer Creek area along the LCL (Reynolds, 1986). These stream deposits are compositionally consistent with nonvolcanics in the Golden Spike Formation and compare in age at 82Ma

(Reynolds, 1986). Well-rounded quartzite and chert clasts in Golden Spike conglomerates underwent weathering and perhaps other episodes of thrusting prior to their current depositional location. A fluvial system within the Sapphire plate and along the western uplifts of the LCL provides possible explanation for the numerous subround to subangular duraclasts in the Golden Spike Formation.

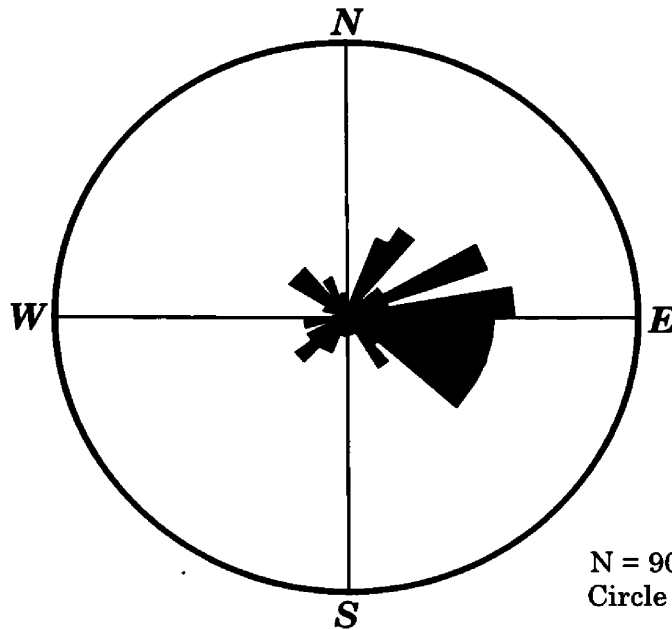
The Golden Spike Formation began as an alluvial pediplain locally dissected by a low-sinuosity fluvial system (Figure 40). Alluvial fan deposition corresponds to eastward propagation of the Sevier thrust plate as indicated by the general eastward dispersal of debris flows (Figure 41a). The inception or increase of movement along the Lombard-Elkhorn thrust (Ruppel et al., 1981) buckled the surface in the east and likely encouraged the predominant southwestern flow of the Golden Spike's meandering fluvial system (Figure 41b).

Alluvial fan facies include noncohesive debris flow and braided stream deposits. The meandering fluvial sandstone and pebble conglomerate laterally and vertically interfinger with crevasse-splay siltstone, floodplain shale and paleosol mudstone. Interfingering of alluvial fans with the meandering fluvial system occurs from two to four times in the basal Golden Spike Formation (Gwinn and Mutch, 1965).

Volcanics gradually occur upsection ("lower mixed unit" of Gwinn and Mutch, 1965) and interfinger with nonvolcanic meandering fluvial strata. Volcanic-related deposits, including lava flows and lahars, originated in the

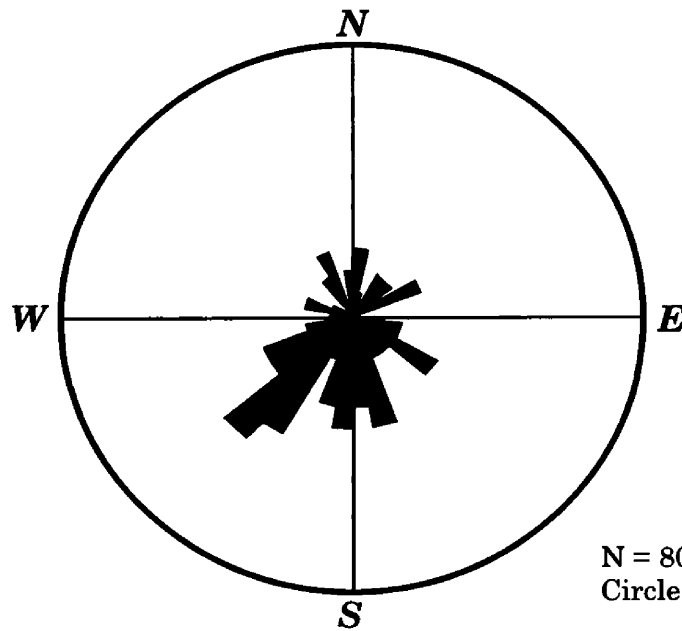


Debris Flow Dispersal on Alluvial Fans
from Clast Imbrication in Sandy Cobble Conglomerate
(Localities 4 & 6)



A

Meandering River and Local Braided Stream Discharge
from Trough Limbs in Sandstone Facies
(Localities 4 & 5)



B

Figure 41:
Paleocurrent Directions
of the lower Golden Spike Formation

Elkhorn Mountain Volcanics that palinspastic restoration suggests were ~30km east of the Sapphire thrust front (J. W. Sears, personal communication, 1997). A Campanian angular unconformity, beneath the Elkhorn Mountain Volcanics, occurs within the Lombard-Elkhorn plate (Viele and Harris, 1965) and implies a contemporaneous relationship between thrust plate movement and volcanic eruption (J. W. Sears, personal communication, 1997).

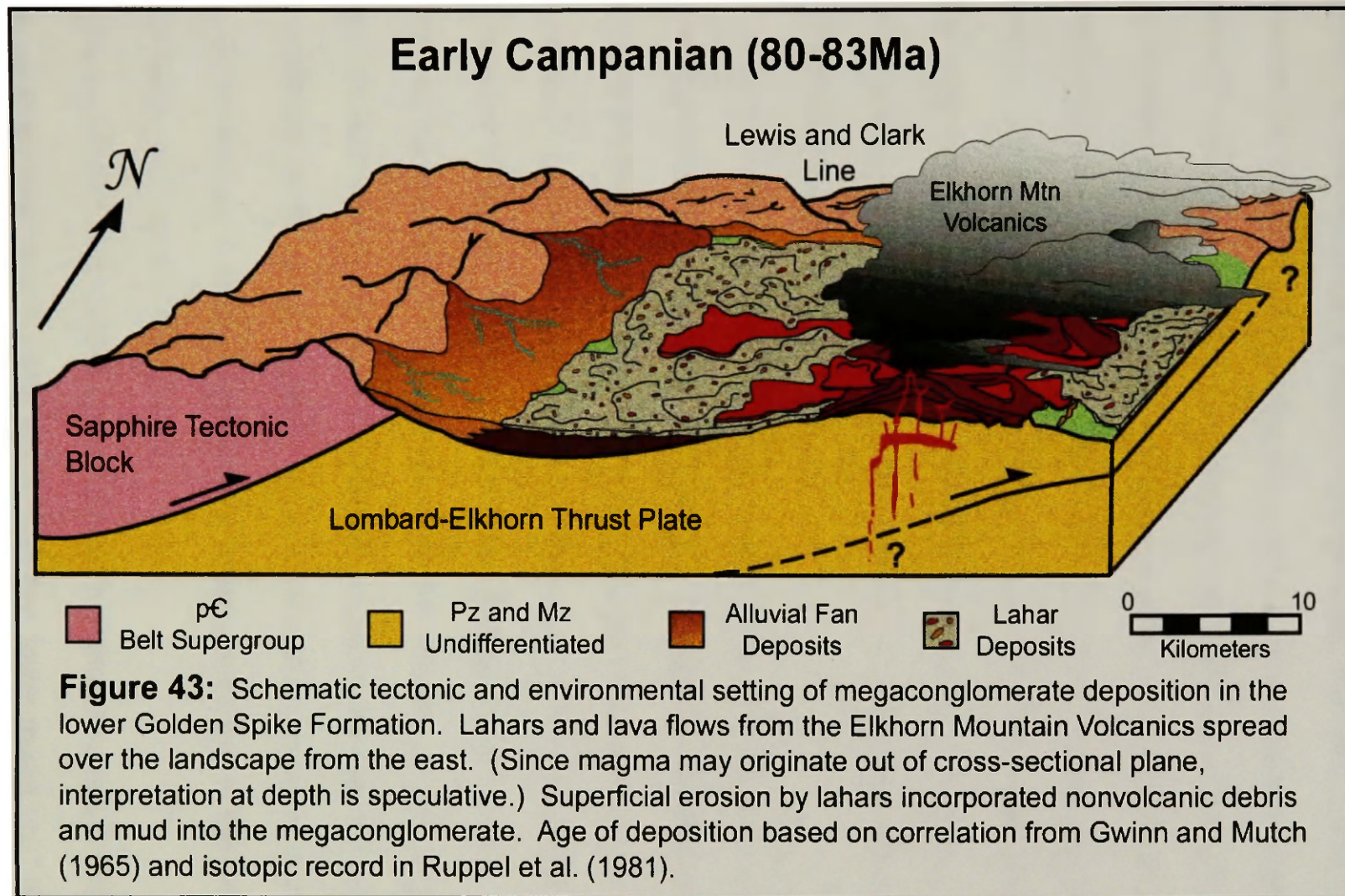
During the advent of volcanics within the Golden Spike, nonvolcanic meandering river deposits also locally interfingered with matrix-rich pebble conglomerate (Figure 23). The pebble conglomerate deposit contains clasts with diameters of ~0.5 to 2cm and is compositionally consistent with alluvial fan facies downsection. The silty-clay matrix and overall thin (~40cm) bedded geometry suggest the pebble conglomerate is the distal extent of a noncohesive debris flow.

The megaconglomerate facies directly overlies and apparently erodes nonvolcanic fluvial sandstone and pebble conglomerate (Figure 42). Megaconglomerate closely follows the initial appearance of volcanoclastics in the Golden Spike Formation and resulted from Elkhorn Mountain lahars and local lava flows spreading over the landscape (Figure 43). Fracturing of the caldera, due to eruptive processes, and debris avalanching may account for the large volcanic boulders embodied in the megaconglomerate facies.

Superficial erosion, by lahars, incorporated nonvolcanic debris and mud into the megaconglomerate. Cannibalized clasts from the lower Golden Spike fluvial deposits indicate erosion of the formation occurred syndepositionally



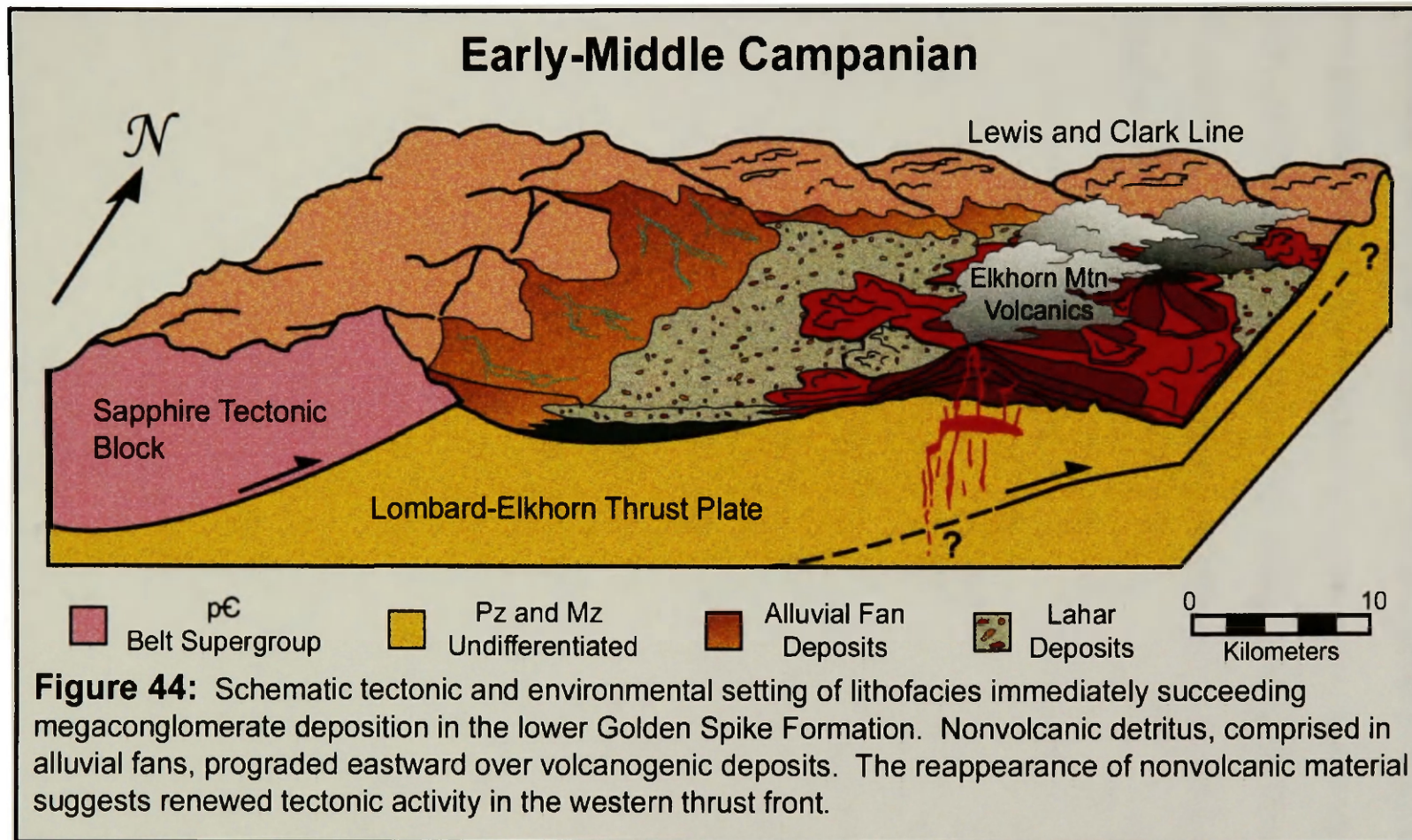
Figure 42: Base of lahar-related megaconglomerate exposed with underlying meandering-fluvial sandstone and pebble conglomerate on the east-side of Locality 5. Scale indicated by decimeter increments on staff.



due to uplift and exposure associated with the active regional tectonics. The most probable sources of large pebble-conglomerate, sandstone and siltstone boulders are the crustal buckling zone induced by Lombard-Elkhorn plate movement in conjunction with intruding magma and uplift along the LCL. Erosion of relatively soft Colorado Group sediments by volcanic-debris flows presumably explains some variation in the matrix texture and provenance composition. Considering the proximity of the Elkhorn Mountain Volcanics, far-reaching lahars perhaps also engulfed material from western nonvolcanic-debris flows. Incorporation of nonvolcanic clasts into the volcanic-debris flows led to the chaotic nature of this unique unit.

In deposition succeeding the megaconglomerate facies, nonvolcanic alluvial fans prograded eastward into the basin and suggest renewed tectonic activity along the Sapphire thrust (Figure 44). Mackie (1986) initially proposed late Cretaceous episodes of Sapphire thrust movement due to provenance cycles recorded in Golden Spike nonvolcanic sandstones. J. W. Sears (personal communication, 1997) postulates that the eastern volcanic eruptions may have created a structural zone of weakness between the Sapphire and Lombard-Elkhorn thrust zones. A decrease in crustal strength in the region of Golden Spike deposition supports reactivated thrust movement of the Sapphire plate (DeCelles and Mitra, 1995).

The remainder of the lower Golden Spike formation includes poorly exposed beds as described in upper sections of the "lower mixed unit" (Gwinn and Mutch, 1965). A reconnaissance survey noted andesitic lava, autoclastic



breccia and mud-rich lahar deposits interfingering with nonvolcanic fluvial sandstone, siltstone, shale and mudstone. Only one other nonvolcanic cobble conglomerate occurs in the Golden Spike Formation and is located in the "middle mixed unit" (Gwinn and Mutch, 1965). This general lack of coarser grained nonvolcanic conglomerates suggests a reduction of tectonic activity within the Sapphire Block.

Implication of Local Stratigraphy on Regional Geology

Opinions differ regarding Cordilleran partitioning and sediment dispersal in the late Cretaceous foreland basin (Gwinn, 1965; Schwartz, 1982; Dickinson et al., 1988; Sears, 1988; et al., in review; Wallace et al., 1990). Deposition typically was wide-spread although foreland basin subsidence was disparate and basement uplift, occurring as early as mid-Cretaceous time, produced disconformities (Schwartz, 1982; Dickinson et al., 1988; Pang and Nummedal, 1995). Wallace et al. (1990) proposed that uplift along the LCL separated the foreland basin during latest Cenomanian to early Turonian time. However, I find the stratigraphic basis of their age interpretation suspect and believe Sears' (1988) suggestion of early Campanian partitioning in the fold-thrust belt to be most plausible.

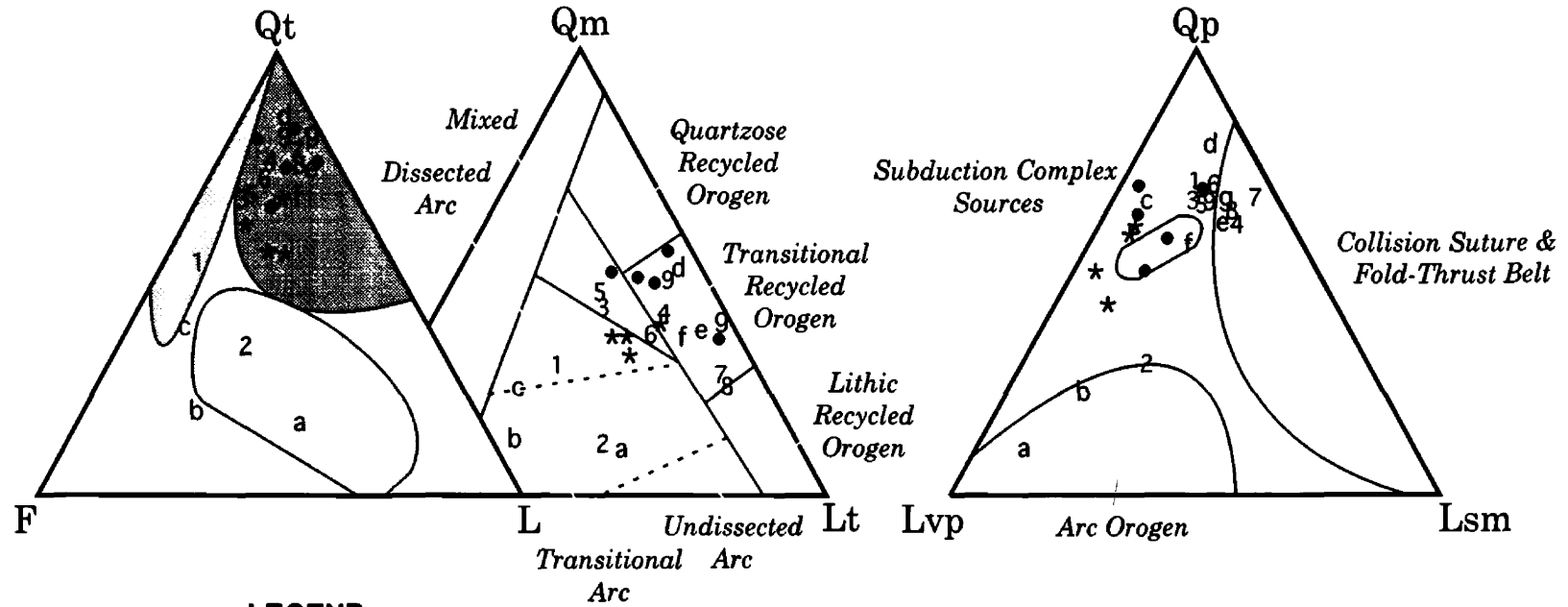
Wallace et al. (1990) allege that the Carten Creek Formation derived from uplift along the LCL because it contains clasts of blue-green argillite that eroded from the Greyson Formation. Provenance analysis conducted for this research disclosed no Greyson argillite in any Carten Creek deposits. I suggest that the clasts in question were either local mudchips that underwent contact-metamorphism from subsequent sill intrusion or green dacite.

According to Wallace et al. (1990), the southern paleocurrent direction indicated in Carten Creek deposits is also the result of uplift along the LCL. My research, like Gwinn's (1965), contends that the Carten Creek Formation derived its sediment from the orogenic wedge to the west. Predominant river

discharge to the south is curious, but likely attributes to high sinuosity in the meandering-fluvial system rather than to a northern provenance.

I resubmit Gwinn's (1965) conviction that early late-Cretaceous deposition correlates across western Montana. For instance, coastal deposition of the Santonian Virgelle sandstone (Larson, 1986), a member of the Milk River Formation, complements the marginal-marine fluvial system proposed for the upper-middle Carten Creek Formation. Depositional environments of the Virgelle include barrier-beach, tidal-inlet channel and brackish marsh (Rice, 1980; Larson, 1986; McCrory and Walker, 1986; Cheel and Leckie, 1990). Carten Creek and Virgelle sandstones are compositionally similar (Figure 45). Both units comprise tan to white sandstone with abundant trough crossbedding, silty mudchips and fossil wood fragments (Rice, 1980; Larson, 1986; McCrory and Walker, 1986; Cheel and Leckie, 1990). Likewise, floodplain facies in the upper Carten Creek Formation also correspond to lagoon and marsh deposits in the Milk River's Deadhorse Coulee Member that overlies the Virgelle (McCrory and Walker, 1986). Other coastal sandstone deposits of similar lithology to the Carten Creek involve the Campanian Two Medicine (lower sandstone facies), upper Campanian Judith River and Maastrichtian Horsethief formations (Viele and Harris, 1965; Rogers, 1993). Since many lithostratigraphic deposits are diachronous from west to east in the foreland basin, correlation of sandstone units suggests a wide-spread time-transgressive progradational shoreline punctuated by the cyclic encroachment of late Cretaceous seas.

Figure 45:
Composition and Tectonic Provenance Comparison
between Upper-Middle Carten Creek and Virgelle Sandstones



LEGEND

- Recycled Orogen
- Continental Block
- Magmatic Arc

- 1 - 9 Carten Creek Sandstone from Measured Section (Locality 1)
- a - g Carten Creek Sandstone from Photomosaic Section (Locality 2)
- Carten Creek Sandstone from Reconnaissance Random Sampling
- * Virgelle Sandstone from Reconnaissance Random Sampling

The shoreline prograded east at ~80km/Ma (Gill and Cobban, 1973 in Rice, 1980) during Virgelle deposition due to the ample supply of sediment carried by river systems (Rice, 1980). Distributary deltas forming along the Cretaceous coast were reworked by wave and tidal activity as identified in the Milk River Formation (Rice, 1980; Larson, 1986; McCrory and Walker, 1986; Cheel and Leckie, 1990). Longshore drift in the Cretaceous seaway generally flowed south, but reversals occurred seasonally (Rice, 1980; Parrish et al., 1984; Cheel and Leckie, 1990). Since Larson (1986) reported northeastern longshore sediment-transport during Virgelle deposition near Wolf Creek, Montana, Santonian Carten Creek fluvial deposits potentially represent part of the deltaic system seasonally feeding the Virgelle sandstone (Figure 46).

Propagation of the western orogenic wedge into central-western Montana locally increased structural deformation. Elevated tectonic activity is represented by erosion and dramatic textural difference between formations. Detailed sedimentologic and stratigraphic research suggests that foreland deposition across the LCL was uninterrupted until early Campanian time. Impressive textural and compositional contrasts within the Campanian Golden Spike Formation reflect multiple sediment sources that include the Sapphire Tectonic Block, Elkhorn Mountain Volcanics and uplift along the LCL.

Subsidence of the Clark Fork Sag behind the active, contemporaneous Lombard-Elkhorn thrust margin implies that the Golden Spike Formation

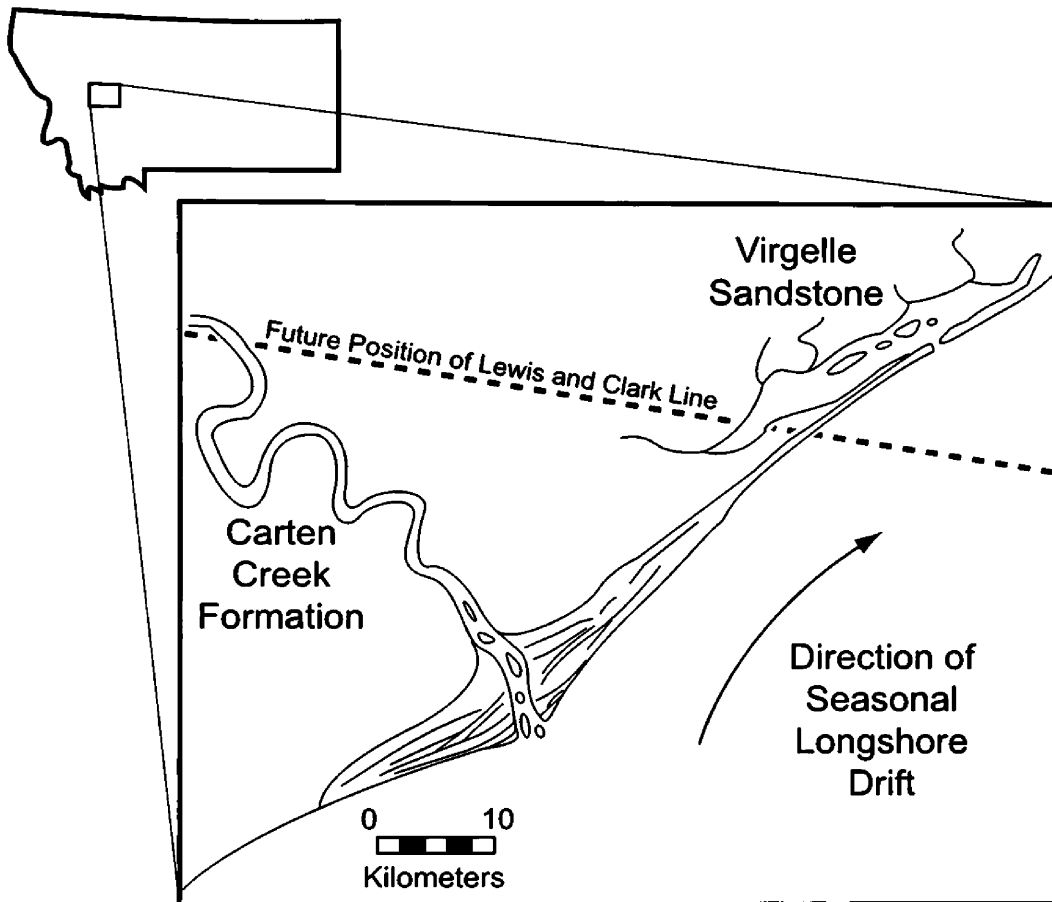


Figure 46: Schematic relationship of Carten Creek and Virgelle deposition during Santonian time. Paleoshoreline and longshore sediment-transport based on Larson (1986). Environmental settings modified from Cheel and Leckie (1990).

developed in a wedge-top depozone (Figure 47) (DeCelles and Giles, 1996).

Consistent with sedimentation atop an orogenic wedge, the Golden Spike Formation thins west in the direction of the thrust belt and thickens east toward the craton (Gwinn and Mutch, 1965; DeCelles and Giles, 1996). Accordingly, cannibalization of and multiple unconformities involving Golden Spike strata are important characteristics of wedge-top deposits (DeCelles and Giles, 1996).

Regional and local unconformities possibly created through eastward propagation of the late Cretaceous orogenic wedge include the following:

- 1) Campanian Golden Spike deposits rest in slight angular unconformity above more gently dipping beds of the Santonian Carten Creek Formation (Gwinn and Mutch, 1965; Mackie, 1986).
- 2) Near the mouth of Brock Creek, tilted basal Golden Spike deposits lie directly beneath volcanic breccias in the formation's uppermost "lower mixed unit" (Gwinn and Mutch, 1965). According to Gwinn and Mutch (1965), this intraformational unconformity may explain the disappearance of megaconglomerate in sections 4 and 5 of T9N-R10W north of the Clark Fork River. However, the lack of megaconglomerate in the northwest may also be attributed to a lateral facies change.
- 3) In the southwest, Golden Spike beds dip towards the southwest and are flatly overlain by early Miocene unconsolidated sediments (Gwinn and Mutch, 1965; Mackie, 1986), although this second regional unconformity could also be the result of post-Cretaceous extension.

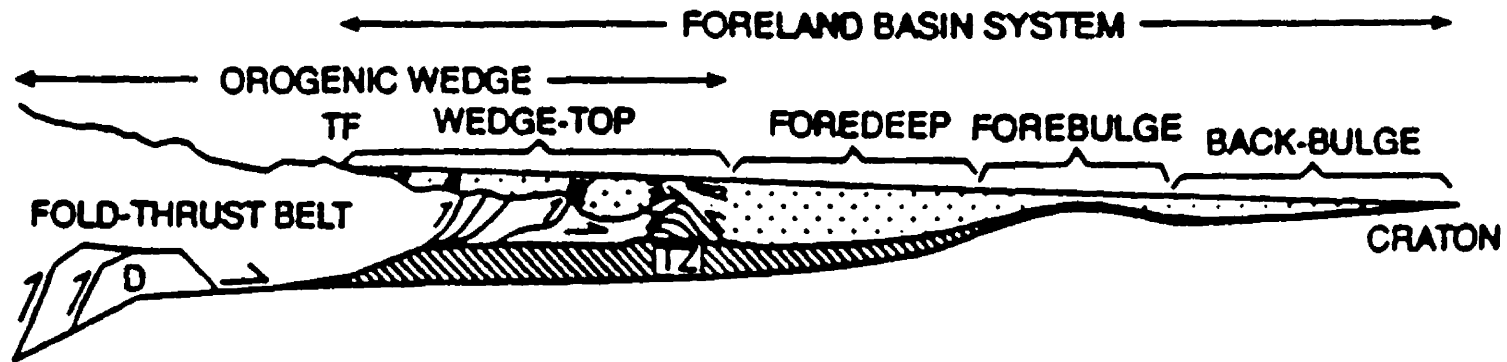


Figure 47: Schematic cross-section of revised foreland basin system by DeCelles and Giles (1996) with labeled depozones at approximately true scale. TF = Topographic front of the fold-thrust belt; D = Duplex in hinterland; TZ = Frontal triangle zone

Correlative deposition of Beaverhead conglomerate above active contemporaneous thrusts (Perry and Sando, 1982) suggests that the wedge-top depozone regionally extended southward, although localized basement uplift partially complicated the fold-thrust belt in south-western Montana (Weimer, 1984; Dickinson et al., 1988). Wilson (1970) described deposits of a major southeast-flowing meandering-river system in the Beaverhead Formation that compare compositionally and texturally to fluvial facies of the lower Golden Spike. Apparently, transverse drainage of the wedge-top basin continued south toward Monida, Montana during Campanian time.

Fluvial deposits in the lower Golden Spike Formation provide clues to the climatic conditions present during deposition. Stratigraphic indicators of climate include local red oxidized paleosols, desiccated caliche nodules and mud drapes in sandstone. Specifically, caliche development represents sporadic or insufficient rainfall generally between 100 and 600mm/yr (Lorenz, 1986; Varricchio, 1993). Lorenz (1981) and Gavin (1986) interpreted similar stratigraphic features present in the correlative Two Medicine Formation as indicative of a seasonal, semi-arid climate with warm temperatures and a long dry season. A seasonal dry climate and prevalent wind direction from the west suggest that the Cordillera produced a rainshadow effect over late Cretaceous deposition in the foreland basin (Carpenter, 1987 in Rogers, 1991; Varricchio, 1993).

Conclusions

- The upper-middle section of the Carten Creek Formation developed during Santonian time in a marginal-marine meandering-fluvial system as suggested by multiple point-bar sequences overlying basal, Coniacian brackish water deposits. Carten Creek sandstone is generally characterized by abundant trough crossbedding, rip-up mud chips and woody debris. Lateral accretion surfaces are common and suggest the high-sinuosity of channels within the formation. The proximity of the Carten Creek river system to a deltaic environment is also implied by local longitudinal bar forms.
- Provenance analysis of the Carten Creek Formation indicates that the sublithic-feldspathic sediment eroded from the Sevier orogenic wedge to the west. Lithic framework-grains of dacite and andesite record earlier volcanism within the fold-thrust belt that is presumably related to the Idaho Batholith.
- Reinterpretation of lower Golden Spike deposits suggests that sandy cobble conglomerate and megaconglomerate resulted respectively from noncohesive nonvolcanic-debris flows with local reworking by braided streams and multiple, superficially erosive lahars. The megaconglomerate facies specifically records lahar deposition related to a concurrent volcanic-event occurring in the foreland basin system. Other Golden Spike facies

represent a low-sinuosity meandering-river that drained the Clark Fork Sag towards the south and may connect to a similar fluvial system in the correlative Beaverhead Formation.

- Compositional analysis of lower Golden Spike sandstone and conglomerate implies various provenance for the formation. Previous work by Gwinn and Mutch (1965) and Mackie (1986) also reported multiple provenance as evidenced by opposing paleocurrent directions of the interbedded volcanic and nonvolcanic strata. Three sources of Golden Spike sediment include the Sapphire Tectonic Block, Elkhorn Mountain Volcanics and uplift along the Lewis and Clark Line.
- Collectively, the Carten Creek and Golden Spike formations record Coniacian to Maastrichtian deposition in the Northern Rocky Mountain foreland basin of central-western Montana. Lithostratigraphic correlation with other late Cretaceous shoreface and near-shore deposits, such as the Santonian Virgelle Sandstone, implies that Coniacian-Santonian Carten Creek rivers provided sediment to a wide-spread, time-transgressive progradational shoreline. The Campanian to Maastrichtian Golden Spike Formation represents wedge-top deposition above the Sevier fold-thrust belt that was punctuated by active volcanism in the foreland basin. This succession of late Cretaceous deposition in central-western Montana suggests that uplift along the Lewis and Clark Line and subsequent partitioning of the Cordillera occurred during the early Campanian Age.

Suggestions for Future Study

These areas of study would provide additional insight into the Carten Creek and Golden Spike formations:

- Detailed characterization of the lower Carten Creek Formation including interpretation of deposystems and provenance analysis.
- Characterization and mapping of individual volcanogenic flows and deposits in the Golden Spike Formation.
- Reconstruction by lithofacies assemblage of the Garrison-area geologic maps made by Gwinn and Mutch (1965) and Mackie (1986).
- Magnetostratigraphic survey of clasts in the megaconglomerate facies of the Golden Spike Formation to determine lahar temperature during deposition.

Bibliography

- Alt, D., and Hyndman, D. W., 1986, *Roadside Geology of Montana: Missoula, MT*, Mountain Press, 427 p.
- Bennett, E. H., and Kiilsgaard, T. H., 1983, The Geology of the Idaho Batholith (Atlanta Lobe) in the Challis 2⁰ Quadrangle, Idaho: *Geological Society of America Abstracts with Programs*, v. 15, no. 5, p. 334.
- Blair, T. C., and McPherson, J. G., 1994, Alluvial Fans and Their Natural Distinction from Rivers based on Morphology, Hydraulic Processes, Sedimentary Processes, and Facies Assemblages: *Journal of Sedimentary Research*, v. 64, no. 3, p. 450-489.
- Boggs, S. J., 1995, *Principles of Sedimentology and Stratigraphy*: Englewood Cliffs, NJ, Prentice Hall, 774 p.
- Cheel, R. J., and Leckie, D. A., 1990, A Tidal-Inlet Complex in the Cretaceous Epeiric Sea of North America: Virgelle Member, Milk River Formation, Southern Alberta, Canada: *Sedimentology*, v. 37, p. 67-81.
- Collinson, J. D., and Thompson, D. B., 1982, *Sedimentary Structures*: London, England, Unwin Hyman Ltd., 207 p.
- DeCelles, P. G., and Giles, K. A., 1996, Foreland Basin Systems: *Basin Research*, v. 8, p. 105-123.
- DeCelles, P. G., and Mitra, G., 1995, History of the Sevier Orogenic Wedge in terms of Critical Taper Models, Northeast Utah and Southwest Wyoming: *Geological Society of America Bulletin*, v. 107, no. 4, p. 454-462.
- Dickinson, W. R., 1970, Interpreting Detrital Modes of Graywacke and Arkose: *Journal of Sedimentary Petrology*, v. 40, p. 695-707.
- Dickinson, W. R., Klute, M. A., Hayes, M. J., Janecke, S. U., Lundin, E. R., McKittrick, M. A., and Olivares, M. D., 1988, Paleogeographic and Paleotectonic Setting of Laramide Sedimentary Basins in the Central Rocky Mountain Region: *Geological Society of America Bulletin*, v. 100, p. 1023-1039.
- Dickinson, W. R., and Suczek, C. Z., 1979, Plate Tectonics and Sandstone Compositions: *American Association of Petroleum Geologists Bulletin*, v. 63, no. 12, p. 2164-2182.

- Gavin, W. M. B., 1986, A Paleoenvironmental Reconstruction of the Cretaceous Willow Creek Anticline Dinosaur Nesting Locality: North Central Montana [MS Thesis]: Montana State University, 148 p.
- Graham, S. A., Hendrix, M. S., Wang, L. B., and Carroll, A. R., 1993, Collisional Successor Basins of Western China: Impact of Tectonic Inheritance on Sand Composition: Geological Society of America Bulletin, v. 105, no. 3, p. 323-344.
- Gwinn, V. E., 1965, Cretaceous Rocks of the Clark Fork Valley, Central Western Montana, Geology of the Flint Creek Range, Montana: 16th Annual Field Conference, Billings Geological Society, p. 34-57.
- Gwinn, V. E., and Mutch, T. A., 1965, Intertongued Upper Cretaceous Volcanic and Nonvolcanic Rocks, Central-Western Montana: Geological Society of America Bulletin, v. 76, p. 1125-1144.
- Hamilton, W., 1983, Depth-Related Contrasts between Idaho and Sierra Nevada Batholiths: Geological Society of America Abstracts with Programs, v. 15, no. 5, p. 334.
- Hyndman, D. W., 1977, Mylonitic Detachment Zone and the Sapphire Tectonic Block, Field Conference No. 1, 30th Annual Meeting Rocky Mountain Section, Geological Society of America, p. 25-31.
- Hyndman, D. W., 1979, Major Tectonic Elements and Tectonic Problems along the line from Northeastern Oregon to West-Central Montana: Geological Society of America Map and Chart Series, MC-28c.
- Johnson, A. M., 1965, A Model for Debris Flow [PhD Dissertation]: Pennsylvania State University, 232 p.
- Jordan, B. T., and Rodgers, D. W., 1994, Systematic Variation of Emplacement Pressure of the Southeastern Atlanta Lobe, Idaho Batholith: Geological Society of America Abstracts with Programs, v. 26, no. 6, p. 21.
- Jordan, T. E., 1981, Thrust Loads and Foreland Basin Evolution, Cretaceous, Western United States: American Association of Petroleum Geologists Bulletin, v. 65, no. 12, p. 2506-2520.
- Larson, J. E., 1986, Stratigraphy and Sedimentation of the Upper Cretaceous Montana Group of Northwestern Montana, with Detailed Bedform Analysis of Two Medicine Formation Complexly Cross-bedded Sandstone [MS Thesis]: University of Montana, 105 p.

- Lorenz, J. C., 1981, Sedimentary and Tectonic History of the Two Medicine Formation, Late Cretaceous (Campanian), Northwestern Montana [PhD Dissertation]: Princeton University, 215 p.
- Mack, G. H., and James, W. C., 1992, Paleosols for Sedimentologists: Geological Society of America Short Course Notes, p. 127.
- Mackie, T. L., 1986, Tectonic Influences on the Petrology, Stratigraphy and Structures of the Upper Cretaceous Golden Spike Fm., Central-Western Montana [MS Thesis]: Washington State University, 132 p.
- Mallory, W. W., 1972, Geologic Atlas of the Rocky Mountain Region: Denver, CO, Rocky Mountain Association of Geologists, p. 331.
- McCrory, V. L. C., and Walker, R. G., 1986, A Storm and Tidally-Influenced Prograding Shoreline -- Upper Cretaceous Milk River Formation of Southern Alberta, Canada: *Sedimentology*, v. 33, p. 47-60.
- Miall, A. D., 1984, Principles of Sedimentary Basin Analysis: New York, NY, Springer-Verlag Inc., 668 p.
- Myers, P. E., and Carlson, D. H., 1982, Tectonic Elements and Plutonic Evolution of the Mesozoic Cratonic Margin, South Fork of the Clearwater River, Idaho: Geological Society of America Abstracts with Programs, v. 14, no. 6, p. 343.
- Nemec, W., and Steel, R. J., 1984, Alluvial and Coastal Conglomerates: Their Significant Features and Some Comments on Gravelly Massflow Deposits, *in* Koster, E. H., and Steel, R. J., eds., *Sedimentology of Gravels and Conglomerates: Canadian Society of Petroleum Geologists Memoir*, 10, p. 295-320.
- Palmer, B. A., Alloway, B. V., and Neall, V. E., 1991, Volcanic-Debris-Avalanche Deposits in New Zealand -- Lithofacies Organization in Unconfined, Wet-Avalanche Flows, *in* Fisher, R. V., and Smith, G. A., eds., *Sedimentation in Volcanic Settings: Society for Sedimentary Geology (SEPM) Special Publication*, 45, p. 89-106.
- Pang, M., and Nummedal, D., 1995, Flexural Subsidence and Basement Tectonics of the Cretaceous Western Interior Basin, United States: *Geology*, v. 23, no. 2, p. 173-176.
- Parrish, J. T., Gaynor, G. C., and Swift, D. J. P., 1984, Circulation in the Cretaceous Western Interior Seaway of North America, a review, *in* Stott,

- D. F., and Glass, D. J., eds., *The Mesozoic of Middle North America*: Canadian Society of Petroleum Geologists, Memoir 9, p. 221-231.
- Perry, W. J. J., and Sando, W. J., 1982, Sequence of Deformation of Cordilleran Thrust Belt in Lima, Montana Region, *in* Blake-Powers, R., ed., *Geologic Studies of Cordilleran Thrust Belt*, Rocky Mountain Association of Geologists, p. 137-144.
- Peterson, J., 1981, General Stratigraphy and Regional Paleostructure of the Western Montana Overthrust Belt, *in* Tucker, T. E., ed., *Field Conference and Symposium Guidebook to Southwest Montana*: Montana Geological Society, p. 5-35.
- Reynolds, P. H., 1983, *Structural Geology of the Blackfoot Thrust System in the Cramer Creek Area, Missoula County, Montana [MS Thesis]*: University of Montana, 70 p.
- Rice, D. D., 1980, Coastal and Deltaic Sedimentation of Upper Cretaceous Eagle Sandstone: Relation to Shallow Gas Accumulations, North-Central Montana: *American Association of Petroleum Geologists Bulletin*, v. 64, no. 3, p. 316-338.
- Robinson, G. D., Klepper, M. R., and Obradovich, J. D., 1968, Overlapping Plutonism, Volcanism, and Tectonism in the Boulder Batholith Region, Western Montana: *Geological Society of America Memoir*, 116, p. 557-575.
- Rogers, R. R., 1990, Taphonomy of Three Dinosaur Bone Beds in the Upper Cretaceous Two Medicine Formation of Northwestern Montana: Evidence for Drought-Related Mortality: *Palaios*, v. 5, p. 394-413.
- Rogers, R. R., 1993, Marine Facies of the Judith River Formation (Campanian) in the Type Area, North-Central Montana, *in* Hunter, L. D. V., ed., *Energy and Mineral Resources of Central Montana: 1993 Field Conference Guidebook*: Montana Geological Society, p. 61-69.
- Ross, C. P., Andrews, D. A., and Witkind, I. J., 1955, *Geologic Map of Montana*: United States Geological Survey, scale 1:500000.
- Ruppel, E. T., Wallace, C. A., Schmidt, R. G., and Lopez, D. A., 1981, Preliminary Interpretation of the Thrust Belt in Southwest and West-Central Montana and East-Central Idaho, *Field Conference and Symposium Guidebook to Southwest Montana*: Montana Geological Society, p. 139-159.

- Schwartz, R. K., 1982, Broken Early Cretaceous Foreland Basin in Southwestern Montana: Sedimentation Related to Tectonism, *in* Blake-Powers, R., ed., *Geologic Studies of Cordilleran Thrust Belt*, Rocky Mountain Association of Geologists, p. 159-183.
- Schwartz, R. K., and DeCelles, P. G., 1988, Cordilleran Foreland Basin Evolution in response to Interactive Cretaceous Thrusting and Foreland Partitioning, Southwestern Montana, *in* Schmidt, C. J., and Perry, W. J. J., eds., *Interaction of the Rocky Mountain Foreland and the Cordilleran Thrust Belt: Geological Society of America Memoir*, 171, p. 489-513.
- Sears, J. W., 1988, Two Major Thrust Slabs in the West-Central Montana Cordillera, *in* Schmidt, C. J., and Perry, W. J. J., eds., *Interaction of the Rocky Mountain Foreland and the Cordilleran Thrust Belt: Geological Society of America Memoir*, 171, p. 165-170.
- Sears, J. W., 1994, Thrust Rotation of the Belt Basin, Canada and United States: *Northwest Geology*, v. 23, p. 81-92.
- Sears, J. W., Hendrix, M. S., and Waddell, A. M., in review, Late Cretaceous-Paleocene Sinistral Shear along the Lewis and Clark Line and Its Influence on Foreland Basin Sedimentation, Montana.
- Smith, G. A., and Lowe, D. R., 1991, Lahars: Volcano-Hydrologic Events and Deposition in the Debris Flow -- Hyperconcentrated Flow Continuum, *in* Fisher, R. V., and Smith, G. A., eds., *Sedimentation in Volcanic Settings: Society for Sedimentary Geology (SEPM) Special Publication*, 45, p. 59-70.
- Smith, R. C. M., 1991, Landscape Response to a Major Ignimbrite Eruption, Taupo Volcanic Center, New Zealand, *in* Fisher, R. V., and Smith, G. A., eds., *Sedimentation in Volcanic Settings: Society for Sedimentary Geology (SEPM) Special Publication*, 45, p. 123-137.
- Sylvester, A. G., 1988, Strike-Slip Faults: *Geologic Society of America Bulletin*, v. 100, p. 1666-1703.
- Tucker, M. E., 1991, *Sedimentary Petrology: an Introduction to the Origin of Sedimentary Rocks*: Oxford, England, Blackwell Scientific Publications, 260 p.
- Varricchio, D., 1993, Montana Climatic Changes Associated with the Cretaceous Claggett and Bearpaw Transgressions, *in* Hunter, L. D. V., ed., *Energy and Mineral Resources of Central Montana: 1993 Field Conference Guidebook: Montana Geological Society*, p. 97-102.

- Viele, G. W., and Harris, F. G. I., 1965, Montana Group Stratigraphy, Lewis and Clark County, Montana: American Association of Petroleum Geologists Bulletin, v. 49, no. 4, p. 379-417.
- Waddell, A. M., and Webb, B., 1997, Stratigraphic and Sedimentologic Analysis of Nonvolcanic Strata in the Upper Cretaceous Golden Spike Formation, Western Montana: American Association of Petroleum Geologists Annual Convention Program with Abstracts, v. 6, p. A121.
- Walker, R. G., 1984, Facies Model, Geosciences Canada Reprint Series 1: Toronto, Canada, Geological Association of Canada, p. 317.
- Wallace, C. A., Lidke, D. J., and Schmidt, R. G., 1990, Faults of the Central Part of the Lewis and Clark Line and Fragmentation of the Late Cretaceous Foreland Basin in West-Central Montana: Geological Society of America Bulletin, v. 102, p. 1021-1037.
- Weimer, R. J., 1984, Relationship of Unconformities, Tectonics, and Sea Level Changes in the Cretaceous of the Western Interior, United States, *in* Schlee, J. S., ed., Interregional Unconformities and Hydrocarbon Accumulation: American Association of Petroleum Geologists Memoir, 36, p. 7-35.
- Wilson, M. D., 1970, Upper Cretaceous-Paleocene Synorogenic Conglomerates of Southwestern Montana: American Association of Petroleum Geologists Bulletin, v. 54, no. 10, p. 1843-1867.
- Winston, D., 1986, Sedimentation and Tectonics of the Middle Proterozoic Belt Basin and Their Influence on Phanerozoic Compression and Extension in Western Montana and Northern Idaho, *in* Peterson, J., ed., Paleotectonics and Sedimentation in the Rocky Mountain Region, United States: American Association of Petroleum Geologists Memoir, 41, p. 87-118.
- Ziebell, W. R., 1943, Minerals of the Idaho Batholith [MS Thesis]: University of Illinois, 44 p.

Appendix

		PAGE
PHOTOMOSAICS		
<hr/>		
Plate 1a-f	Carten Creek Formation - Locality 2	(in pocket)
Plate 2	Golden Spike Formation - Locality 4	(in pocket)
Plate 3	Golden Spike Frm. - East-side of Loc. 5	(in pocket)
Plate 4a,b & c	Golden Spike Formation - Locality 5	(in pocket)
Plate 5	Golden Spike Formation - Locality 6	(in pocket)
Plate 6a & b	Golden Spike Frm. - South Hill of Loc. 6	(in pocket)
POINT COUNT DATA		
<hr/>		
Carten Creek Formation and Virgelle Sandstone		117
Golden Spike Formation		119
CLAST COUNT DATA		
<hr/>		
Map of Sampling Localities		121
Clast Counts in Facing Stratigraphic Order		
SCC CC1	Population Totals	122
	Area-based Totals and Ratios	124
SCC CC2	Population Totals	127
	Area-based Totals and Ratios	128
CB CC1,2 & 3	Population and Area-based Totals	131
CB CC4	Population Totals	132
	Area-based Totals and Ratios	133
CB CC5	Population Totals	136
	Area-based Totals and Ratios	138
CB CC6	Population Totals	142
	Area-based Totals and Ratios	143
SCC CC3	Population Totals	145
	Area-based Totals and Ratios	146
SCC CC4	Population and Area-based Totals	148

POINT COUNT DATA

Sample#	Location/description	Q m	Q p	Cht.	K	P	Lv	Lp	Lcl	Lnoncl	Lmsed	Lm	unid	L	bt	ms	chl	pyrx	heav.	Cmt	Matr.	Unid T	CHK
CARTEN CREEK FRM																							
AW Kv 4-1	Garrison-random	185	24	30	21	49	27	11	3			13	5	1						94	36	1	500
AW Kv 4-2A	Garrison-random	188	72	24	1	17	16	21	2	2	1									135	21		500
AW Kvc 4-3	Garr. meas. sect. -4m	91	33	33	10	132	7	9	3		11			9					1	141	20		500
AW Kvc 4-4	Garr. meas. sect. -24m	33	6	35	4	131	60	11	7		29		1	2					1	157	23		500
AW Kvc 4-5	Garr. meas. sect. -35m	147	43	32	15	84	15	6	5		14			4	1					87	47		500
AW Kvc 4-6	Garr. meas. sect. -52m	144	47	54	19	42	14	9	11		28	1		3						97	31		500
AW Kvc 4-7	Garr. meas. sect. -75m	149	40	27	18	73	10	9	7		10									92	65		500
AW Kvc 4-8	Garr. meas. sect. -92m	119	56	45	9	58	11	11	12		14			4					5	106	50		500
AW Kvc 4-9	Garr. meas. sect. -114m	95	72	80	4	35	11	6	22	1	30	11								90	43		500
AW Kvc 4-10	Garr. meas. sect. 130m	82	64	83	3	35	21	11	22	2	30	1		2						77	67		500
AW Kvc 4-11	Garr. meas. sect. -140m	178	64	39	5	36	19	7	11		18			1	1					69	52		500
AW Kvc 5-1	photomosaic plate 1e&f	109	53	53	2	15	15	9	7	8	17		1	1					14	112	84		500
AW Kvc 5-2	photomosaic pl. 1d,e&f	127	62	57	13	27	20	13	22	2	17		2	2						103	32	1	500
AW Kvc 5-3	photomosaic pl. 1c&d	172	64	49	5	29	15	2	6		11			2	2					111	32		500
AW Kvc 5-4	photomosaic plate 1e	113	36	56	7	48	30	16	13		17		2	1	1				3	106	51		500
AW Kvc 5-5	photomosaic plate 1b	73	21	22	7	168	9	12	2		1		5	8	3				3	90	76		500
AW Kvc 5-6	photomosaic plate 1a&b	34	8	10	5	189	10	42	4	2	4		9	1	1		2			159	20		500
AW Kvc 5-7	photomosaic plate 1a	26	2	12	1	128	50	81	5		7				1				1	168	18		500
AW Kcc 1A	random-Warm Springs	114	53	57		15	20	32	9	3	16	1	1	2						116	61		500
AW Kcc 1B	random-Warm Springs	153	47	32	21	24	10	6			21		1	6	1					105	71	2	500
AW Kcc 1C	random	130	34	33	4	27	14	18	2	1	4		5	2						177	49		500
VIRGELLE SANDSTONE																							
AW Kv 1-1	Route 278 roadcut	88	38	21	6	63	36	17			4	1	7	8	3					177	30	1	500
AW Kv 1-2	Route 278 roadcut	100	31	17	8	57	27	24	2		3	7	7	6						196	15		500
AW Kv 2-1	Route 200 roadcut	118	58	21		89	8	32			6	3	2	2						142	17	2	500
AW Kv 3-1	Hoodoo locale	132	63	30	1	55	20	33	5		3	4	1	4	6	3				116	24		500

POINT COUNT DATA

Sample#	QM	F	LT	QT	F	L	CP	LVP	LSM	QM	P	K	P/F	%Mica	%hvy	%CaCO3
CARTEN CREEK FRM																
AW Kv 4-1	50.3	19.0	30.7	64.9	19.0	16.0	50.0	35.2	14.8	72.5	19.2	8.2	0.7	0.2	0.0	0.0
AW Kv 4-2A	54.7	5.2	40.1	82.8	5.2	11.9	69.6	26.8	3.6	91.3	8.3	0.5	0.9	0.0	0.0	0.4
Std. Dev.	3.1	9.8	6.7	12.7	9.8	2.9	13.8	5.9	7.9	13.2	7.8	5.5	0.2	0.1	0.0	0.3
AW Kvc 4-3	27.7	43.2	29.2	51.1	43.2	5.8	68.8	16.7	14.6	39.1	56.7	4.3	0.9	1.8	0.2	0.0
AW Kvc 4-4	10.4	42.6	47.0	32.5	42.6	24.9	27.7	48.0	24.3	19.6	78.0	2.4	1.0	0.4	0.2	0.0
AW Kvc 4-5	40.7	27.4	31.9	65.4	27.4	7.2	65.2	18.3	16.5	59.8	34.1	6.1	0.8	1.0	0.0	0.0
AW Kvc 4-6	39.0	16.5	44.4	74.0	16.5	9.5	61.6	14.0	24.4	70.2	20.5	9.3	0.7	0.6	0.0	0.0
AW Kvc 4-7	43.4	26.5	30.0	65.9	26.5	7.6	65.0	18.4	16.5	62.1	30.4	7.5	0.8	0.0	0.0	0.0
AW Kvc 4-8	35.5	20.0	44.5	69.9	20.0	10.1	67.8	14.8	17.4	64.0	31.2	4.8	0.9	0.8	1.0	0.0
AW Kvc 4-9	25.9	10.6	63.5	75.5	10.6	13.9	65.2	7.3	27.5	70.9	26.1	3.0	0.9	0.0	0.0	0.2
AW Kvc 4-10	23.2	10.7	66.1	73.2	10.7	16.1	62.8	13.7	23.5	68.3	29.2	2.5	0.9	0.4	0.0	0.4
AW Kvc 4-11	47.1	10.8	42.1	79.1	10.8	10.1	65.2	16.5	18.4	81.3	16.4	2.3	0.9	0.2	0.0	0.0
Std. Dev.	13.7	22.8	9.1	19.8	22.8	3.0	2.5	0.1	2.7	29.9	28.4	1.4	0.0	1.1	0.1	0.0
AW Kvc 5-1	37.7	5.9	56.4	80.3	5.9	13.8	65.4	14.8	19.8	86.5	11.9	1.6	0.9	0.2	2.8	1.6
AW Kvc 5-2	35.1	11.0	53.9	72.7	11.0	16.3	61.7	17.1	21.2	76.0	16.2	7.8	0.7	0.4	0.0	0.4
AW Kvc 5-3	48.7	9.6	41.6	83.9	9.6	6.5	76.9	11.6	11.6	83.5	14.1	2.4	0.9	0.8	0.0	0.0
AW Kvc 5-4	33.4	16.3	50.3	65.7	16.3	18.0	54.8	27.4	17.9	67.3	28.6	4.2	0.9	0.4	0.6	0.0
AW Kvc 5-5	22.8	54.7	22.5	36.6	54.7	8.8	64.2	31.3	4.5	29.4	67.7	2.8	1.0	2.2	0.6	0.0
AW Kvc 5-6	10.7	61.2	28.1	17.7	61.2	21.1	22.5	65.0	12.5	14.9	82.9	2.2	1.0	0.4	0.0	0.4
AW Kvc 5-7	8.3	41.3	50.3	15.1	41.3	43.6	8.9	83.4	7.6	16.8	82.6	0.6	1.0	0.2	0.2	0.0
Std. Dev.	20.8	25.1	4.3	46.1	25.1	21.0	40.0	48.5	8.6	49.3	50.0	0.7	0.1	0.0	1.8	1.1
AW Kcc 1A	35.5	4.7	59.8	74.8	4.7	20.6	57.6	27.2	15.2	88.4	11.6	0.0	1.0	0.4	0.0	0.6
AW Kcc 1B	48.6	14.3	37.1	80.3	14.3	5.4	68.1	13.8	18.1	77.3	12.1	10.6	0.5	1.4	0.0	0.0
AW Kcc 1C	47.8	11.4	40.8	73.9	11.4	14.7	63.2	30.2	6.6	80.7	16.8	2.5	0.9	0.4	0.0	0.2
Std. Dev.	8.7	4.8	13.4	0.6	4.8	4.1	4.0	2.1	6.1	5.4	3.6	1.8	0.1	0.0	0.0	0.3
VIRGELLE SANDSTONE																
AW Kv 1-1	31.3	24.6	44.1	53.7	24.6	21.7	50.4	45.3	4.3	56.1	40.1	3.8	0.9	2.2	0.0	0.0
AW Kv 1-2	35.3	23.0	41.7	53.4	23.0	23.7	43.2	45.9	10.8	60.6	34.5	4.8	0.9	1.2	0.0	0.0
AW Kv 2-1	35.0	26.4	38.6	60.2	26.4	13.4	61.7	31.3	7.0	57.0	43.0	0.0	1.0	0.4	0.0	0.0
AW Kv 3-1	38.0	16.1	45.8	65.7	16.1	18.2	58.9	33.5	7.6	70.2	29.3	0.5	1.0	2.6	0.0	0.0
Std. Dev.	4.8	6.0	1.2	8.5	6.0	2.5	6.0	8.3	2.3	10.0	7.7	2.3	0.0	0.3	0.0	0.0

POINT COUNT DATA

Sample#	Location/description	Q m	Q p	Cht.	K	P	Lv	Lp	Lcl	Lnocl	Lmsed	Lm	unid	L	bt	ms	chl	pyrx	heav.	Cmt	Matr.	Unid T	CHK	
GOLDEN SPIKE FRM																								
Aw Kgs 1-34	pebble mudstone	80	19	24	1	3	17	3		31	5		2							80	235	500		
AW Kgs 1-40	Moby Dick	218	56	19	9	12	35	16			3		1							108	21	2	500	
AW Kgs 1-4	Moby Dick	142	57	19	3	12	74	17	1		2									102	71	500		
AW Kgs 1E	float ss (east Loc. 5)	103	50	39	3	1	75	10			8		8							115	86	2	500	
Aw Kgs 1-33A	east Loc. 5 white ss	132	63	13	12	22	27	19					1							169	39	3	500	
Aw Kgs 1-33B	east Loc. 5 white ss	76	65	38	14	12	64	30			7								1	140	52	1	500	
Aw Kgs 1-21	east Loc. 5 fluvial ss	110	40	83		1	34	5	4	24	5	1	3							168	19	3	500	
Aw Kgs 1-23	east Loc. 5 fluvial ss	212	43	32	2	1	25	4			2		1						1	137	39	1	500	
Aw Kgs 1-24	east Loc. 5 fluvial ss	159	29	19	5	5	22	3		6	5		4	1	1					180	58	3	500	
AW Kgs 1-25	east Loc. 5 fluvial ss	162	24	15	7	5	17	4		5	6		2	1		1				183	67	1	500	
AW Kgs 3-4	Loc. 4 fluvial ss	144	39	88		22	8	2	12	29	20									70	66	500		
AW Kgs 3-5	Loc. 4 fluvial ss	147	46	65		14	4	2	4	7	15			2						100	93	1	500	
Aw Kgs 3-6	Loc. 4 fluvial ss	98	35	88		21	10	1	18	20	35		2	4					1	96	70	1	500	
AW Kgs 2-11	ss in Loc. 6 SCC	119	63	71		6	4	18			34		2			1				112	70	500		
AW Kgs 3-1	ss in Loc. 4 SCC	83	24	17		8	20	49	68	28	1	3								93	106	500		
AW Kgs 3-2	ss in Loc. 4 SCC	109	79	71		25	8	3	8	1	47		1			1				88	59	500		
AW Kgs 3-3	ss in Loc. 4 SCC	115	49	85		27	22	3	24		18	1	1	1		1				62	90	1	500	
AW Kgs 4-1	ss in Loc. 3 SCC	118	89	90		2	2	1	10	1	32	2								96	57	500		
AW Kgs 1-7	Loc. 5 matrix	27	10	12	6	57	90	8	11	29			7	2	6				15	70	146	4	500	
AW Kgs 1-2	Loc. 5 matrix	102	18	20	11	23	20	6	7	21		2		2	5					2	43	217	1	500
AW Kgs 1-16	Loc. 5 St. 0+1 matr	38	8	5	2	24	89	5		5			3							6	25	287	3	500
AW Kgs 1-17	Loc. 5 St. 1+2 matr	160	27	22	5	22	62	8		6			2							76	104	6	500	
AW Kgs 1-37	Loc. 5 St. 3+1 matr	64	13	14	3	8	17	5		5			4							1	69	294	3	500
AW Kgs 1-41	Loc.5 matrix plate 2	50	13	21	2	71	81	6	3	12	2		3	3		1				2	34	193	3	500
AW Kgs 2-12	Loc. 6 CB matrix	66	20	22		44	50	6	1	10	6		3	3		3				51	214	1	500	
AW Kgs 2-2	s hill Loc 6 SCC mtr	96	61	54	3	8	45	12		17	8		3							95	98	500		
AW Kgs 3-7	s hill Loc 6 SCC mtr	95	19	95		4	11	30	75	46			2							77	46	500		
AW Kgs 4-2	s hill Loc 6 SCC mtr	86	28	94		4	11	46	50	47			3							91	40	500		

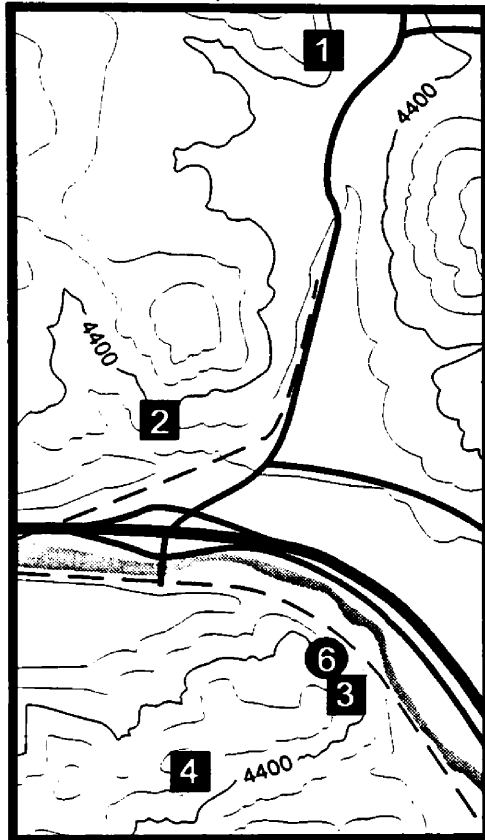
POINT COUNT DATA

Sample#	QM	F	LT	QT	F	L	QP	LVP	LSM	QM	P	K	P/F	%Mica	%hvy	%CaCO3
GOLDEN SPIKE FRM																
Aw Kgs 1-34	43.2	2.2	54.6	69.2	2.2	28.6	43.4	20.2	36.4	95.2	3.6	1.2	0.8	0.0	0.0	6.2
Std. Dev.	-	-	-	-	-	-	-	-	-	-	-	-	-	-	-	-
AW Kgs 1-40	59.2	5.7	35.1	80.4	5.7	13.9	58.1	39.5	2.3	91.2	5.0	3.8	0.6	0.2	0.0	0.0
AW Kgs 1-4	43.4	4.6	52.0	67.3	4.6	28.1	44.7	53.5	1.8	90.4	7.6	1.9	0.8	0.0	0.0	0.0
Std. Dev.	11.2	0.8	12.0	9.3	0.8	10.1	9.5	9.9	0.4	0.5	1.9	1.3	0.2	0.1	0.0	0.0
AW Kgs 1E	34.7	1.3	64.0	67.3	1.3	31.3	48.9	46.7	4.4	96.3	0.9	2.8	0.3	0.0	0.0	0.0
Aw Kgs 1-33A	45.7	11.8	42.6	72.0	11.8	16.3	62.3	37.7	0.0	79.5	13.3	7.2	0.6	0.0	0.0	0.0
Aw Kgs 1-33B	24.8	8.5	66.7	60.8	8.5	30.7	50.5	46.1	3.4	74.5	11.8	13.7	0.5	0.0	0.2	0.0
Aw Kgs 1-21	35.5	0.3	64.2	76.8	0.3	22.9	62.8	19.9	17.3	99.1	0.9	0.0	1.0	0.0	0.0	4.8
Aw Kgs 1-23	65.8	0.9	33.2	89.8	0.9	9.3	70.8	27.4	1.9	98.6	0.5	0.9	0.3	0.0	0.2	0.0
Aw Kgs 1-24	61.9	3.9	34.2	82.5	3.9	13.6	57.1	29.8	13.1	94.1	3.0	3.0	0.5	0.4	0.0	1.2
AW Kgs 1-25	65.6	4.9	29.6	83.8	4.9	11.3	54.9	29.6	15.5	93.1	2.9	4.0	0.4	0.4	0.0	1.0
AW Kgs 3-4	39.6	6.0	54.4	79.9	6.0	14.0	64.1	5.1	30.8	86.7	13.3	0.0	1.0	0.0	0.0	5.8
AW Kgs 3-5	48.4	4.6	47.0	89.8	4.6	5.6	77.6	4.2	18.2	91.3	8.7	0.0	1.0	0.4	0.0	1.4
Aw Kgs 3-6	29.9	6.4	63.7	78.0	6.4	15.5	59.4	5.3	35.3	82.4	17.6	0.0	1.0	0.8	0.2	4.0
Std. Dev.	3.4	3.6	0.2	7.6	3.6	11.1	7.4	29.3	21.8	9.8	11.8	2.0	0.5	0.6	0.1	2.8
AW Kgs 2-11	37.5	1.9	60.6	90.5	1.9	7.6	70.5	2.1	27.4	95.2	4.8	0.0	1.0	0.2	0.0	0.0
AW Kgs 3-1	27.6	2.7	69.8	50.5	2.7	46.8	19.8	9.7	70.5	91.2	8.8	0.0	1.0	0.0	0.0	13.6
AW Kgs 3-2	31.0	7.1	61.9	86.9	7.1	6.0	69.1	5.1	25.8	81.3	18.7	0.0	1.0	0.2	0.0	0.2
AW Kgs 3-3	33.3	7.8	58.8	77.4	7.8	14.8	66.3	12.4	21.3	81.0	19.0	0.0	1.0	0.4	0.0	0.0
AW Kgs 4-1	34.0	0.6	65.4	94.8	0.6	4.6	78.9	1.3	19.8	98.3	1.7	0.0	1.0	0.0	0.0	0.2
Std. Dev.	2.5	0.9	3.4	3.0	0.9	2.1	5.9	0.6	5.3	2.2	2.2	0.0	0.0	0.1	0.0	0.1
AW Kgs 1-7	10.5	24.5	65.0	19.1	24.5	56.4	13.8	61.3	25.0	30.0	63.3	6.7	0.9	1.6	3.0	5.8
AW Kgs 1-2	44.3	14.8	40.9	60.9	14.8	24.3	40.4	27.7	31.9	75.0	16.9	8.1	0.7	1.4	0.4	4.2
AW Kgs 1-16	21.2	14.5	64.2	28.5	14.5	57.0	11.6	83.9	4.5	59.4	37.5	3.1	0.9	0.0	1.2	1.0
AW Kgs 1-17	51.0	8.6	40.4	66.6	8.6	24.8	39.2	56.0	4.8	85.6	11.8	2.7	0.8	0.0	0.0	1.2
AW Kgs 1-37	48.1	8.3	43.6	68.4	8.3	23.3	50.0	40.7	9.3	85.3	10.7	4.0	0.7	0.0	0.2	1.0
AW Kgs 1-41	18.9	27.7	53.4	32.6	27.7	39.8	24.6	63.0	12.3	40.7	57.7	1.6	1.0	0.8	0.4	2.4
AW Kgs 2-12	28.9	19.3	51.8	50.0	19.3	30.7	36.5	48.7	14.8	60.0	40.0	0.0	1.0	1.2	0.0	2.0
Std. Dev.	13.0	3.7	9.4	21.9	3.7	18.2	16.1	8.9	7.2	21.2	16.5	4.7	0.1	0.3	2.1	2.7
AW Kgs 2-2	31.3	3.6	65.1	71.3	3.6	25.1	58.4	28.9	12.7	89.7	7.5	2.8	0.7	0.0	0.0	3.4
AW Kgs 3-7	25.2	1.1	73.7	67.6	1.1	31.3	41.3	4.0	54.7	96.0	4.0	0.0	1.0	0.0	0.0	15.0
AW Kgs 4-2	23.3	1.1	75.6	69.1	1.1	29.8	44.2	4.0	51.8	95.6	4.4	0.0	1.0	0.0	0.0	10.0
Std. Dev.	5.6	1.8	7.4	1.6	1.8	3.3	10.0	17.6	27.7	4.1	2.1	2.0	0.2	0.0	0.0	4.7

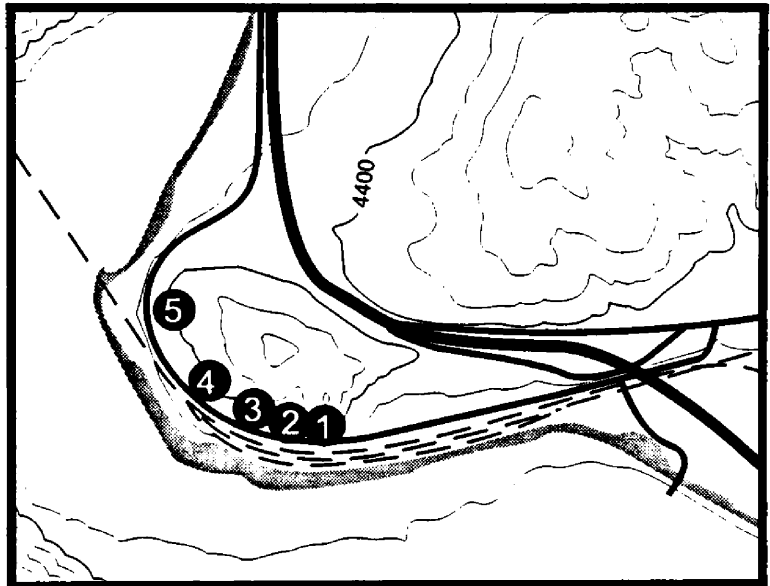
Clast Count Sampling Localities

Garrison, MT Quadrangle -- Montana-Powell Co.
 T9N - R10W
 Contour Interval 80 Feet

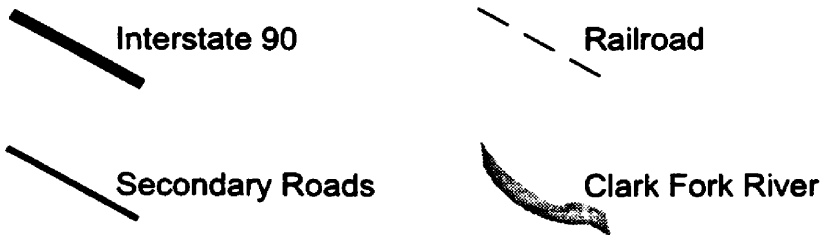
Phosphate Exit



Garrison Junction Exit



- # Megaconglomerate Stations (CB)
- # Sandy Cobble Conglomerate Stations (SCC)



SANDY-COBBLE-CONGLOMERATE CLAST COUNT - SCC CC1: Population Totals

Lithology	1x1	1.5x1	1.5x1.5	2x1	2x1.5	2x2	2.5x1	2.5x1.5	2.5x2	2.5x2.5	3x1.5	3x2	3x2.5	3x3	3.5x1.5	3.5x2	3.5x2.5	SubTTL:
Red Quartzite		1		1		2				1	2	3		1		1	1	13
Other Quartzite		2	1		4	2		1	1			1				2	1	15
Limestone	1	4			1	3	1		1			3	5	1		2		22
Blk Chert	1		1	3	3	1		1	2	1	1	4	2			1	1	22
Other Chert			1			2			1							1		5
Volcanics																		
Dolomite						1						1				1		3
Vein Quartz				1									2					3
Marble?(pink gray spar)																		
Red/pink sublithfeld ss		1	2	1	2	1	1	5							1			14
White & pink subfeld ss				1														1
Green sublithfeld ss									1			1				3		5
Wh/gry subli.fel. ss/meta	1				2	1			1				2			1		8
Subtotal:	3	8	5	7	12	13	2	7	7	2	3	13	11	2	1	12	3	111
Lithology	3.5x3	3.5x3.5	4x2	4x2.5	4x3	4x4	4.5x2.5	4.5x3	4.5x3.5	4.5x4	5x2	5x2.5	5x3	5x3.5	5x4	5x5	5.5x3	SubTTL:
Red Quartzite															2	1		3
Other Quartzite	1		1	1	1	1								2				7
Limestone	2			2	4		1		2	1				1	1		1	15
Blk Chert	3	1		1	3		1			2					1		1	13
Other Chert	1			1									1					3
Volcanics																		
Dolomite								1										1
Vein Quartz																		
Marble?(pink gray spar)									1							1		2
Red/pink sublithfeld ss				3			1	2	1		1	1	1	1				11
White & pink subfeld ss																		
Green sublithfeld ss																		
Wh/gry subli.fel. ss/meta																		
Subtotal:	7	1	1	8	8	1	3	3	4	3	1	1	3	4	5	1	1	55

SANDY-COBBLE-CONGLOMERATE CLAST COUNT - SCC CC1: Population Totals

Lithology	5.5x3.5	5.5x4	5.5x4.5	5.5x5	5.5x5.5	6x3	6x4	6x4.5	6x5	6x5.5	6x6	SubTTL:	
Red Quartzite	2		1				2					5	
Other Quartzite				1		1			1			3	
Limestone									1			1	
Blk Chert		1				1	1	1		1		5	
Other Chert								1				1	
Volcanics								1				1	
Dolomite											1	1	
Vein Quartz													
Marble?(pink gray spar)													
Red/pink sublithfeld ss													
White & pink subfeld ss													
Green sublithfeld ss													
Wh/gry subli.fel. ss/meta													
Subtotal:	2	1	1	1	1	2	4	1	2	1	1	17	
Lithology	6.5x3	6.5x4	6.5x5	7x3.5	7x4.5	7x5	7.5x6	8x4.5	9x5	9.5x5	11.5x10	SubTTL:	TOTAL:
Red Quartzite	1		2	1	1		1			1	1	6	27 13.6%
Other Quartzite										1		2	27 13.6%
Limestone		1						1	1			3	41 20.7%
Blk Chert						1						1	41 20.7%
Other Chert						1						1	10 5.1%
Volcanics					1							1	2 1.0%
Dolomite													5 2.5%
Vein Quartz													3 1.5%
Marble?(pink gray spar)													2 1.0%
Red/pink sublithfeld ss										1		1	26 13.1%
White & pink subfeld ss													1 0.5%
Green sublithfeld ss													5 2.5%
Wh/gry subli.fel. ss/meta													8 4.0%
Subtotal:	1	1	2	1	2	2	1	1	2	1	1	15	198 100%

SANDY-COBBLE-CONGLOMERATE CLAST COUNT - SCC CC1: Area-based Totals and Ratios

WGT RATIO		Category 1																			SubTTL:	
CLAST DIMENSION:	4x3	3.5x3.5	5x2.5	4.5x3	5x3	4x4	4.5x3.5	5.5x3	5x3.5	4.5x4	6x3	5.5x3.5	5x4	5.5x4	6x4	5.5x4.5	5x5	6x4.5	5.5x5	6x5	SubTTL:	
TOTAL:	8	1	1	3	3	1	4	1	4	3	2	2	5	1	4	1	1	1	1	2	49	
CLAST AREA:	9.42	8.62	8.82	10.6	11.78	12.57	12.37	12.96	13.74	14.14	14.14	15.12	15.71	17.28	18.85	19.44	19.63	21.21	21.6	23.56	SubTTL:	
TOTAL:	75.36	9.62	9.82	31.8	35.34	12.57	49.48	12.96	54.96	42.42	28.28	30.24	78.55	17.28	75.4	19.44	19.63	21.21	21.6	47.12	693.08	
AREA %																					SubTTL:	
CLAST DIMENSION:	4x3	3.5x3.5	5x2.5	4.5x3	5x3	4x4	4.5x3.5	5.5x3	5x3.5	4.5x4	6x3	5.5x3.5	5x4	5.5x4	6x4	5.5x4.5	5x5	6x4.5	5.5x5	6x5	SubTTL:	
CLAST AREA:	9.42	9.62	9.82	10.6	11.78	12.57	12.37	12.96	13.74	14.14	14.14	15.12	15.71	17.28	18.85	19.44	19.63	21.21	21.6	23.56	SubTTL:	
Red Quartzite												2	2		2		1	1			8	
Other Quartzite	1					1			2		1									1	1	7
Limestone	4						2	1	1	1			1								1	11
Blk Chert	3	1			1					2	1		1	1					1			11
Other Chert					1											1						2
Volcanics																1						1
Dolomite					1																	1
Vein Quartz																						
Marble?(pink gray spar)							1						1									2
Red/pink sublithfeld ss			1	2	1		1		1													6
White & pink subfeld ss																						
Green sublithfeld ss																						
Wh/gry sublithfeld ss/meta																						

SANDY-COBBLE-CONGLOMERATE CLAST COUNT - SCC CC1: Area-based Totals and Ratios

WGTR RATIOS		Category 1																				SubTTL:		
CLAST DIMENSION:	1x1	1.5x1	2x1	1.5x1.5	2.5x1	2x1.5	2.5x1.5	2x2	3x1.5	2.5x2	3.5x1.5	3x2	2.5x2.5	3.5x2	3x2.5	4x2	3.5x2.5	3x3	4x2.5	5x2	3.5x3	4.5x2.5	SubTTL:	
TOTAL:	3	8	7	5	2	12	7	13	3	7	1	13	2	12	11	1	3	2	8	1	7	3	131	
CLAST AREA:	0.79	1.18	1.57	1.77	1.96	2.35	2.95	3.14	3.53	3.93	4.12	4.71	4.91	5.5	5.89	6.28	6.87	7.07	7.85	7.85	8.25	8.84	SubTTL:	
TOTAL:	2.37	9.44	10.99	8.85	3.92	28.2	20.65	40.82	10.59	27.51	4.12	61.23	9.82	66	64.79	6.28	20.61	14.14	62.8	7.85	57.75	26.52	565.25	
AREA %																						SubTTL:		
CLAST DIMENSION:	1x1	1.5x1	2x1	1.5x1.5	2.5x1	2x1.5	2.5x1.5	2x2	3x1.5	2.5x2	3.5x1.5	3x2	2.5x2.5	3.5x2	3x2.5	4x2	3.5x2.5	3x3	4x2.5	5x2	3.5x3	4.5x2.5	SubTTL:	
CLAST AREA:	0.79	1.18	1.57	1.77	1.96	2.35	2.95	3.14	3.53	3.93	4.12	4.71	4.91	5.5	5.89	6.28	6.87	7.07	7.85	7.85	8.25	8.84	SubTTL:	
Red Quartzite			1	1				2	2			3	1	1			1	1					13	
Other Quartzite			2		1		4	1	2		1		1		2		1	1		1		1	18	
Limestone		1	4			1	1		3		1		3		2	5			1	2		2	1	27
Bk Chert		1		3	1		3	1	1	1	2		4	1	1	2		1		1		3	1	27
Other Chert					1				2		1				1					1		1	7	
Volcanics																								
Dolomite									1				1		1								3	
Vein Quartz				1												2							3	
Marble?(pink gray spar)																								
Red/pink sublithfeld ss			1	1	2	1	2	5	1			1								3	1		1	19
White & pink subfeld ss				1																			1	
Green sublithfeld ss											1		1		3								5	
Wh/gry subli.fel. ss/mela		1					2		1		1				1	2							8	

SANDY-COBBLE-CONGLOMERATE CLAST COUNT - SCC CC1: Area-based Totals and Ratios

WGTR RATIOS	Category 1			Category 2											SubTTL	TOTAL	Category 1 Category 2 Category 3					
CLAST DIMENSION:	5.5x5.5	6x5.5	6x6	6.5x3	7x3.5	6.5x4	7x4.5	6.5x5	7x5	8x4.5	7.5x6	9x5	9.5x5	11.5x10	18	198	Category TTL:	183	15	.		
TOTAL:	1	1	1	1	1	1	2	2	2	1	1	2	1	1	18	198	Cat. Area TTL:	1336.28	472.42	0		
CLAST AREA:	23.76	25.92	28.27	15.32	19.24	20.42	24.74	25.53	27.49	28.27	35.34	35.34	37.31	90.32	550.37	1808.7	Cat. Mean Area:	7.30	31.49	0		
TOTAL:	23.76	25.92	28.27	15.32	19.24	20.42	24.74	25.53	27.49	28.27	35.34	35.34	37.31	90.32	550.37	1808.7	Ratio:	1	4	-		
AREA %																						
CLAST DIMENSION:	5.5x5.5	6x5.5	6x6	6.5x3	7x3.5	6.5x4	7x4.5	6.5x5	7x5	8x4.5	7.5x6	9x5	9.5x5	11.5x10	SubTTL	TOTAL						
CLAST AREA:	23.76	25.92	28.27	15.32	19.24	20.42	24.74	25.53	27.49	28.27	35.34	35.34	37.31	90.32	SubTTL	TOTAL						
Red Quartzite				1	1		1	2			1				6	27	Med. Area & Dim.:	15.12	408.24	29.7		
Other Quartzite													1	1	2	27	5.5x3.5	5.5	148.5	10.8		
Limestone							1			1		1				3	41	3.5x2	5.89	241.49	17.6	
Blk Chert	1	1														3	41	3x2.5	5.89	241.49	17.6	
Other Chert										1				1	10	6.68	66.8	4.9				
Volcanics							1							1	2	21.8	43.6	3.2				
Dolomite	1																1	5	avg 6x4&7x4.5	5.5	27.5	2.0
Vein Quartz																	3	3	3.5x2	5.89	17.67	1.3
Marble?(pink gray spar)																	2	2	3x2.5	14.04	28.08	2.0
Red/pink sublithfeld ss													1	1	26	3.63	94.38	6.9				
White & pink subfeld ss																	1	1	avg 2x2&3.5x1.5	1.57	1.57	0.1
Green sublithfeld ss																	5	5	2x1	5.5	27.5	2.0
Wh/gry subli.fel. ss/meta																	8	8	3.5x2	3.54	28.32	2.1
																			1375.14	100		

SANDY-COBBLE-CONGLOMERATE CLAST COUNT - SCC CC2: Population Totals

Lithology	1.5x1	2x1	2x1.5	2.5x1.5	2.5x2	2.5x2.5	3x1.5	3x2	3x2.5	3x3	3.5x2	3.5x3	4x2.5	4x3	4x3.5	4.5x3	4.5x3.5	5x2.5	SubTTL:
Red Quartzite	1	1	1		1	2	1	1		1	1	1		1		1			13
Other Quartzite	1					1	1				1			2	1				7
Limestone	1	1		1	2			1	4	1	1	1		3				1	18
Blk Chert		2	4	1	4	2		3	1	2			1	1					22
Other Chert																			
White calcareous ss																			
Volcanics			1																1
Pink sucrosic spar/mic														1					1
Dolomite					1														1
Marble? (blocky spar)											1								1
Hema spar w/mic cl											1								1
Subtotal:	3	4	6	2	8	5	2	5	5	4	5	2	1	8	1	1	2	1	65
Lithology	5x3	5x3.5	5x4	5x4.5	5.5x3	5.5x4.5	5.5x5	6x2.5	6x3.5	6x4	6x4.5	6x5	6x6	6.5x4	6.5x5	7x4	7x4.5	8x3	SubTTL:
Red Quartzite		1								1								1	3
Other Quartzite			2			1		1	1		1	1		1					6
Limestone	1	3	2	1		1		1		1	1	1							12
Blk Chert														1					1
Other Chert					1														1
White calcareous ss															1				1
Volcanics																			
Pink sucrosic spar/mic																			
Dolomite														1	1	1			3
Marble? (blocky spar)																			
Hema spar w/mic cl																			
Subtotal:	1	4	4	1	1	1	1	1	1	2	2	1	1	1	2	1	1	1	27
Lithology	8x5	8x7.5	8.5x6	8.5x8	9x9	9.5x4	9.5x6	10x6	10x9	10.5x6	11x3.5	11x9	13x7	17x8	17x12	17x14	SubTTL:	TOTAL:	
Red Quartzite				1							1						2	18	16.5%
Other Quartzite									1				1	1			3	16	14.7%
Limestone	1		1		1	1									1	1	6	36	33.0%
Blk Chert																		23	21.1%
Other Chert																		1	0.9%
White calcareous ss																		1	0.9%
Volcanics																		1	0.9%
Pink sucrosic spar/mic																		1	0.9%
Dolomite		1					1	2		1				1			6	10	9.2%
Marble? (blocky spar)																		1	0.9%
Hema spar w/mic cl																		1	0.9%
Subtotal:	1	1	1	1	1	1	1	2	1	1	1	1	1	1	1	1	17	109	100%

SANDY-COBBLE-CONGLOMERATE CLAST COUNT - SCC CC2: Area-based Totals and Ratios

WGTR RATIOS		Category 1																				SubTTL:				
CLAST DIMENSION:	1.5x1	2x1	2x1.5	2.5x1.5	3x1.5	2.5x2	3x2	2.5x2.5	3.5x2	3x2.5	3x3	4x2.5	3.5x3	4x3	5x2.5	4.5x3	4x3.5	5x3	6x2.5	4.5x3.5	5.5x3	5x3.5	5x4	6x3.5	SubTTL:	
TOTAL:	3	4	6	2	2	8	5	5	5	5	4	1	2	8	1	1	1	1	1	2	1	4	4	1	77	
CLAST AREA:	1.18	1.57	2.35	2.95	3.53	3.93	4.71	4.91	5.5	5.89	7.07	7.85	8.25	9.42	9.82	10.6	11	11.78	11.78	12.37	12.96	13.74	15.71	16.49	SubTTL:	
TOTAL:	3.54	6.28	14.1	5.9	7.06	31.44	23.55	24.55	27.5	29.45	28.28	7.85	16.5	75.36	9.82	10.6	11	11.78	11.78	24.74	12.96	54.96	62.84	16.49	528.33	
AREA %																						SubTTL:				
CLAST DIMENSION:	1.5x1	2x1	2x1.5	2.5x1.5	3x1.5	2.5x2	3x2	2.5x2.5	3.5x2	3x2.5	3x3	4x2.5	3.5x3	4x3	5x2.5	4.5x3	4x3.5	5x3	6x2.5	4.5x3.5	5.5x3	5x3.5	5x4	6x3.5	SubTTL:	
CLAST AREA:	1.18	1.57	2.35	2.95	3.53	3.93	4.71	4.91	5.5	5.89	7.07	7.85	8.25	9.42	9.82	10.6	11	11.78	11.78	12.37	12.96	13.74	15.71	16.49	SubTTL:	
Red Quartzite	1	1	1		1	1	1	2	1		1		1	1			1						1		14	
Other Quartzite	1				1			1	1					2			1							2	1	10
Limestone	1	1		1		2	1		1	4	1		1	3	1			1	1	1			3	2	25	
Blk Chert		2	4	1		4	3	2		1	2	1		1							1				22	
Other Chert																								1	1	
White calcareous ss																										
Volcanics			1																						1	
Pink sucrosic spar/mic														1											1	
Dolomite						1																			1	
Marble? (blocky spar)									1																1	
Hema spar w/mic cl									1																1	

SANDY-COBBLE-CONGLOMERATE CLAST COUNT - SCC CC2: Area-based Totals and Ratios

WGT RATIOS	Category 1								Category 2												SubTTL				
CLAST DIMENSION:	5x4.5	6x4	5.5x4.5	6x4.5	5.5x5	6x5	6x6	8x3	6.5x4	7x4	7x4.5	6.5x5	9.5x4	11x3.5	8x5	8.5x6	9.5x6	8x7.5	10x6	10.5x6	8.5x6	9x9	10x9	SubTTL	
TOTAL:	1	2	1	2	1	1	1	1	1	1	1	2	1	1	1	1	1	1	2	1	1	1	1	1	27
CLAST AREA:	17.67	18.85	19.44	21.21	21.6	23.56	28.27	18.85	20.42	21.99	24.74	25.53	29.85	30.24	31.42	40.06	44.77	47.12	47.12	49.48	53.41	63.62	70.69	SubTTL:	
TOTAL:	17.67	37.7	19.44	42.42	21.6	23.56	28.27	18.85	20.42	21.99	24.74	51.06	29.85	30.24	31.42	40.06	44.77	47.12	94.24	49.48	53.41	63.62	70.69	882.62	
AREA %	Category 1								Category 2												SubTTL				
CLAST DIMENSION:	5x4.5	6x4	5.5x4.5	6x4.5	5.5x5	6x5	6x6	8x3	6.5x4	7x4	7x4.5	6.5x5	9.5x4	11x3.5	8x5	8.5x6	9.5x6	8x7.5	10x6	10.5x6	8.5x6	9x9	10x9	SubTTL	
CLAST AREA:	17.67	18.85	19.44	21.21	21.6	23.56	28.27	18.85	20.42	21.99	24.74	25.53	29.85	30.24	31.42	40.06	44.77	47.12	47.12	49.48	53.41	63.62	70.69	SubTTL:	
Red Quartzite		1						1						1								1		4	
Other Quartzite				1	1		1																	1	4
Limestone	1	1	1	1		1							1		1	1						1		9	
Blk Chert									1																1
Other Chert																									
White calcareous ss												1													1
Volcanics																									
Pink sucrosic spar/mic																									
Dolomite										1	1	1					1	1	2	1					8
Marble? (blocky spar)																									
Hema spar w/mic cl																									

SANDY-COBBLE-CONGLOMERATE CLAST COUNT - SCC CC2: Area-based Totals and Ratios

WGT RATIOS		Category 2					SubTTL: TOTAL:		Category 1	Category 2	Category 3
CLAST DIMENSION:	13x7	11x9	17x8	17x12	17x14	5	109	Category TTL:	86	23	-
TOTAL:	1	1	1	1	1	5	109	Cat. Area TTL:	718.99	1295.13	0
CLAST AREA:	71.47	77.75	106.81	160.22	186.92	603.17	2014.12	Cat. Mean Area:	8.36	31.26	0
TOTAL:	71.47	77.75	106.81	160.22	186.92	603.17	2014.12	Ratio:	1	4	-
AREA %											
CLAST DIMENSION:	13x7	11x9	17x8	17x12	17x14	SubTTL: TOTAL:					
CLAST AREA:	71.47	77.75	106.81	160.22	186.92	SubTTL: TOTAL:					
Red Quartzite						18		Med. Area & Dim:	6.29	113.22	8.0
Other Quartzite	1	1				16		avg 3.5x2&3x3	15.71	251.36	17.7
Limestone				1	1	36		5x4	11.78	424.08	29.9
								avg 5x3&6x2.5			
Blk Chert						23		4.71	108.33	7.6	
Other Chert						1		3x2	12.96	0.9	
White calcareous ss						1		5.5x3	25.53	1.8	
								6.5x5			
Volcanics						1		2.35	2.35	0.2	
								2x1.5			
Pink sucrosic spar/mic						1		9.42	9.42	0.7	
								4x3			
Dolomite			1			10		45.95	459.5	32.4	
								avg 9.5x6&8x7.5			
Marble? (blocky spar)						1		5.5	5.5	0.4	
								3.5x2			
Hema spar w/mic cl						1		5.5	5.5	0.4	
								3.5x2			
									1417.75	100	

MEGACONGLOMERATE CLAST COUNT - CB CC1,2 and 3:
Population and Area (Weighted) Totals

CB CC1 - 1x2 sq. m	Category 1 (1-6cm)	Category 2 (>6-<50cm)	Category 3 (>50cm)	Weighted	
Lithology				Percent	Percent
Red Quartzite	26	4		16.2	12.4
Other Quartzite	6			3.2	1.1
Limestone	74	18		49.7	48.1
Black Chert	13	3		8.6	8.1
Other Chert	5	1		3.2	2.8
Volcanics	9	3		6.5	7.4
Black Argillite	1	1		1.1	2.1
Marble(?)	10	4		7.6	9.6
Micritic Nodule	3	1		2.2	2.5
Sublithic/cherty ss		3		1.6	5.8
				100.0	100.0
Sub Totals:	147	38	0		
Total:	185				
Weighted Sub Totals:	147	418	0		
Weighted Total:	565				

CB CC2 - 1x3 sq. m	Category 1 (1-6cm)	Category 2 (>6-<50cm)	Category 3 (>50cm)	Weighted	
Lithology				Percent	Percent
Red Quartzite	55	1		11.5	10.5
Other Quartzite	26	3		6.0	9.4
Limestone	319	5		66.5	59.6
Black Chert	37	1		7.8	7.7
Other Chert	5	1		1.2	2.6
Volcanics	31			6.4	4.9
Black Argillite				0.0	0.0
Pink sucrosic sparite		1		0.2	1.8
Micritic Nodule				0.0	0.0
Sublithic/cherty ss		2		0.4	3.5
				100.0	100.0
Sub Totals:	473	14	0		
Total:	487				
Weighted Sub Totals:	473	154	0		
Weighted Total:	627				

CB CC3 - 1x3 sq. m	Category 1 (1-6cm)	Category 2 (>6-<50cm)	Category 3 (>50cm)	Weighted	
Lithology				Percent	Percent
Red Quartzite	33	5		18.9	7.9
Other Quartzite	21	1		10.9	2.9
Limestone	116	8		61.7	18.4
Black Chert	5			2.5	0.5
Other Chert	1			0.5	0.1
Volcanics	8			4.0	0.7
Black Argillite	1			0.5	0.1
Marble(?)				0.0	0.0
Micritic Nodule				0.0	0.0
Sublithic/cherty ss			2	1.0	69.4
				100.0	100.0
Sub Totals:	185	14	2		
Total:	201				
Weighted Sub Totals:	185	154	768		
Weighted Total:	1107				

MEGACONGLOMERATE CLAST COUNT - CB CC4: Population Totals

Lithology	1x1	1.5x1	1.5x1.5	2x1	2x1.5	2x2	2.5x1.5	2.5x2	2.5x2.5	3x1.5	3x2	3x2.5	3x3	3.5x2	3.5x2.5	3.5x3	3.5x3.5	4x2	SubTTL:
Red Quartzite	15	7	8	2	9				2		2		1						46
Other Qtzite	2	5			4	1		1	1										14
Limestone	37	30	7	1	22	13	1	4	14	1	8	2	3	2	11	2	3	2	163
Blk Chert	17	5			1				4		1			1				1	30
Other Chert	5	2			1														8
Vein Quartz		1				1													2
Volcanics	6	2			3	1		2	4				1	2		2	2		25
Sublithic ss					2											1			3
Hematized ss	1																		1
Marble(?)	1	6	4		2	2			1						1				17
Subtotal:	84	58	19	3	44	18	1	7	26	1	11	2	5	5	12	5	5	3	309
Lithology	4x2.5	4x3	4x3.5	4.5x2	4.5x3	4.5x3.5	4.5x4	4.5x4.5	5x2	5x3	5x3.5	5x4	5x4.5	5x5	5.5x3	5.5x3.5	5.5x4	5.5x4.5	SubTTL:
Red Quartzite		3			3				1									1	8
Other Qtzite	1	1										1				1			4
Limestone	1	5	1	1	1	1	1	1		1	3	2	2	1			1	2	24
Blk Chert		1																	1
Other Chert																			
Vein Quartz																			
Volcanics	1	1										1				1			5
Sublithic ss																			
Hematized ss																			
Marble(?)					1														1
Subtotal:	3	11	1	1	5	1	1	1	1	1	3	4	2	1	2	1	3	1	43
Lithology	6x2.5	6X3	6x3.5	6x4	6x5	6x5.5	6x6	6.5x4	7x5	8x6.5	9x6	14x11	50x23	SubTTL:	TOTAL:				
Red Quartzite				1										1	55	15.0%			
Other Qtzite					1				1	1				3	21	5.7%			
Limestone	1	1	1			3		1			1	1		9	196	53.4%			
Blk Chert															31	8.4%			
Other Chert															8	2.2%			
Vein Quartz															2	0.5%			
Volcanics							1							1	31	8.4%			
Sublithic ss													1	1	4	1.1%			
Hematized ss															1	0.3%			
Marble(?)															18	4.9%			
Subtotal:	1	1	1	1	1	3	1	1	1	1	1	1	1	15	367	100%			

MEGACONGLOMERATE CLAST COUNT - CB CC4:
Area-based Totals and Ratios

WGT RATIOS		Category 1																							
CLAST DIMEN:	1x1	1.5x1	2x1	1.5x1.5	2x1.5	2.5x1.5	2x2	3x1.5	2.5x2	3x2	2.5x2.5	3.5x2	3x2.5	4x2	3.5x2.5	3x3	4.5x2	4x2.5	5x2	3.5x3	4x3	3.5x3.5	4.5x3	SubTTL:	
TOTAL:	84	58	3	19	44	1	18	1	7	11	26	5	2	3	12	5	1	3	1	5	11	5	5	330	
CLAST AREA:	0.79	1.18	1.57	1.77	2.35	2.95	3.14	3.53	3.93	4.71	4.91	5.5	5.89	6.28	6.87	7.07	7.07	7.85	7.85	8.25	9.42	9.62	10.6	SubTTL:	
TOTAL:	66.36	68.44	4.71	33.63	103.4	2.95	56.52	3.53	27.51	51.81	127.66	27.5	11.78	18.84	82.44	35.35	7.07	23.55	7.85	41.25	103.62	48.1	53	1006.87	
AREA %																									
CLAST DIMEN:	1x1	1.5x1	2x1	1.5x1.5	2x1.5	2.5x1.5	2x2	3x1.5	2.5x2	3x2	2.5x2.5	3.5x2	3x2.5	4x2	3.5x2.5	3x3	4.5x2	4x2.5	5x2	3.5x3	4x3	3.5x3.5	4.5x3	SubTTL:	
CLAST AREA:	0.79	1.18	1.57	1.77	2.35	2.95	3.14	3.53	3.93	4.71	4.91	5.5	5.89	6.28	6.87	7.07	7.07	7.85	7.85	8.25	9.42	9.62	10.6	SubTTL:	
Red Quartzite	15	7	2	8	9					2	2					1			1		3		3	53	
Other Qtzite	2	5			4		1		1		1								1			1		16	
Limestone	37	30	1	7	22	1	13	1	4	8	14	2	2	2	11	3	1	1		2	5	3	1	171	
Blk Chert	17	5			1					1	4	1		1								1		31	
Other Chert	5	2			1																			8	
Vein Quartz		1					1																	2	
Volcanics	6	2			3		1		2		4	2				1		1		2	1	2		27	
Sublithic ss					2																1			3	
Hematized ss	1																							1	
Marble(?)	1	6		4	2		2				1				1								1	18	

MEGACONGLOMERATE CLAST COUNT - CB CC4
Area-based Totals and Ratios

WGT RATIOS	Category 1																				Category 2		
CLAST DIMEN:	4x3.5	5x3	6x2.5	4.5x3.5	5.5x3	5x3.5	4.5x4	6X3	5.5x3.5	5x4	4.5x4.5	6x3.5	5x4.5	5x5	5.5x4	6x4	5.5x4.5	6x5	6x5.5	6x6	6.5x4	7x5	SubTTL:
TOTAL:	1	1	1	1	2	3	1	1	1	4	1	1	2	1	3	1	1	1	3	1	1	1	33
CLAST AREA:	11	11.78	11.78	12.37	12.96	13.74	14.14	14.14	15.12	15.71	15.9	16.49	17.67	19.63	17.28	18.85	19.44	23.56	25.92	28.27	20.42	27.49	SubTTL:
TOTAL:	11	11.78	11.78	12.37	25.92	41.22	14.14	14.14	15.12	62.84	15.9	16.49	35.34	19.63	51.84	18.85	19.44	23.56	77.76	28.27	20.42	27.49	575.3
AREA %																							
CLAST DIMEN:	4x3.5	5x3	6x2.5	4.5x3.5	5.5x3	5x3.5	4.5x4	6X3	5.5x3.5	5x4	4.5x4.5	6x3.5	5x4.5	5x5	5.5x4	6x4	5.5x4.5	6x5	6x5.5	6x6	6.5x4	7x5	SubTTL:
CLAST AREA:	11	11.78	11.78	12.37	12.96	13.74	14.14	14.14	15.12	15.71	15.9	16.49	17.67	19.63	17.28	18.85	19.44	23.56	25.92	28.27	20.42	27.49	SubTTL:
Red Quartzite																1	1						2
Other Qtzite					1					1									1			1	4
Limestone	1	1	1	1		3	1	1	1	2	1	1	2	1	2					3	1		23
Blk Chert																							
Other Chert																							
Vein Quartz																							
Volcanics					1					1								1			1		4
Sublithic ss																							
Hematized ss																							
Marble(?)																							

MEGA CONGLOMERATE CLAST COUNT - CB CCA:
Area-based Totals and Ratios

WGT RATIOS	Category 2			Category 3				Category 1	Category 2	Category 3
CLAST DIMEN:	8x6.5	9x6	14x11	50x23	SubTTL:	TOTAL:	Median Dimension:	2x1.5	8x6.5	50x23
TOTAL:	1	1	1	1	4	367	Category TTL:	361	5	1
CLAST AREA:	40.84	42.41	120.95	903.21	SubTTL:	TOTAL:	Median Area:	2.35	40.84	903.21
TOTAL:	40.84	42.41	120.95	903.21	1107.41	2689.58	Ratio:	1	17	384
AREA %										
CLAST DIMEN:	8x6.5	9x6	14x11	50x23	SubTTL:	TOTAL:				
CLAST AREA:	40.84	42.41	120.95	903.21						
Red Quartzite						55	Med. Area & Dim.:	1.77	97.35	9.9
Other Qtzite	1				1	21		1.5x1.5		
Limestone		1	1		2	196		2.35	49.35	5.0
Blk Chert						31		2x1.5		
Other Chert						8		3.05	597.8	60.6
Vein Quartz						2		avg 2.5x1.5&2x2		
Volcanics						31		0.79	24.49	2.5
Sublithic ss				1	1	4		1x1		
Hematized ss						1		0.79	6.32	0.6
Marble(?)						18		1x1		
								2.16	4.32	0.4
								avg 1.5x1&2x2		
								4.91	152.21	15.4
								2.5x2.5		
								5.3	21.2	2.2
								avg 2x1.5&3.5x3		
								0.79	0.79	0.1
								1.77	31.86	3.2
								1.5x1.5		
									985.69	100

MEGACONGLOMERATE CLAST COUNT - CB CC5: Population Totals

Lithology	1x1	1.5x1	1.5x1.5	2x1	2x1.5	2x2	2.5x1	2.5x1.5	2.5x2	2.5x2.5	3x1.5	3x2	3x2.5	3x3	3.5x1	3.5x1.5	5x3.5	SubTTL:
Red Quartzite		2	1	1	2	1		2	1	2		4	4			1	1	21
Other Quartzite				1		1		1	3		1		1	1		1		10
Limestone		7	3	1	5	4	1	3	13	4	3	2	6	2			2	56
Blk Chert	2		1	1							1	1	1					8
Other Chert								2					1					3
Volcanics		1	1		2	1		1				1	1	1				9
Vein Quartz																		
Sublithfeld ss															1	1		2
Dolomite																		
Blocky spar/marble?					1													1
White sucrosic sparite					1													1
Black siltstone				1														1
Tan metasiltst. w/CO3 cem									1			1						2
Hematitic spar w/mic clst																		
Subtotal	2	10	6	5	11	7	1	10	18	6	5	9	14	5	1	4	1	114
Lithology	3.5x2	3.5x2.5	3.5x3	3.5x3.5	4x2	4x2.5	4x3	4x3.5	4x4	4.5x2	4.5x2.5	4.5x3	4.5x3.5	4.5x4	5x2.5	5x3	7x5	SubTTL:
Red Quartzite	2	1	2	2			3	3			1			1	1			17
Other Quartzite											1	1	1	1				4
Limestone	4	5	6			3	7	1	1			1				2		30
Blk Chert							1	1					1					3
Other Chert			2				1	1										4
Volcanics							1											1
Vein Quartz								1										1
Sublithfeld ss				1														1
Dolomite							1											1
Blocky spar/marble?																		
White sucrosic sparite										1					2			3
Black siltstone																		
Tan metasiltst. w/CO3 cem	1									1							1	3
Hematitic spar w/mic clst																		
Subtotal:	7	6	10	2	1	6	14	4	2	1	1	3	3	4	2	1	1	68

MEGACONGLOMERATE CLAST COUNT - CB CC5 Population Totals

Lithology	5x4	5x4.5	5.5x2.5	5.5x3	5.5x3.5	5.5x4	5.5x4.5	6x4	6x4.5	6.5x3.5	6.5x4	6.5x4.5	6.5x5	6.5x6	6.5x6.5	7x3.5	SubTTL:			
Red Quartzite			1	1					1		1		1				5			
Other Quartzite			1		1						1						3			
Limestone	2		1		2	2	1	2		1		1			1	1	15			
Blk Chert		1												1			2			
Other Chert																				
Volcanics								2									2			
Vein Quartz																				
Sublithfeld ss			1														1			
Dolomite																				
Blocky spar/marble?			1														1			
White sucrosic sparite																				
Black siltstone																				
Tan metasiltst. w/CO3 cem																				
Hematitic spar w/mic clst																				
Subtotal:	2	1	5	1	3	2	1	2	3	1	3	1	1	1	1	1	29			
Lithology	7x6	7.5x5.5	7.5x6	8x5.5	8x6	8x6.5	8x7	8.5x5.5	9x8	9x8.5	9.5x4.5	9.5x6.5	10x9	14x8	14.5x9.5	30x20	SubTTL: TOTAL:			
Red Quartzite	1	1	1	1					1	1							6	50 21.6%		
Other Quartzite																		17	7.3%	
Limestone					1	2					1	1		1			6	107	46.1%	
Blk Chert																		0	13	5.6%
Other Chert																			7	3.0%
Volcanics		1							1				1			1	4	16	6.9%	
Vein Quartz																			1	0.4%
Sublithfeld ss							1			1					1		3	7	3.0%	
Dolomite																			1	0.4%
Blocky spar/marble?																			2	0.9%
White sucrosic sparite																			4	1.7%
Black siltstone																			1	0.4%
Tan metasiltst. w/CO3 cem																			5	2.2%
Hematitic spar w/mic clst											1						1	1	0.4%	
Subtotal:	1	2	1	1	1	2	1	2	1	1	2	1	1	1	1	1	20	232	100%	

MEGA CONGLOMERATE CLAST COUNT - CBCC5
Area-based Totals and Ratios

WGT RATIOS		Category 1																				SubTTL:			
CLAST DIMENSION:	1x1	1.5x1	2x1	1.5x1.5	2.5x1	2x1.5	3.5x1	2.5x1.5	2x2	3x1.5	2.5x2	3.5x1.5	3x2	2.5x2.5	3.5x2	3x2.5	4x2	3.5x2.5	3x3	4.5x2	4x2.5	3.5x3	4.5x2.5	4x3	SubTTL:
TOTAL:	2	10	5	6	1	11	1	10	7	5	18	4	9	6	7	14	1	6	5	1	6	10	1	14	160
CLAST AREA:	0.79	1.18	1.57	1.77	1.96	2.35	2.75	2.95	3.14	3.53	3.93	4.12	4.71	4.91	5.5	5.89	6.28	6.87	7.07	7.07	7.85	8.25	8.84	9.42	SubTTL:
TOTAL:	1.58	11.8	7.85	10.62	1.96	25.85	2.75	29.5	21.98	17.65	70.74	16.48	42.39	29.46	38.5	82.46	6.28	41.22	35.35	7.07	47.1	82.5	8.84	131.88	771.81
AREA %																						SubTTL:			
CLAST DIMEN:	1x1	1.5x1	2x1	1.5x1.5	2.5x1	2x1.5	3.5x1	2.5x1.5	2x2	3x1.5	2.5x2	3.5x1.5	3x2	2.5x2.5	3.5x2	3x2.5	4x2	3.5x2.5	3x3	4.5x2	4x2.5	3.5x3	4.5x2.5	4x3	SubTTL:
CLAST AREA:	0.79	1.18	1.57	1.77	1.96	2.35	2.75	2.95	3.14	3.53	3.93	4.12	4.71	4.91	5.5	5.89	6.28	6.87	7.07	7.07	7.85	8.25	8.84	9.42	SubTTL:
Red Quartzite		2	1	1		2		2	1		1	1	4	2	2	4		1		1	3	2		3	33
Other Quartzite			1					1	1	1	3	1				1			1				1		11
Limestone		7	1	3	1	5		3	4	3	13	2	2	4	4	6		5	2		3	6		7	81
Blk Chert	2		1	1				1		1			1			1								1	9
Other Chert								2								1						2		1	6
Volcanics		1		1		2		1	1				1			1				1				1	10
Vein Quartz																									
Sublithifed ss							1										1		1						3
Dolomite																								1	1
Blocky spar/marble?						1																			1
White sucrosic spar						1																			1
Black siltstone			1																						1
Tan metasiltst. w/CO3 cem											1		1		1										3
Hematitic spar w/mic clst																									

MEGACONGLOMERATE CLAST COUNT - CBCCS:
Area-based Totals and Ratios

WGT RATIOS	Category 1																		Category 2				SubTTL:	
CLAST DIMENSION:	3.5x3.5	5x2.5	4.5x3	5.5x2.5	4x3.5	5x3	4.5x3.5	4x4	5.5x3	5x3.5	4.5x4	5.5x3.5	5x4	5.5x4	5x4.5	6x4	5.5x4.5	6x4.5	6.5x3.5	7x3.5	6.5x4	6.5x4.5	SubTTL:	
TOTAL:	2	2	3	5	4	1	3	2	1	1	4	3	2	2	1	2	1	3	1	1	3	1	48	
CLAST AREA:	9.62	9.02	10.6	10.8	11	11.78	12.37	12.57	12.96	13.74	14.14	15.12	15.71	17.28	17.67	18.85	19.44	21.21	17.87	19.24	20.42	22.97	SubTTL:	
TOTAL:	19.24	19.64	31.8	54	44	11.78	37.11	25.14	12.96	13.74	56.56	45.36	31.42	34.56	17.67	37.7	19.44	63.63	17.87	19.24	61.26	22.97	697.09	
AREA %	Category 1																		Category 2				SubTTL:	
CLAST DIMEN:	3.5x3.5	5x2.5	4.5x3	5.5x2.5	4x3.5	5x3	4.5x3.5	4x4	5.5x3	5x3.5	4.5x4	5.5x3.5	5x4	5.5x4	5x4.5	6x4	5.5x4.5	6x4.5	6.5x3.5	7x3.5	6.5x4	6.5x4.5	SubTTL:	
CLAST AREA:	9.62	9.02	10.6	10.8	11	11.78	12.37	12.57	12.96	13.74	14.14	15.12	15.71	17.28	17.67	18.85	19.44	21.21	17.87	19.24	20.42	22.97	SubTTL:	
Red Quartzite	2			1			1		1	1	1							1				1	9	
Other Quartzite				1	1		1				1	1										1	6	
Limestone			2	1	1	1			1				2	2	2		2	1		1	1	1	1	19
Blk Chert					1		1								1								3	
Other Chert					1																		1	
Volcanics																		2					2	
Vein Quartz					1																		1	
Sublithfeld ss					1																		1	
Dolomite																								
Blocky spar/marble?					1																		1	
White sucrosic spar				1							2												3	
Black siltstone																								
Tan metasilst. w/CO3 cem						1		1															2	
Hematitic spar w/mic clst																								

MEGACONGLOMERATE CLAST COUNT - CBCC5
Area-based Totals and Ratios

WGT RATIOS		Category 2																			SubTTL:	TOTAL:		
CLAST DIMENSION:	6.5x5	7x5	6.5x6	7.5x5.5	7x6	6.5x6.5	9.5x4.5	8x5.5	7.5x6	8.5x5.5	8x6	8x6.5	8x7	9.5x6.5	9x8	9x8.5	10x9	14x8	14.5x9.5	30x20				
TOTAL:	1	1	1	2	1	1	2	1	1	2	1	2	1	1	1	1	1	1	1	1		24	232	
CLAST AREA:	25.53	27.49	30.63	32.4	32.99	33.18	33.58	34.56	35.34	36.72	37.7	40.84	43.98	48.5	56.55	60.01	70.69	87.96	108.19	471.24		1491.62	2960.52	
TOTAL:	25.53	27.49	30.63	64.8	32.99	33.18	67.16	34.56	35.34	73.44	37.7	81.68	43.98	48.5	56.55	60.01	70.69	87.96	108.19	471.24		1491.62	2960.52	
AREA %																					SubTTL:	TOTAL:		
CLAST DIMEN:	6.5x5	7x5	6.5x6	7.5x5.5	7x6	6.5x6.5	9.5x4.5	8x5.5	7.5x6	8.5x5.5	8x6	8x6.5	8x7	9.5x6.5	9x8	9x8.5	10x9	14x8	14.5x9.5	30x20				
CLAST AREA:	25.53	27.49	30.63	32.4	32.99	33.18	33.58	34.56	35.34	36.72	37.7	40.84	43.98	48.5	56.55	60.01	70.69	87.96	108.19	471.24				
Red Quartzite	1	1		1	1			1	1	1					1							8	50	
Other Quartzite																								17
Limestone						1	1				1	2		1				1				7	107	
Blk Chert			1																			1	13	
Other Chert																								7
Volcanics				1						1							1				1	4	16	
Vein Quartz																								1
Sublithfeld ss													1			1			1			3	7	
Dolomite																								1
Blocky spar/marble?																								2
White sucrosic spar																								4
Black siltstone																								1
Tan metasiltst. w/CO3 cem																								5
Hematitic spar w/mic clst							1															1	1	

MEGACONGLOMERATE CLAST COUNT - CBCC5:
Area-based Totals and Ratios

WGT RATIOS		Category 1	Category 2	Category 3
CLAST DIMENSION:	TOTAL:	Median Dimension: 3.5x2	8x5.5 & 9.5x4.5	.
TOTAL:	232	Category TTL: 202	30	0
CLAST AREA:	TOTAL:	Median Area: 5.5	34.07	0
TOTAL:	2960.52	Ratio:	1	6

AREA %		Med. Area & Dim.:	Med. Avg. Area:	Percentage:
CLAST DIMEN:	TOTAL:			
Red Quartzite	50	7.46 avg 4.5x2&4x2.5	373	24.1
Other Quartzite	17	5.89 3x2.5	100.13	6.5
Limestone	107	5.89 3x2.5	630.23	40.7
Blk Chert	13	4.71 3x2	61.23	4.0
Other Chert	7	8.25 3.5x3	57.75	3.7
Volcanics	16	6.48 avg 3x2.5&3x3	103.68	6.7
Vein Quartz	1	11 4x3.5	11	0.7
Sublithfield ss	7	10.8 5.5x2.5	75.6	4.9
Dolomite	1	9.42 4x3	9.42	0.6
Blocky spar/marble?	2	6.58 avg 2x1.5&5.5x2.5	13.16	0.9
White sucrosic spar	4	12.37 avg 4.5x3&4.5x4	49.48	3.2
Black siltstone	1	1.57 2x1	1.57	0.1
Tan metasiltst. w/CO3 cen	5	5.5 3.5x2	27.5	1.8
Hematitic spar w/mic clst	1	33.58 9.5x4.5	33.58	2.2
			1547.33	100

MEGACONGLOMERATE CLAST COUNT - CB CC6: Population Totals

Lithology	1.5x1	2x1	2x1.5	2x2	2.5x1	2.5x1.5	2.5x2	2.5x2.5	3x1.5	3x2	3x2.5	3x3	3.5x2	3.5x3	4x3	4x3.5	4.5x2	4.5x3	4.5x4	SubTTL:
Red Quartzite			1				2								1					4
Rd/org subfeld metass	1								1											2
Limestone	2	1	1	1	1	1	3			3	3	1	1			2	1			21
Blk Chert	1		1				1							1		1				5
Other Chert	1			1																2
Micritic Nodule	1	2					1			1							1			6
Volcanics								1												1
Sublithfeld ss(blu gry)							2											1	1	4
Dolomite					1					1					1					3
White sublith ss w/jas							1													1
Hema spar w/mic cl															1					1
Subtotal:	6	3	3	2	1	2	10	1	1	5	3	1	1	1	3	3	2	1	1	50
Lithology	5x2.5	5x3	5x3.5	5x4	5.5x2.5	5.5x4	5.5x4.5	6x3.5	6x4	6.5x5	7x4	7.5x4	8x6.5	13x8	32x25	42x8	SubTTL:	TOTAL:		
Red Quartzite																		4	5.9%	
Rd/org subfeld metass																		2	2.9%	
Limestone		1		1		1		1			1	1		1				7	28	41.2%
Blk Chert	1	1																2	7	10.3%
Other Chert																			2	2.9%
Micritic Nodule				1														1	7	10.3%
Volcanics																			1	1.5%
Sublithfeld ss(blu gry)	1				1		1		1	1			1		1	1		8	12	17.6%
Dolomite																			3	4.4%
White sublith ss w/jas																			1	1.5%
Hema spar w/mic cl																			1	1.5%
Subtotal:	2	2	1	1	1	1	1	1	1	1	1	1	1	1	1	1		18	68	100%

MEGACONGLOMERATE CLAST COUNT - CBCC6
Area-based Totals and Ratios

WGT RATIOS		Category 1																									
CLAST DIMEN:	1.5x1	2x1	2.5x1	2x1.5	2.5x1.5	2x2	3x1.5	2.5x2	3x2	2.5x2.5	3.5x2	3x2.5	3x3	4.5x2	3.5x3	4x3	5x2.5	4.5x3	5.5x2.5	4x3.5	5x3	5x3.5	4.5x4	5x4	6x3.5	SubTTL:	
TOTAL:	6	3	1	3	2	2	1	10	5	1	1	3	1	2	1	3	2	1	1	3	2	1	1	1	1	1	
CLAST AREA:	1.18	1.57	1.96	2.35	2.95	3.14	3.53	3.93	4.71	4.91	5.5	5.89	7.07	7.07	8.25	9.42	9.82	10.6	10.8	11	11.78	13.74	14.14	15.71	16.49	SubTTL:	
TOTAL:	7.09	6.28	1.96	7.05	5.9	6.28	3.53	39.3	23.55	4.91	5.5	17.67	7.07	14.14	8.25	28.26	19.64	10.6	10.8	33	23.56	13.74	14.14	15.71	16.49		
AREA %																											
CLAST DIMEN:	1.5x1	2x1	2.5x1	2x1.5	2.5x1.5	2x2	3x1.5	2.5x2	3x2	2.5x2.5	3.5x2	3x2.5	3x3	4.5x2	3.5x3	4x3	5x2.5	4.5x3	5.5x2.5	4x3.5	5x3	5x3.5	4.5x4	5x4	6x3.5	SubTTL:	
CLAST AREA:	1.18	1.57	1.96	2.35	2.95	3.14	3.53	3.93	4.71	4.91	5.5	5.89	7.07	7.07	8.25	9.42	9.82	10.6	10.8	11	11.78	13.74	14.14	15.71	16.49	SubTTL:	
Red Quartzite				1					2																	4	
Rd/org subfeld metass	1									1																2	
Limestone	2	1	1	1	1	1			3	3		1	3	1	1						2	1			1	1	24
Blk Chert	1			1					1							1		1			1	1				7	
Other Chert	1						1																			2	
Micritic Nodule	1	2							1	1					1									1		7	
Volcanics												1														1	
Sublithfeld ss(blu gry)									2									1	1	1				1		6	
Dolomite						1				1							1									3	
White sublith ss w/jas									1																	1	
Hema spar w/mic cl																	1									1	

MEGA CONGLOMERATE CLAST COUNT CBCC6:
Area-based Totals and Ratios

WGTRATIOS	Category 1			Category 2						SubTTL:	TOTAL:	Category 1 Category 2 Category 3								
CLAST DIMEN:	5.5x4	6x4	5.5x4.5	7x4	7.5x4	6.5x5	8x6.5	13x8	42x8	32x25	10	68	Median Dimension:	3x2	8x6.5	-				
TOTAL:	1	1	1	1	1	1	1	1	1	1	10	68	Category TTL:	61	7	0				
CLAST AREA:	17.28	18.85	19.44	21.99	23.56	25.53	40.84	81.68	263.89	628.32	1141.38	1485.79	Median Area:	4.71	40.84	0				
TOTAL:	17.28	18.85	19.44	21.99	23.56	25.53	40.84	81.68	263.89	628.32	1141.38	1485.79	Ratio:	1	9	-				
AREA %																				
CLAST DIMEN:	5.5x4	6x4	5.5x4.5	7x4	7.5x4	6.5x5	8x6.5	13x8	42x8	32x25	SubTTL:	TOTAL:	Med. Area & Dim.: Med. Avg. Area Percentage:							
CLAST AREA:	17.28	18.85	19.44	21.99	23.56	25.53	40.84	81.68	263.89	628.32										
Red Quartzite											4	28	3.93	15.72	3.1					
Rd/org subfeld metass											2		2.5x2	2.36	4.72	0.9				
Limestone	1											4	28	avg 1.5x1.8x1.5	5.7	159.6	31.9			
				1	1													avg 3.5x2.8x2.5		
Blk Chert											7		8.25	57.75	11.5					
Other Chert											2		3.5x3	2.16	4.32	0.9				
Micritic Nodule											7		avg 1.5x1.8x2x2	3.93	27.51	5.5				
													2.5x2							
Volcanics											1		4.91	4.91	1.0					
Sublithfeld ss(blu gry)		1	1											6	12	2.5x2.5	16.5	198	39.8	
				1	1													avg 4.5x4.8x4		
Dolomite											3		4.71	14.13	2.8					
													3x2							
White sublith ss w/jas											1		3.93	3.93	0.8					
													2.5x2							
Hema spar w/mic cl											1		9.42	9.42	1.9					
													4x3							
													500.01	100						

SANDY-COBBLE-CONGLOMERATE CLAST COUNT - SCC CC3: Population Totals

Lithology	1x1	2.5x1	2.5x2	2.5x2.5	3x2	3x2.5	3x3	3.5x2.5	3.5x3	3.5x3.5	4x2	4x2.5	4x3	4x3.5	SubTtl:	
Red Quartzite												1			1	
Other Quartzite													1		1	
Limestone	2	1	1		2	2	1	2	3		1	2	2	2	21	
Blk Chert		1										1			2	
White Marble																
Wh/gry dolomite			1	1			1	1	1	1	1	1		1	8	
Red sucrosic sparmicrite													1		1	
Subtotal:	2	2	2	1	2	2	2	3	4	1	1	5	4	3	34	
Lithology	4x4	4.5x2.5	4.5x3.5	5x3	5x3.5	5x4	5x4.5	5x5	5.5x3	6x2.5	6x4	6x5	6.5x4.5	7x4	SubTtl:	
Red Quartzite										1					1	
Other Quartzite						1									1	
Limestone	2	1		1		2	1	1	1			1		3	13	
Blk Chert																
White Marble													1		1	
Wh/gry dolomite	1		1	1	1	2					1				7	
Red sucrosic sparmicrite			1												1	
Subtotal:	3	1	2	2	1	5	1	1	1	1	1	1	1	3	24	
Lithology	8x5	8x7	8.5x4	9x5	9x6	9x7	11x7	11x8	14x10	7x5	7x6	7x7	7.5x5	SubTtl:	TOTAL:	
Red Quartzite															2	2.8%
Other Quartzite							1								2	2.8%
Limestone	2		1	1	1	1	1	1		1	1		1	11	43	60.6%
Blk Chert															2	2.8%
White Marble															1	1.4%
Wh/gry dolomite		1								1	1		1	4	19	26.8%
Red sucrosic sparmicrite															2	2.8%
Subtotal:	2	1	1	1	1	1	1	1	1	2	1	1	1	15	71	100%

SANDY-COBBLE-CONGLOMERATE CLAST COUNT - SCC CC3: Area-based Totals and Ratios

WGTR RATIOS		Category 1																				SubTTL	
CLAST DIMENSION:	1x1	2.5x1	2.5x2	3x2	2.5x2.5	3x2.5	4x2	3.5x2.5	3x3	4x2.5	3.5x3	4.5x2.5	4x3	3.5x3.5	4x3.5	5x3	6x2.5	4.5x3.5	4x4	5.5x3	5x3.5	SubTTL	
TOTAL:	2	2	2	2	1	2	1	3	2	5	4	1	4	1	3	2	1	2	3	1	1	45	
CLAST AREA:	0.79	1.96	3.93	4.71	4.91	5.89	6.28	6.87	7.07	7.85	8.25	8.84	9.42	9.62	11	11.78	11.78	12.37	12.57	12.96	13.74	SubTTL	
TOTAL:	1.58	3.92	7.86	9.42	4.91	11.78	6.28	20.61	14.14	39.25	33	8.84	37.68	9.62	33	23.56	11.78	24.74	37.71	12.96	13.74	366.38	
AREA %																							
CLAST DIMENSION:	1x1	2.5x1	2.5x2	3x2	2.5x2.5	3x2.5	4x2	3.5x2.5	3x3	4x2.5	3.5x3	4.5x2.5	4x3	3.5x3.5	4x3.5	5x3	6x2.5	4.5x3.5	4x4	5.5x3	5x3.5	SubTTL	
CLAST AREA:	0.79	1.96	3.93	4.71	4.91	5.89	6.28	6.87	7.07	7.85	8.25	8.84	9.42	9.62	11	11.78	11.78	12.37	12.57	12.96	13.74	SubTTL	
Red Quartzite										1								1				2	
Other Quartzite													1									1	
Limestone	2	1	1	2		2	1	2	1	2	3	1	2		2	1			2	1		26	
Blk Chert		1								1												2	
White Marble																							
Wh/gry dolomite			1		1			1	1	1	1			1	1	1			1	1		12	
Red sucrosic spar/mic													1						1			2	
WGTR RATIOS		Category 1										Category 2										SubTTL	TOTAL:
CLAST DIMENSION:	5x4	5x4.5	6x4	5x5	6x5	7x4.5x4.5	8.5x4	7x5	7.5x5	8x5	7x6	9x5	7x7	9x6	8x7	9x7	11x7	11x8	14x10	SubTTL:	TOTAL:		
TOTAL:	5	1	1	1	1	3	1	1	2	1	2	1	1	1	1	1	1	1	1	1	28	73	
CLAST AREA:	15.7	17.67	18.85	19.6	23.56	21.99	23	26.7	27.49	29.45	31.42	32.99	35.34	38.48	42.41	43.98	49.48	60.48	69.11	110	SubTTL:	TOTAL:	
TOTAL:	78.6	17.67	18.85	19.6	23.56	65.97	23	26.7	54.98	29.45	62.84	32.99	35.34	38.48	42.41	43.98	49.48	60.48	69.11	109.96	903.4	1269.8	
AREA %																							
CLAST DIMENSION:	5x4	5x4.5	6x4	5x5	6x5	7x4.5x4.5	8.5x4	7x5	7.5x5	8x5	7x6	9x5	7x7	9x6	8x7	9x7	11x7	11x8	14x10	SubTTL:	TOTAL:		
CLAST AREA:	15.7	17.67	18.85	19.6	23.56	21.99	23	26.7	27.49	29.45	31.42	32.99	35.34	38.48	42.41	43.98	49.48	60.48	69.11	110	SubTTL:	TOTAL:	
Red Quartzite																						2	
Other Quartzite	1																					1	2
Limestone	2	1		1	1	3		1	1	1	2	1	1		1		1	1	1		19	45	
Blk Chert																						2	
White Marble							1															1	1
Wh/gry dolomite	2		1						1					1		1					1	7	19
Red sucrosic spar/mic																							2

SANDY-COBBLE-CONGLOMERATE CLAST COUNT - SCC CC3: Area-based Totals and Ratios

WGTR RATIOS				
		Category 1	Category 2	Category 3
CLAST DIMENSION:	TOTAL:	Category TTL:	54	19
TOTAL:	73	Cat. Area TTL:	524.64	745.14
CLAST AREA:	TOTAL:	Cat. Mean Area:	9.72	39.22
TOTAL:	1269.78	Ratio:	1	4
AREA %				
CLAST DIMENSION:				
CLAST AREA:		TOTAL:		
		Med. Area & Dim.:	Med. Avq. Area	Percentage:
Red Quartzite	2	9.82	19.64	2.2
		avg 4x2.5&6x2.5		
Other Quartzite	2	12.57	25.14	2.8
		avg 4x3&5x4		
Limestone	45	12.57	565.65	62.8
		4x4		
Blk Chen	2	4.91	9.82	1.1
		avg 2.5x1&4x2.5		
White Marble	1	22.97	22.97	2.6
		6.5x4.5		
Wh/gry dolomite	19	12.37	235.03	26.1
		4.5x3.5		
Red sucrosic spar/mic	2	10.9	21.8	2.4
		avg 4x3&4.5x3.5		
			900.05	100

SANDY-COBBLE-CONGLOMERATE CLAST COUNT - SCC CC4:
Population and Area (Weighted) Totals

Lithology	Category 1 (1-6cm)	Category 2 (>6-<50cm)	Category 3 (≥50cm)	Percent	Weighted Percent
Red Quartzite	8	2		5.7	5.1
Other Quartzite	20	10		17.2	19.2
Limestone	57	28		48.9	54.2
Black Chert	17			9.8	5.4
Other Chert	2			1.1	0.6
Volcanics	2			1.1	0.6
Dolomite	4	4		4.6	6.4
Marble(?)	5			2.9	1.6
Grn-pnk ss/siltstone	5			2.9	1.6
Subfeldlith ss	4	2		3.4	3.8
Whi/gry suc. sparmic	4			2.3	1.3
				100.0	100.0
Sub Totals:	128	46	0		
Total:	174				
Weighted Sub Totals:	128	184	0		
Weighted Total:	312				